LFAA DEMONSTRATOR TEST REPORT

Document number SKA-TEL-LFAA-0800001
Context ..... REP
Revision 02
Author ..... D B Davidson
Date 2018-11-05
Document Classification..... FOR PROJECT USE ONLY
Status..... Released

Name	Designation	Affiliation	Signature	
Authored by:				
David Davidson and others	Director: Engineering	Curtin University		
			Date:	Nov 6, 2018
Owned by:				
David Davidson	Director: Engineering	Curtin University		
			Date:	Nov 6, 2018
Approved by:				
P. Gibbs	LFAA EPM	SKAO	Philip Gibbs	
			Date:	Nov 5, 2018
Released by:				
J. G. Bij de Vaate	Consortium Lead	AADC		
			Date:	Nov 5, 2018

DOCUMENT HISTORY

Revision	Date Of Issue	Engineering Change Number	Comments
A	2018-07-12	-	First draft release for July 2018 face-to-face
B	2018-09-28	-	Second draft for management team review
C	2018-10-12	-	Third draft for SKAO review
01	2018-11-01	-	Final draft, incorporating SKAO feedback.
02	2018-11-05		Several errata corrected.

DOCUMENT SOFTWARE

	Package	Version	Filename
Wordprocessor	MsWord	Word 2016	SKA-TEL-LFAA-0800001_Demonstrator Test Report_DBD20181101.docx
Block diagrams			
Other			

ORGANISATION DETAILS

Name	LFAA Station Resolution Team
Registered Address	(TBC) SKA Organisation Jodrell Bank Observatory, Lower Withington, Cheshire, Macclesfield, England SK11 9DL United Kingdom
Fax.	
Website	www.skatelescope.org/lfaa/

Copyright

Document owner	LFAA Station Resolution Team
	This document is written for internal use in the SKA project

TABLE OF CONTENTS

LIST OF FIGURES

LIST OF TABLES

LIST OF ABBREVIATIONS

AADC	Aperture Array Design and construction Consortium
AAVS	Aperture Array Verification System
ADC	Analog to Digital converter
Ad-n	n-th document in the list of Applicable Documents
AIV	Assembly Integration and Verification
APIU	Antenna Power Interface Unit
ASIC	Application Specific Integrated Circuit
CAD	Computer Aided Design
CCB	Configuration Control Board
CDR	Critical Design Review
CEM	Computational Electromagnetics
CI	Configuration Item
COTS	Commercial Off The Shelf
CPF	Central Processing Facility
CM	Configuration Manager
CW	Continuous Wave
DMS	Document/Data Management System
ECP	Engineering Change Proposal
EEP	Embedded Element Pattern
EMC	Electromagnetic Compatibility
EMI	Electromagnetic Interference
FoV	Field of View
FPGA	Field Programmable Gate Array
FTR	Full Text Retrieval
HW	Hardware
ICD	Interface Control Document
INFRAAUS	Infrastructure Australia
ISO	International Organisation for Standardisation
LFAA	Low Frequency Aperture Array
LFAA-DN	Low Frequency Aperture Array – Data Network
LNA	Low Noise Amplifier
LMC	Local monitoring and Control
LOFAR	Low Frequency Aperture Array
MBSE	Model Based Systems Engineering
MCCS	Monitor, Control and Calibration Sub-system
MOM	Minutes of Meeting
MPO	Multi-Purpose Optic (connector)
MRI	Master Record Index
MRO	Murchison Radio-astronomy Observatory
MWA	Murchison Widefield array
NRE	Non Recurring Engineering
OCR	Optical Character Recognition
PA	Product Assurance
PDF	Portable Document Format
PDR	Preliminary Design Review
PC	Project Controller
PO	Project Officer
QA	Quality Assurance
RBS	Re-Baselining Submission
RD-n	n-th document in the list of Reference Documents
RF	Radio Frequency

RFI	Radio Frequency Interference
RFoF	Radio Frequency signal over Fibre
RPF	Remote Processing Facility
SaDT	Signal and Data Transport
SDP	Signal Data Processing
SEMP	System Engineering Management Plan
SFDR	Spurious Free Dynamic Range
SKA	Square Kilometre Array
SKA-LOW	SKA low frequency part of the full telescope
SKAO	SKA Office
S/N	Signal to noise
SOW	Statement of Work
SW	Software
TCP-IP	Transmission Control Protocol – Internet Protocol
TBC	To Be Continued
TBD	To Be Done
TBS	To Be Supplied
TM	Telescope Management
TPM	Tile Processing Module
TRB	Test Review Board
WBS	Work Breakdown Structure
WDM	Wavelength Division Multiplexing
WP	Work Package

Executive summary

This report discusses the Aperture Array Verification System (AAVS), a full station of 256 low-frequency antennas deployed on CSIRO's Murchison Radio Astronomy Observatory (MRO) in Western Australia. The aim of this demonstrator was to provide a full-scale Low Frequency Aperture Array (LFAA) station prototype deployed on the Australian SKA site, to assist the design team to investigate, mitigate and retire key risks.

Section 1 provides an introductory overview of the motivation, implementation and current status of the AAVS. Its relationship to LFAA is also discussed, and the point is made that AAVS is not a pre-production prototype of LFAA. Visually, the most striking difference is that AAVS uses the 2nd generation SKALA2 dual-polarised log-periodic antennas, whereas the current LFAA reference design used the 4th generation of this antenna, but there a number of other distinguishing features. An extensive list of authorship and contributors is provided.

Section 2 lists applicable and reference documents.

Section 3 discusses the status of key parameters, including electromagnetics and sensitivity; the analogue RF chain; digital processing; local monitoring and control; correlation; network; and environmental. The electronic (in)stability of the overall RF front-end caused significant delays following deployment until a satisfactory work-around could be found, and remains a risk for the current design.

Section 4 presents results from initial calibration work, much done at 160 MHz, and discusses the calibratability of the station beam in detail. This has emerged as a key risk of the current design. Both experimental and simulation-based work is reported. The key issue is not whether AAVS can be calibrated (results in this section clearly demonstrate that it can be), but rather to what level of accuracy and stability this can be accomplished - and further, at what computational cost. Appendix A.1 provides additional supporting evidence of risk via an independent study of the complexity of AAVS and LFAA station calibration. That work also establishes a useful framework of four classes of calibration for aperture arrays.

Section 5 addresses the maturity of a sub-systems comprising AAVS, and connects with material in Section 3 as appropriate.

Section 6 lists the LFAA level 2 requirements at the time of writing, and outlines how AAVS impacts on the compliance of LFAA for each of these requirements, where relevant.

Section 7 provides a summary of the report, and an outline of future work. The most pressing item is to resolve the highest priority technical risk in the SKA-LOW station reference design identified at CDR, namely station calibratability. A high-level summary of the pre-EPA bridging project proposal currently under development is presented.

Several appendices provide further technical details on a number of topics covered in the main body of the report, including: an analysis of the complexity of LFAA station calibration; a discussion addressing the simulation of embedded element patterns; measured results on optical fibre and power stability, as well as measured temperature effects on the RF

front-end chain and LNA, and an overview of the relevant laboratory measurement procedures; EMC/RFI considerations for AAVS; simulated AAVS station beams at 110 MHz; and finally a detailed analysis of the statistics of the phase solutions obtained during commissioning.

1 Introduction

1.1 Document context

An appreciation of the intent and objectives of the Aperture Array Verification System (AAVS[1]) and its relationship to the LFAA design are essential to the proper interpretation of this document. This section contains information intended to provide the reader with the context required to recognise and derive utility from the document.

1.1.1 Aperture Array Verification System

1.1.1.1 Motivation

The AAVS was conceived and implemented as a vehicle to support the LFAA engineering design process during the SKA preconstruction phase [RD1-2]. The principal motivation for AAVS was to provide a platform to help the design team investigate, mitigate and retire key risks. The objectives of the AAVS program are:

- to validate the architecture (as distinct from implementation) and key enabling technologies of the LFAA baseline design;
- to assess sub-system prototypes in a realistic operating environment and inform their subsequent engineering development and detailed design;
- to validate key performance requirements and assess, by measurement, progress toward compliance with them;
- to support development and assessment of LFAA deployment and installation techniques;
- to progress development of tools and techniques—including correlation, calibration and digital signal processing—required to commission and operate SKA_LOW; and
- to improve the completeness and maturity of the LFAA cost model and budget estimates.

The AAVS is not an LFAA pre-production prototype and, as such, is not intended to demonstrate LFAA compliance with the SKA System Requirements Specification.

1.1.1.2 Implementation

This section describes the fielded implementation of AAVS that has been used (to date) to conduct the analysis presented in this report.

This section does not detail performance specifications, targeted or achieved. These are discussed in Sections 3, 4 and 5, and in the Appendices.

Scope. AAVS is representative of a single LFAA Station. It includes a single Field Node (FN) of 256 antennas deployed in the field; and 256 independent analogue signal paths to the input of a digital signal processing system intended to generate a calibrated station beam. AAVS also includes a Monitor, Control and Calibration system; and a management system that emulates the necessary functions of Telescope Manager. The AAVS FN is shown in Figure 1.

[1] AAVS is also often referred to as AAVS1.

Figure 1: AAVS Field Node deployed on the MRO

FN Dimensions. The AAVS FN has nominal dimensions—determined by the extent of the Ground Plane (GP)—described by a 40m-diametre circle. This provides for a maximum, centre-to-centre, separation of 38m between antennas.

FN Ground Plane. As installed, the FN GP is made up of L6000mm x W2400mm rectangular panels of steel wire mesh arranged in a polygon dimensioned to contain a 40m-diameter circle. The general arrangement of the AAVS GP is shown in Figure 2. The pitch of the wire mesh is 200mm x 200mm. Adjacent panels of mesh are clipped together in order to prevent movement and loss of orientation. The wire mesh AAVS GP is visible under the SKALA2 antenna in Figure 3.

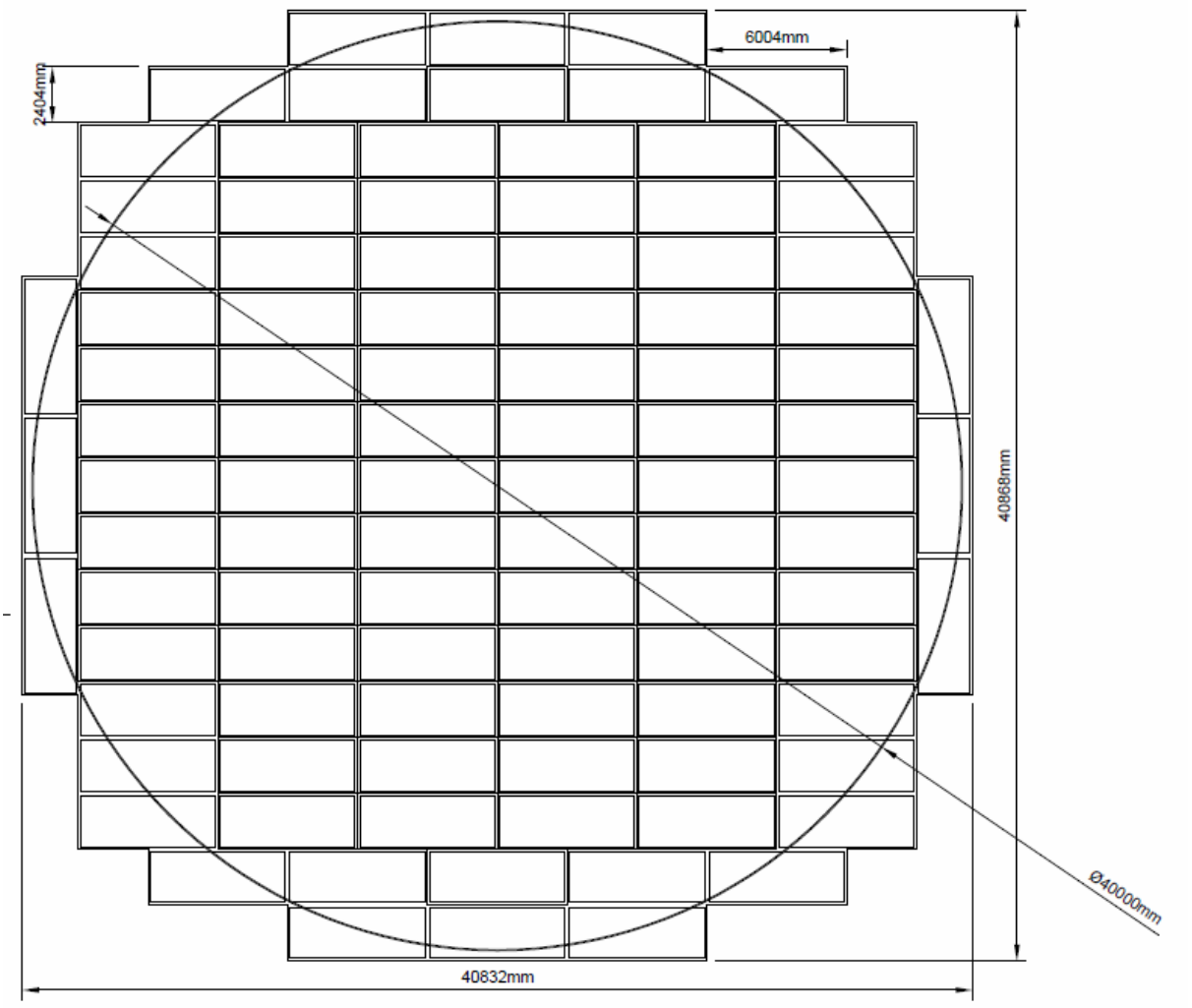

Figure 2: AAVS FN Ground Plane – general arrangement

Antenna system. The AAVS FN has 256 Log-Periodic Dipole Antennas (LPDA). The specific LPDA utilised in AAVS is the SKA Low Antenna, Version 2 (SKALA2). Each antenna incorporates two Low Noise Amplifiers (LNA)—one for each polarisation—followed by analogue amplification and filtering. The antennas incorporate Wavelength Division Multiplexing (WDM) analogue laser drivers, to transmit signals over optical fibre to the MRO processing facility. Each antenna has a factory connected (and thus 'captive' for the purposes of the deployed system) combination (hybrid) copper (for power) and fibre (for signal) cable to connect it to a FN power and fibre distribution hub (Antenna Power Interface Unit [APIU]). The SKALA2 is described in detail in [RD3-6]. The antenna is fixed to a concrete base that is placed on top of the FN GP. The general arrangement of the SKALA2 antenna system used in AAVS is shown in Figure 3.

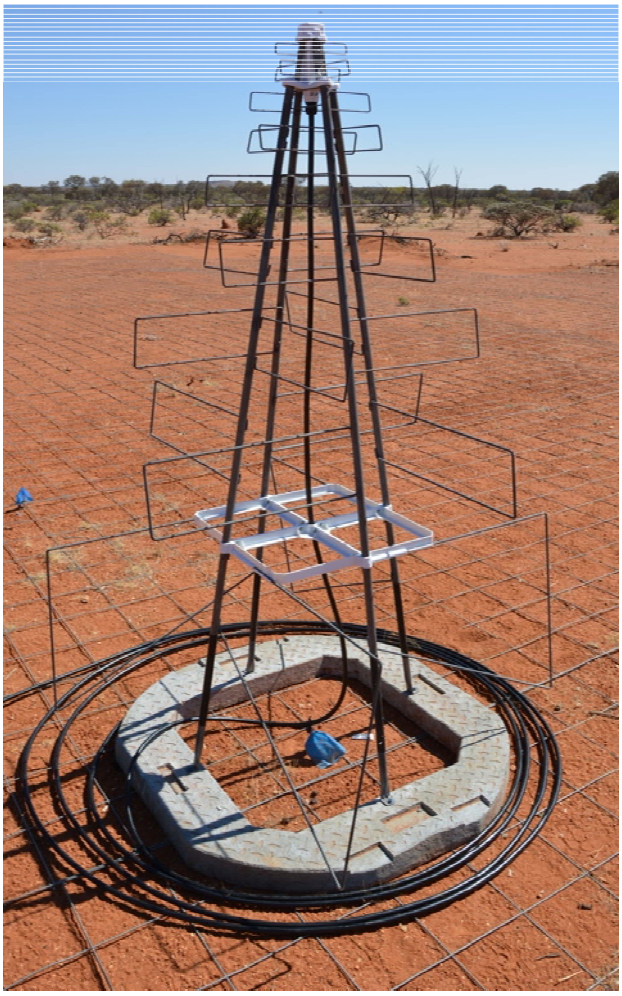

Figure 3: SKALA2 antenna installed in AAVS at the MRO

Antenna distribution. The antennas in the AAVS FN are laid out in random, sparse and constant density configuration. The minimum centre-to-centre antenna separation is 1500mm. The average centre-to-centre antenna separation is 1900mm. Figure 4 shows the distribution of the 256 SKALA2 antennas within the AAVS FN, and their mapping to the Tile Processing Modules (TPM) that provide the AAVS DSP.

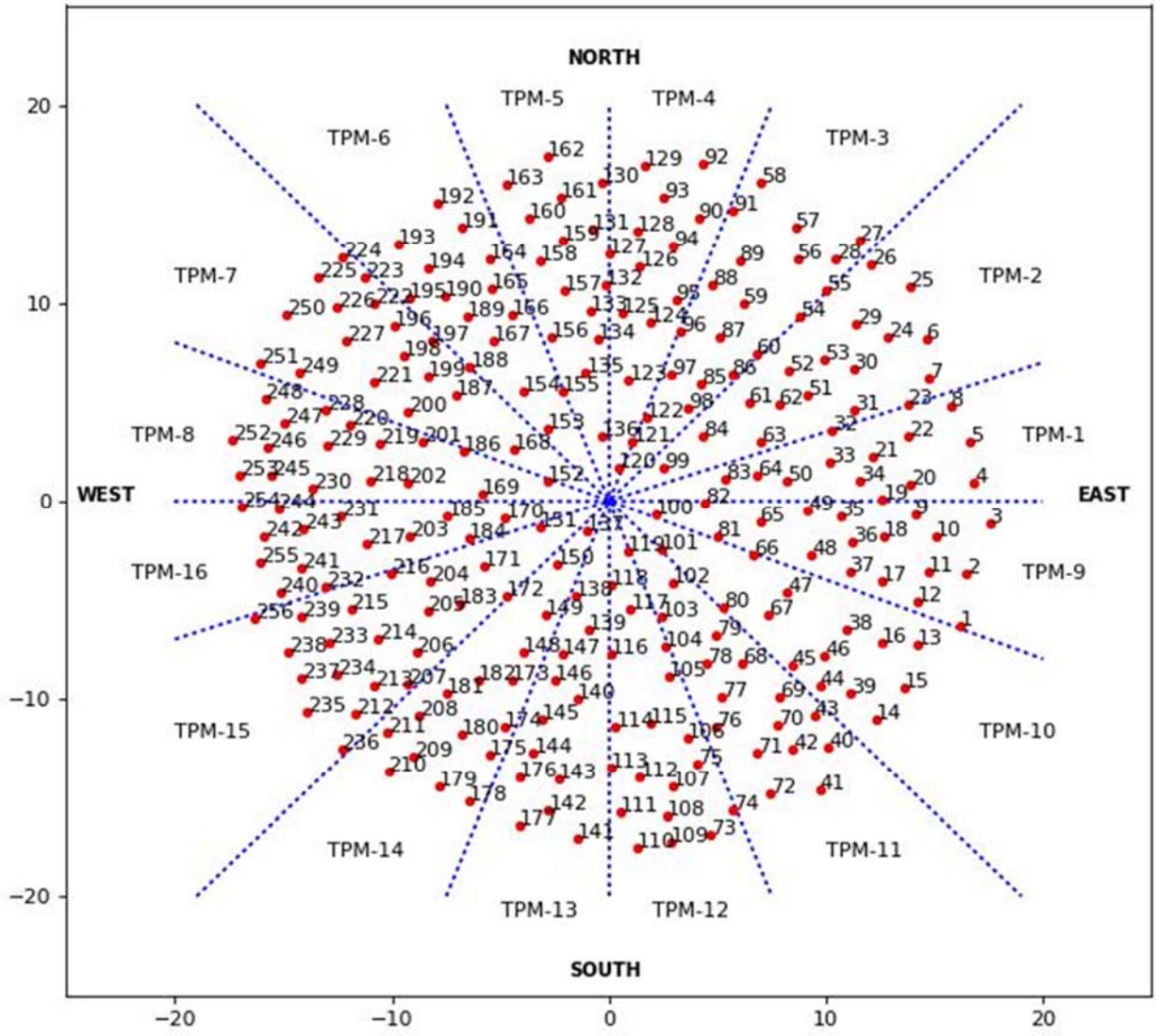

Figure 4: AAVS.1 antenna distribution

Power distribution. An APIU at the centre of the AAVS FN provides power to all 256 antennas. The APIU receives 230V_{ac} on the input side and reticulates low voltage DC at 5V_{dc} to each antenna. The AAVS APIU does not provide any power control or monitoring.

Fibre distribution. The APIU at the centre of the AAVS FN is also the point of connection and aggregation for the individual signal-carrying optical-fibres from the antennas. A fibre-optic breakout module within the APIU presents an LC-APC connect point for the incoming antenna cables and aggregates the individual fibres into a 288-core trunk cable that carries the signals to the MRO processing facility. The 288-core fibre-optic trunk cable is surface laid for the ~5000m route between the AAVS FN and the MRO processing facility.

Figure 5 (left) shows (black surface laid) antenna cables tracking to the APIU positioned at the centre of the AAVS FN; and (right) 128 (of 256) hybrid (copper and optical-fibre) antenna cables entering the APIU. The single black cable at the top-centre of the right image is the 288-core trunk cable that runs to the MRO processing facility.

Figure 5: AAVS APIU and cable entry

Signal path. Figure 6 outlines the AAVS signal path, including the format transitions (in blue) that the signal undergoes.

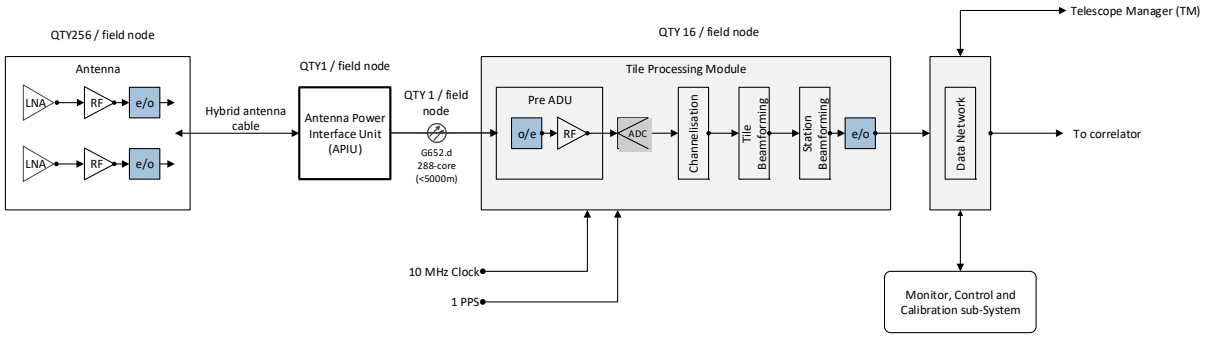

Figure 6: AAVS signal path

Signal processing. AAVS employs a distributed digital beamforming scheme. The TPM is the primary component responsible for the processing of the RF signals received by the AAVS FN. Each TPM performs analogue signal conditioning and digitisation for 16 antennas (dual polarisation). The TPMs perform the following functions: RF-analogue-to-electric conversion; anti-alias filtering and conditioning; variable attenuation; digitisation; channelization; signal chain calibration; buffering; partial-beam assembly and forwarding.

Networking. AAVS uses COTS switching hardware to provide high-speed inter-connect between signal processing units, control processing, and to output to a correlator.

Timing reference and distribution. AAVS sources its timing reference from the MRO station clock which is derived from a local hydrogen maser disciplined by a GPS timing signal. 10MHz and 1pps references are delivered to the signal processing system. Distribution is implemented with COTS devices.

Monitor, Control and Calibration. The Monitoring Control and Calibration Sub-system (MCCS) performs the local monitoring, control and calibration functions for AAVS station. COTS servers are used to support all local monitor and control MCCS functions. These servers are racked with the signal processing system and connected to it via the high-speed switched network.

Telescope Management Controller. A virtual machine running within the LMC server is used to support telescope management (TM) functions. The TMC is a simple emulation of the functions provided by the anticipated SKA1_LOW TM system used to control and monitor AAVS.

1.1.1.3 Current status

The physical implementation of AAVS described above was completed in November 2017. The software required to realise the MCCS and signal processing functionality of AAVS has been incrementally deployed and tested on AAVS since that time. This process is ongoing.

1.1.2 AAVS relationship to LFAA

1.1.2.1 Requirements

There is a tendency by many engaged in SKA pre-construction to view and treat LFAA (and by extension AAVS) as synonymous with SKA_LOW. This is not only technically inappropriate but also detrimental to the proper assessment of the LFAA and SKA_LOW designs. The propensity to measure LFAA against Level 1 system requirements that involve complex and inter-dependent contributions from a number of system elements often manifests as an unnecessarily critical appraisal of the LFAA design's correctness and/or maturity. A potentially problematic corollary effect is that other elements of the system are not as closely scrutinised and may, as a result, ultimately give rise to issues when they are integrated into the SKA_LOW system.

A clear statement of the applicability and flow of requirements as they relate to LFAA (and AAVS) is therefore critical to the proper interpretation of this document, and to distilling robust and credible conclusions from it:

> Level 1 requirements are applicable to the SKA1_LOW telescope.
>
> Level 2 requirements are applicable to the LFAA.
>
> Level 3 requirements are applicable to the Level 3 products within the LFAA Product Breakdown Structure (PBS), being the 'Field Node'; 'Signal Processing Sub-system' (SPS); and 'Monitor Control and Calibration Sub-system' (MCCS).

Figure 7 shows 'product levels' 2 to 4 of the LFAA PBS annotated with the applicable 'requirement levels'.

AAVS does not fit neatly into this model. AAVS incorporates elements of all of the level 3 products, but, as has been established above, is not identical or complete at this level. The

limited scope of AAVS also means that even if it was identical and complete at Level 3, it cannot be considered synonymous with LFAA.

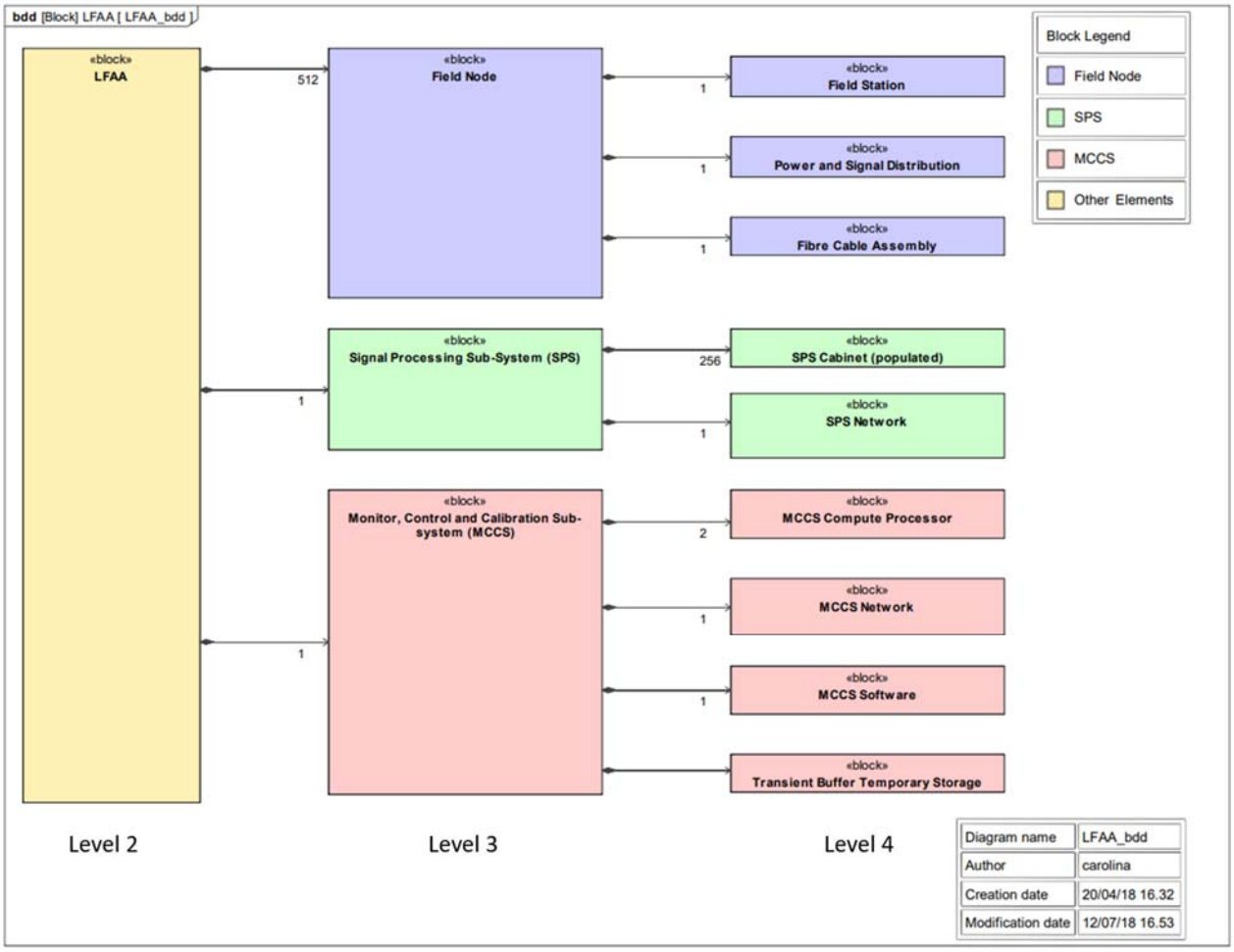

Figure 7: LFAA Product Breakdown Structure

1.1.2.2 Implementation

The implementation of AAVS differs from LFAA design presented for CDR for a number of reasons. These reasons include:

Requirements. The AAVS implementation was informed by the key SKA Level 1 functional performance requirements that were in place in 2013 (System Requirement Specification Rev3). These requirements have evolved significantly since that time. As such and noting the motivation and objectives of AAVS (outlined at 1.1.1.1), it is not appropriate to consider or measure AAVS in the context of the current (2018) SKA Level 1 requirements (System Requirement Specification Rev11, [AD2]).

Objectives. The primary objective of the LFAA is to meet SKA functional performance requirements whereas the primary objective of the AAVS is to provide a design-phase platform to investigate and mitigate risks. These different objectives give rise to vastly different considerations, priorities and imperatives.

Program context. Activities at the MRO are governed and constrained by a regime of authorities, instruments and agreements that (among other things) limited the physical extent, location, and installation of AAVS.

System context. The LFAA will be a discrete sub-system within SKA_LOW. It has a variety of external dependencies (interfaces) that mean it will not provide a 'telescope' capability except in the context of SKA_LOW. In order to serve as an effective risk mitigation platform, the AAVS must be capable of operating in the absence of the external contributions that other elements of the SKA_LOW system will provide for LFAA. AAVS achieves this by relying on existing MRO infrastructure, provided via the MWA, and the use of limited-function emulators.

Schedule. Good engineering practice and precedent suggest that many technical risks and issues do not manifest until realistic procurement, manufacturing, deployment, installation, and operational processes are exercised. This creates a strong imperative to get representative systems (hardware and software) into a realistic environment as early as possible. This imperative shaped the approach to AAVS and has seen numerous lessons learned [RD7] that might otherwise not have become evident until the SKA construction phase.

Budget and cost. AAVS was entirely paid for by the membership of the AADC Consortium and, as such, the scale and scope of budget and cost considerations were different than will be the case for the SKA. Key details of the implementation that were influenced by cost include:

- Overall scope: the overall scope of AAVS was limited by the funding available within the Consortium;
- Site preparation: the extent of civil works possible to establish the AAVS FN locations was limited by the funds available. The limited 'scrape to clear' approach taken in AAVS is an excellent test of whether clearing the ground to the prevailing terrain profile is sufficient for LFAA;
- Fibre installation: the budget did not allow for the ~5000m optical-fibre trunk cable that connects the AAVS FN to the MRO processing facility to be buried. Having this cable surface laid and therefore exposed to the environment represents a 'worst case' scenario for SKA_LOW. AAVS provides an excellent opportunity to evaluate the feasibility of this implementation should it become necessary for any reason.
- Representative components: in many areas AAVS makes use of functionally representative COTS components where LFAA will utilise custom specified items which would be prohibitively expensive in AAVS quantities. The benefits and/or difficulties experienced using COTS components in AAVS can help to inform the custom specification for LFAA, or even demonstrate the feasibility/utility of using the COTS component for LFAA.

Technology readiness. Some key enabling technologies in the LFAA design, such as the SKALA and RFoF, have continued to undergo rapid development throughout the pre-construction design phase. The imperative to deploy AAVS so that it could serve its purpose as a risk identification and mitigation platform meant that the versions of these key technologies deployed in AAVS were never going to be the 'production' specification. The same general premise and approach—accepting the likelihood of a specification update between various system releases (baselines) during the design process to take advantage of

improving technology—is common in the specification of computing components that evolve rapidly. Section 5 discusses the maturity of key elements of the LFAA design.

Despite the differences between the objectives and implementations of AAVS and LFAA, AAVS remains directly relevant to LFAA for the following reasons:

Environment. AAVS is located on the intended site of SKA_LOW. AAVS is subject to the same physical environment (including RFI) that SKA_LOW must endure and so its performance—particularly of critical elements installed in the field such as the antenna, LNA and RFoF transmitters—is directly relevant to LFAA.

Architecture. While the detailed implementations—including specifications, functional allocations, and packaging—of 'products' in AAVS and LFAA differ, the underlying architecture—signal path and format transitions, signal processing approach, and MCCS strategy—is common. AAVS can therefore be used to validate and assess the underlying LFAA architecture without necessarily verifying the performance of a specific implementation.

FN configuration. Though not identical, the AAVS and LFAA FNs are sufficiently alike with respect to their overall dimensions, component make-up, and environmental contexts as to make AAVS a relevant source of lessons learned for both deployment and installation, and through-life-support.

Antenna. AAVS and LFAA are sufficiently alike electromagnetically—based on the lineage of the antenna type and the similarity of the general FN arrangement—as to support credible extrapolation of 'on-sky' measurements and results derived from AAVS to validate models and simulations used to evaluate the LFAA design, including calibration.

Signal processing. Though the detailed hardware specification and configuration of the signal processing systems of AAVS and LFAA differ, the underlying architecture and approach is the same. As such, AAVS signal processing functionality and performance are directly relevant to LFAA.

Switched network. Again, the detailed hardware specification and configuration of the high speed switched network that connects signal processing units, MCCS and the correlator will differ between AAVS and LFAA but the underlying approach and architecture are consistent. Lessons learned in relation to this element of the system are directly relevant to LFAA.

Table 1 compares the AAVS implementation with the CDR baseline of the LFAA design.

Table 1: AAVS and LFAA implementations compared

	AAVS	**LFAA**	
Scope	1 station	512 stations	

FN Dimensions	40m diameter	40m diameter	Both implemented as straight-edged polygons dimensioned to contain the 40m [2]diameter circle required
FN Ground Plane	200mm pitch square pattern wire mesh	50mm pitch square pattern wire mesh	Change motivated by lessons learned from AAVS and evolution of the SKALA design
Antenna System	SKALA2	SKALA4	SKALA evolved in response to lessons learned from AAVS and changing performance specifications
Antenna distribution	Random, sparse and constant density	Random, sparse and constant density	Centre-to-centre minimum and average spacing have remained the same, but SKALA is larger and thus edge-to-edge separation is reduced
Power distribution Fibre distribution	Single APIU supporting 256 antennas Fibre trunk cable surface laid	Four APIUs supporting 64 antennas each Fibre trunk cable buried	Change motivated by 'constructability' and 'maintainability' lessons learned from AAVS
Signal path and transitions	RF > E > O > E > O	RF > E > O > E > O	No change
Signal processing	Distributed digital beamforming	Distributed digital beamforming	No change
Networking	COTS, high-speed	COTS, high-speed	No change
Timing reference and distribution	Source = MRO station clock 10MHz and 1pps	Source = MRO station clock 10MHz and 1pps	Implementation for SKA1_LOW likely to be different that current MRO, but functionally equivalent
Monitor, Control and Calibration	COTS servers High-speed interconnects	COTS servers High-speed interconnects	No change

[2] Now 42m as of July 2018.

Telescope Management	Limited function emulator	SKA1_LOW TM	Constraint of demonstration system environment

1.1.2.3 Compliance

Having established that LFAA compliance was not the primary imperative shaping the derivation of the AAVS implementation, it is nonetheless clear that AAVS can support LFAA's progress toward compliance in a number of important areas. With that in mind, this document canvasses compliance as and where appropriate, consistent with the motivation and primary objective(s) of AAVS.

Section 6 of this document uses the Level 2 (LFAA) requirements as a framework in order to ensure that the status/performance/relevance of the demonstration system (AAVS) to the LFAA design is comprehensively canvassed. Treating all of the L2 requirements also supports the objective of validating LFAA requirements through AAVS.

Using the Level 2 requirements as a framework also makes it logical and easy for the key points of this report to inform/flow directly into other key documents including the Verification Plan and Development Plan.

1.2 Document purpose

The purpose of this document is to report how the AAVS program has contributed to the management of LFAA's risk profile, and to document the maturity levels of elements of the LFAA design.

1.3 Document scope

The document presents a summary of the progress of key functional performance parameters achieved with AAVS; evaluates the maturity of a number of elements of the LFAA design based on outcomes of the AAVS program—including verification of models and simulations; and discusses progress toward compliance with requirements, as and where appropriate.

The document does not include any detailed treatment of the SPS or MCCS elements of the AAVS. These elements are discussed in detail in [RD24], which can be considered a companion to this document.

This document should not be construed to be a compliance report against System (Level 1); Element (Level 2); or Product (Level 3 and below) requirements and, in particular, absence of such content should not be considered indicative of non-compliance.

The document devotes particular attention to work on the calibration of AAVS. At the time of writing, a number of questions remain open regarding this issue and work continues on this.

1.4 Document structure

Section 1: Provides context and information that is important to the proper interpretation of the document.

Section 2: References.

Section 3: Provides a summary of the outcomes and progress achieved with AAVS in a number of key areas of performance and design.

Section 4: Address a key risk associated with AAVS and LFAA, namely station-level calibration.

Section 5: Discusses the status of a range of key risks addressed by AAVS and evaluates the maturity of a number of key elements of the LFAA design.

Section 6: Discusses the validity of and progress toward compliance with Level 2 (LFAA) requirements based on the outcomes of AAVS.

Section 7: Summarises the document and outlines future work.

Several appendices provide additional technical details and measured data for topics addressed in Sections 3, 4 and 5.

1.5 Document status

The document has been structured and drafted with a view to its continued expansion as AAVS continues to function as a risk mitigation platform.

This first version of the document has been drafted with limited input from outside of Curtin University. The objective of the next version of the document will be to fold in analyses and results from other members of the AADC Consortium. This will see improvement in the coverage and treatment of the DSP and MCCS elements of the AAVS in particular.

This document is intended to complement the myriad practical lessons learned from AAVS that are documented in SKA-TEL-LFAA-0900012 – Lessons Learned from AAVS [RD7].

This document must be read in concert with SKA-TEL-LFAA-0500047 – LFAA Signal Processing Sub-system Prototype Test Report [RD24] to achieve a comprehensive understanding of the outcomes of AAVS.

This document is intended to inform subsequent design iterations, analyses and planning documents including SKA-TEL-LFAA-0200050 LFAA Development Plan [AD3], and the intended SKA-TEL-LFAA-0000022 SKA1 LFAA Assembly Integration and Verification Plan [AD4].

1.6 Document authorship

1.6.1 Authors

Authors of this document are DB Davidson, T Booler, and R Wayth (ICRAR-Curtin).

1.6.2 Contributors

This document includes contributions from the following: D Emrich, B Juswardy, B McKinley, A Sutinjo, and D Ung (ICRAR-Curtin); P Benthem, J Broderick and SJ Wijnholds (ASTRON); J Borg, A DeMarco, A Magro, K Zarb Adami (University of Malta), R Chiello (University of Oxford) and G Pupillo (INAF).

2 References

2.1 Applicable documents

The following documents are applicable to the extent stated herein. In the event of conflict between the contents of the applicable documents and this document, **the applicable documents** shall take precedence.

Id	Title	Code	Issue
AD1	SKA System Engineering Management Plan	SKA-TEL-SKO-0000024	02
AD2	SKA1 System Requirement Specification	SKA-TEL-SKO-0000008	11
AD3	LFAA Development Plan	SKA-TEL-LFAA-0200050	-
AD4	SKA1 LFAA Assembly Integration and Verification Plan	SKA-TEL-LFAA-0000022	-

2.2 Reference documents

The following documents are referenced in this document. In the event of conflict between the contents of the referenced documents and this document, **this document** shall take precedence.

Id	Title	Code	Issue
RD1	The Purpose of AAVS1	SKA-TEL-LFAA-0900005	01
RD2	AAVS1 Architecture	SKA-TEL-LFAA-0200003	01
RD3	LFAA Antenna Mechanical Design FP	SKA-TEL-LFAA-0300001	01
RD4	Antenna Design Simulations and Testing Support Document	SKA-TEL-LFAA-0300006	01
RD5	LNA Design FP	SKA-TEL-LFAA-0300002	01
RD6	RX Design Document Wave Division Multiplex 16 Links	SKA-TEL-LFAA-0400024	01
RD7	Lessons Learned from AAVS1	SKA-TEL-LFAA-0900012	01
RD8	Signal Processing Design Document	SKA-TEL-LFAA-0500001	01
RD9	A. T. Sutinjo, T. M. Colegate, R. B. Wayth, et al, ”Characterization of a Low-Frequency Radio Astronomy Prototype Array in Western Australia”, IEEE Trans. Antennas Propag., vol. 63, no. 12, pp. 5433-5442, Dec. 2015.		
RD10	A. T. Sutinjo and P. J. Hall, " Antenna Rotation Error Tolerance for a Low-Frequency Aperture Array Polarimeter”, IEEE Trans. Antennas Propag., vol. 62, no. 6, pp. 3401-3406, Jun. 2014.		
RD11	RFI Standards for Equipment to be Deployed on the MRO	ASKAP-MRO-0001	1.1
RD12	SKA EMI/EMC standards, related procedures & guidelines	SKA-TEL-SKO-0000202	03
RD13	AAVS1 System Requirements Specification	SKA-TEL-LFAA-0200001	1.1
RD14	B. Juswardy, “Temperature Specification Consideration for Outdoor Electronics Deployed at the MRO,” ICRAR/Curtin, Perth, 21 March 2016.		
RD15	RF Front-end Temperature Stability at the MRO	SKA-TEL-LFAA-0800011	1
RD16	J. Abraham and E. de Lera, “LNA Thermal Measurements”, LFAA-AADC Consortium, Cambridge, 28 April 2015.		4
RD17	Memo on the Phase Stability Consideration for Operating Standard Fibre at Non-standard Wavelength: 1550 nm Case Study	SKA-TEL-LFAA-0400018	
RD18	B. Juswardy, “Analysis of ASTRON RFoF on MWA Receiver Front-end,” Rev 1, ICRAR Internal Report, Perth, 2 September 2016.		
RD19	Field Test Result at the MRO to Assess Gain and Phase Variation of Fibre-optic Cable	SKA-TEL-LFAA-0400017	1
RD20	Field Test Result of the 11-km Buried Fibre-optic Cable at the MRO	SKA-TEL-LFAA-0800005	1
RD21	B. Juswardy, “AAVS1 Cable Characterisation Using WDM RFoF Modules,” ICRAR Internal Presentation Slides, Perth, 20 September 2016.		
RD22	LFAA Field Node Deployment Plan	SKA-TEL-LFAA-0700013	D
RD23	LFAA Field Node Deployment Plan Basis of Estimate	SKA-TEL-LFAA-0700014	B
RD24	LFAA Signal Processing Sub-system Prototype Test Report	SKA-TEL-LFAA-0500047	
RD25	Production Specification Field Node Fibre Cable Assembly	SKA-TEL-LFAA-0700026	TBC

RD26	B. Juswardy and A. Sutinjo, “Practical Consideration for Fibre Length and Attenuation Measurements in AAVS1 Deployment,” Internal ICRAR/ Curtin Document, Perth, Rev. 1, 27 July 2015.		
RD27	K.F. Warnick, R. Maaskant, M.V. Ivashina, D.B. Davidson, B.D. Jeffs, ``Phased Arrays for Radio Astronomy, Remote Sensing, and Satellite Communications", Cambridge University Press, 2018.		1st edn
RD28	G. Comoretto et al.: "The Signal Processing Firmware for the Low Frequency Aperture Array", Journal of Astronomical Instrumentation, 6(1), 1641015 (2017) DOI: 10.1142/S2251171716410154		
RD29	C. Wilson, M. Storey and T. Tzioumis, "Measures for Control of EMI and RFI at the Murchison Radioastronomy Observatory," IEEE 2013 Asia-Pacific Symposium on Electromagnetic Compatibility (APEMC), Melbourne, VIC Australia, 20-23 May 2013.		
RD30	G. Naldi et al.: "The Digital Signal Processing Platform for the Low Frequency Aperture Array: Preliminary Results on the Data Acquisition Unit", Journal of Astronomical Instrumentation, 6(1),1641011 (2017) DOI:10.1142/S2251171716410142		
RD31	Software Demonstrator Report	SKA-TEL-LFAA-0600054	A
RD32	“AAVS1 pre-conformance and calibration tests”, Internal ICRAR-Curtin Document, Perth, 27 July 2018.		
RD33	SKA1 Error Budgets	SKA-TEL_SKO-0000641	
RD34	AAVS1 calibration plan	SKA-TEL-LFAA-0200006	1
RD35	CA Jackson et al, “EMC considerations for the ASKAP dish antennas”, APEMC 2013. IEEE 2013 Asia-Pacific Symposium on Electromagnetic Compatibility (APEMC), Melbourne, VIC Australia, 20-23 May 2013,pp 360-363.		
RD36	Station Design Report	SKA-TEL-LFAA-0300034	0.3
RD37	RC Hansen, “Phased Array Antennas”, 2nd edn, Wiley 2009.		
RD38	SJ Wijnholds, “Complexity of LFAA station calibration”, internal note, 12 Sept 2018		
RD39	Analyses of Ambient Temperature Measurements at the MRO and their Implications on RF Front-end Specifications	SKA-TEL-LFAA-08000XX	1
RD40	Balance Utility Solutions, “SKA LFAA AAVS1 Antenna Power Interface Unit: Synchronous Rectifier EMC tests”, Dec 2015		
RD41	Appendix 4: EMC Testing and Assessment Considerations.	SKA-TEL-LFAA-000000	A
RD42	F Schlagenhaufer, “ICRAR EMC Test Report: AAVS1 TPM Subrack”, Internal ICRAR-Curtin report, 8 Mar 2017		
RD43	AT Sutinjo, et al. “Revisiting Hybrid Interferometry With Low-Frequency Radio Astronomy Arrays”, IEEE Trans. Antennas Propag., vol. 65, no. 8, pp. 3967-3975, Aug. 2017.		
RD44	AAVS1 Software Demonstrator Design Report	SKA-TEL-LFAA-0600054	

RD45	S Tingay, J Monari, A Schinckel, A van Es and L Stringhetti, "The pre-EPA bridging project for SKA_LOW", 16 Oct. 2018		Ver 5

3 Status of key parameters

This section provides a summary of the outcomes and progress achieved with AAVS in a number of key areas of performance and design. The sub-sections that follow are largely reprised from section 5 of [RD2] and canvass the primary testable areas where AAVS performance is directly relevant to LFAA. Calibration, and concerns about station beam calibration, emerged as major topic of work in the period preceding CDR, and this is addressed separately in the following section, with supporting results and measurements. Particular emphasis is put on calibration results obtained to date. The issue of station beam calibration emerged as a major risk during this work, and is discussed at length in Section 4 and Appendix A.1.

3.1 Electromagnetics and sensitivity

The current SKALA4 antenna shares the same overall dual-polarised log-periodic dipole array design as the SKALA2 used by AAVS. Although there are significant differences in the detail designs, much can be learnt from the AAVS system using SKALA2 elements in the context of electromagnetic design, sensitivity and station-level calibration. Briefly, the SKALA4 is longer, consists of more elements, and has a central transmission line feed. This impacts on both the electromagnetic performance of the antenna, as well as the mechanical configuration. The largest element has been designed to provide the SKALA4 with better sensitivity at the lower end of the band. The addition of more elements provides a spectrally smoother response in terms of reflection coefficient (and hence noise matching) as well as in terms of element patterns.

As discussed in the section “Models and simulations”, the modelling approaches developed and demonstrated for AAVS0.5 are also applicable to AAVS, but with the caveat of high computational cost. From AAVS, using SKALA2, to an LFAA field node using SKALA4, the simulation methods are similarly applicable, as are beam measurement methods. This report addresses only the SKALA2 antennas deployed in AAVS. Work is in progress on developing station models for LFAA for the SKALA4 antennas.

Drone measurements were envisaged in [RD2] for AAVS; these have not yet been performed on the full AAVS array, only on a 16-element prototype. Comparisons of measured and simulated data from these more limited validation studies will provide useful indications of the reliability of full-scale station simulations. Other methods, such as the use of satellites as test sources, could also be considered, or the use of compact cosmic radio sources combined with interferometry (as in [RD9]).

Prediction using simulation and validation of the full AAVS station beams, using the most appropriate methods, is an activity which should continue to be addressed during bridging as it has not been possible to fully address this before CDR.

Regarding the specific points outlined in [RD2] to evaluate primary testable areas for LFAA that can be addressed by AAVS:

- Sensitivity (and T_{sys}) as a function of frequency and scan angle: Processing of the data is still in progress at the time of writing, and it is difficult to provide an estimate of how much time beyond CDR is likely to be needed, as there are dependencies on the beamformer (which is not currently fully working). Extracting this information from station drift scans is under consideration.

- Polarisation performance: Simulations are currently in progress. For individual elements, the computer simulation problem is readily tractable. For a 256 element station, the problem is challenging, as noted above. As this metric is associated with polarisation leakage, measurements may be very difficult.

- Beam shape predictability: This has been discussed above in the context of AAVS05 and AAVS. For the latter, predictability using numerical simulation is possible, but as noted above, this is a computationally challenging problem due to the large station size combined with the complex SKALA2 (or SKALA4 for LFAA) design and the random element layout. This topic is addressed further below, in the context of initial calibration results. Currently, simulations per frequency point for AAVS require many hours to days of computation time per frequency point. (Note also that beam is assembled from the embedded element patterns, and as outlined in Appendix A.1, numerical simulations ultimately require validation by measurement.)

- Sensitivity to variation in antenna position, orientation, and verticality: The sensitivity of the precursor MWA elements to orientation variation was addressed in [RD10]. A similar analysis has not been undertaken for AAVS. An analysis has been performed on LFAA [RD36].

Summarizing this section, work is currently in progress on evaluating sensitivity, system temperature and polarisation performance; work still required in this area includes AAVS station beam simulations and measurements and sensitivity studies on antenna positioning. This represents a substantial amount of work; since both the simulation methods and metrology impact direct on LFAA, this work should continue, potentially beyond CDR.

3.2 Analogue chain

[RD2] envisaged the data transport through the antenna electronics, RFoF, analogue chain in the bunker to digitisation to be testable using AAVS. However, soon after deployment in early 2017, electronic oscillations were found on the AAVS analogue chains. These were attributed to a feedback loop due to excessive leakage of the RF signal and subsequent coupling back to the antennas due to two factors, namely leakage of the RF line to the DC copper pair in the RFoF transmitter due to poor DC-RF decoupling, and leakage of the RF signal from the copper pair to the outside of the Hybrid cable due to poor grounding of the hybrid cable armour and the RFoF front end transmitter. (It should be noted that measurements of the LNA on its own indicated unconditional stability; the problem occurred when the LNA was installed within the RF front end system).

Changes were proposed and implemented to address this. Several solutions were identified to this problem by Cambridge University, including the use of ferrites, grounding the hybrid cable, and correcting the capacitor value to decouple the RF and DC lines at the RFoF

transmitter [RD7]. INAF and the University of Ferrara (Italy) also independently developed solutions; the use of ferrites below the trumpet and grounding the hybrid cable appropriately were similar to the Cambridge solutions, and they further proposed shorting the hybrid cable jacket to the RFoF chassis. Measurements were also made in the Curtin University laboratories.

This work has reduced the instability issue, but whether is it wise to have the LNA and the RFoF transmitter in close proximity within the "trumpet" of the antenna remains a design issue currently debated for SKALA4.

Specific items which were planned in [RD2] to be tested included:

- Gain appropriate to the site;
- Noise contribution;
- Ensure IP2 and IP3 limits are not reached;
- (Sensitivity - see discussion in the preceding section);
- Crosstalk between polarisations and antennas; and
- Attenuator range.

For many of these, the receiver chain oscillation issue meant that these tests could not be undertaken as intended soon after deployment. Attention has been primarily focussed on getting data out of the system, so most of these items have yet to be tested individually. At the time of writing, only the first and last items in the list above (gain and attenuator range) have been tested, both of which are working as expected. Additionally, during tests to date, it has proven difficult in practise to separate out the intrinsic variations in the analogue chain from the effects of the differing embedded element patterns.

Tests have been made on the optical fibre stability and are include as Appendix A.3 .These summarise the measured optical path length of the cables as well the statistics of the optical power. As indicated in [RD19], it was found that fibre (core) length difference has a relatively small effect on the relative phase variation, provided that the length difference is relatively small compared to the total length of the cable. In this case, a simple physical model of the fibre as discussed in that report indicates that temperature difference among the fibre cores is the factor that most significantly influence the phase variations. Additionally, results for a series of measurements on the front-end module which recorded the optical power of each wavelength are also presented in the same appendix. (It is noted that there is not at present a specification on this.)

Temperature stability of the RF front-end chain is discussed in detail in Appendix A.4. Using the data presented in A.4.3, for a 10-minute interval at 160 MHz, contributions will include of 0.28° from the LNA, 0.75° from the RFoF transmitter and around 7.8° for the 5.2 km of surface laid cable (assuming use of the lower-specification SDGI loose tube cable, 1.5°/km). Adding these contributions predicts a maximum phase variation of around 8.83°; the RMS variation will be approximately 1/3 of this, ie around 3°. This is well within the 20° phase variation currently considered sufficient for LFAA (as of October 2018).

This data is specifically for AAVS. With a buried RFoF link (0.013°/km) as currently planned for LFAA, a 50km cable run will contribute only 0.65°, and the overall phase

variation will be well within the above 20° phase variation. Should the AAVS surface-laid cable option be considered for LFAA, again assuming a 50km FO cable, the phase variation in the FO cable dominates the calculation (at around 75°), with an RMS value of around 25°, which exceeds the above limit - but not by much.

It should be noted that potential overall RF front-end system oscillation remains an issue of concern.

3.3 Digital processing

Available documentation [RD8] does not full address the digital system as implemented for the AAVS. As only the 256-element station (the "primary array" in [RD8]) is currently in the field, only 16 tile processing modules (TPMs), not 25 as planned, are presently in use (all were deployed as planned). These TPMs provide partial beamforming, summing 16 antenna signals together, and then forwarding to another unit. As noted below, the correlation mode currently available is limited to only one of the coarse channels (These are spaced 781.25 kHz apart, but due to oversampling comprise 925.926 kHz).

From [RD2], the intent was to demonstrate the following:

- Digitisation performance in the conditions found on the site. Before shipping, INAF carefully tested each board, and documented the tests. Current tests demonstrate that the digitiser is working, although its detailed performance on-site has not yet been evaluated.
- Beamforming and tracking. Attention with initial testing has focussed on the correlation mode, and beamforming and tracking have yet to be evaluated. Station beamforming functionality was not operational in the period preceding CDR, so this functionality could not be evaluated. The problem was an intermittent hardware fault in one of the TPMs that caused the DDR memory used in beamforming to fail. As far as is known, the firmware is serviceable, but for this reason it has not been thoroughly tested.
- Polarisation correction. Similar comments apply: these have not yet been demonstrated.

SKA-TEL-LFAA-TBD - LFAA Signal Processing System Prototype Test Report [RD24] provides detailed discussion of the AAVS SPS. The TPM is further described in [RD28] and [RD30]. The software design is reported in RD44 - AAVS1 Software Demonstrator Design Report.

3.4 Local monitor and control

Specific tests envisaged in [RD2] included:

- Ability to monitor and control TPMs directly via TANGO;
- Collect antenna data into MCCS servers for calibration;
- Run beamforming coefficient calculations;
- Distribute coefficients effectively and in a timed fashion for good observation;
- Develop and check precision of calibration algorithms;
- Ability to size the MCCS for SKA1_LOW; and
- Effective interface with TM and refine TM/LFAA responsibilities.

As with digital processing, the delayed start due to analogue signal chain issues has delayed testing of these. As it currently stands, the LMC system consists of custom software written specifically for commissioning and testing. It does not specifically address the LFAA design. Nonetheless, this custom AAVS software directly addressing the issues of collecting antenna data, and as such is applicable to LFAA.

SKA-TEL-LFAA-TBD - LFAA Signal Processing System Prototype Test Report [RD24] provides detailed discussion of the AAVS MCCS as a corollary of its treatment of the SPS.

3.5 Correlation

As only the 256-element station was deployed, phase and amplitude closure between stations has not been demonstrated to date.

The calibration plan explicitly included using the MWA as a reference system, and parts of the signal processing required to enable this would re-use infrastructure are already set up in the EDA system. The key issue here is that the signal that is intended to go into the MWA system is a single full-station beam, and there is not yet a working station beamformer, as outlined in the preceding section.

The tests outlined in [RD2] included:

- Validation of the LFAA-CSP ICD using an independently developed correlator;
- An essential part of the test environment for much of the testing work; and
- Multi-beaming capability testing.

Presently, data has only been extracted using a mode of operation on AAVS permitting correlation between individual SKALA2 elements. This can however only be done on one coarse channel at a time.

3.6 Network

SKA-TEL-LFAA-TBD - LFAA Signal Processing System Prototype Test Report [RD24] provides detailed discussion of the AAVS Network as a corollary of its treatment of the SPS.

3.7 Environmental

The discussion in this section is limited to the performance of AAVS components deployed in the field at the MRO. Components and equipment installed in the controlled environment of the MRO control building are not discussed. The impact, if any, of a number of primary environmental factors on the performance of each of the major elements of the deployed array is noted. The environmental factors discussed are briefly defined for the purposes of this document in Table 2.

A number of specific issues arising from factors of the transport environment are mentioned at section 5.3 and documented in detail in [RD7].

Environmental factor	Definition
Solar insolation	Impacts associated with the incidence of solar energy
Temperature	Impacts associated with changes in the ambient temperature caused by, inter alia, time of day, wind, cloud cover, rain etc
Wind	Impacts associated with the electrical and mechanical forces generated by wind and particulate matter acting on objects
Particulate matter	Impacts associated with ingress of dust, dirt and other particulate matter
Rainfall	Impacts arising from rainfall
Water flow	Impacts resulting from the flow of water over the surface of the ground
Flora	Impacts related to the growth of plant material on the site
Fauna	Issues caused by interaction with animals
Radio Frequency	Impacts arising from the radio frequency environment at the MRO

Table 2: Explanation of environmental factors

Table 3 summarises environmental impacts and issues associated with the AAVS Antennas.

Environmental factor	Impacts and issues
Solar insolation	The 'plastic' components of the antenna used in AAVS0.5—including the injection moulded plastic casing of the antenna electronics, and the structural bracing sections—exhibit discolouration and surface flaking after six years deployed at the MRO. They remain structurally robust. The earliest examples of the same components in AAVS have been deployed since early 2016 and exhibit only minor discolouration. Commodity 'cable ties' were used to secure the hybrid antenna cables in place and ensure a deliberate arrangement that formed part of the 'work around' to resolve an 'oscillation' exhibited in the generation of SKALA2 deployed in AAVS. These cable ties perish quickly as a result of solar insolation and must not form part of the production version of the SKALA. Similarly, the heat shrink tubing applied to the antenna hybrid cables as part of the 'oscillation' remediation process is susceptible to perishing due to solar insolation and a number of deployed examples are showing early signs of wear. Tubing used to finish/seal antenna cables in factory production processes must have equivalent solar ratings to the cable sheath so that they do not provide a weak point that undermines the MTBF of the cable component.
Temperature	The deployed antennas have not exhibited any negative response or issue arising from changes in the ambient temperature.
Wind	The antennas deployed for AAVS0.5 (in 2012) were installed by drilling a central pole into the surface of the ground, where the central pole was the only point of contact between the antenna and the ground. This arrangement proved to be unviable as the antenna was prone to vibrate significantly in response to the wind. (The

	actual level was measured and was in the order of a few millimeters; most of the vibration was due to the PVC/composite pipe then in use). The SKALA2 antennas deployed for AAVS (from 2016) no longer have a central pole and have four points of contact with a heavy concrete base. This provides a much more rigid structure and secure attachment/installation. The SKALA2 deployed for AAVS (Figure 3) have not exhibited any negative response or issue that can be definitively attributed to the mechanical forces produced by the wind acting on the antenna. However, the potential for the wind to impact the connection between the antenna hybrid cable and the antenna electronics has been identified as a risk to consider in subsequent versions of the antenna.
Particulate matter	The deployed antennas have not exhibited any negative response or issue arising from ingress of particulate matter. Noting the susceptibility of optical transmission components to ingress, there was considerable risk arising from the need to open and re-finish the antenna electronics casing in the field to implement the 'work-around' fixes for the 'oscillation' exhibited by the deployed SKALA2 antennas. Careful handling and precautions—including completing the work in as protected an environment as possible, and not working in windy conditions—mitigated this risk during AAVS deployment but highlight important considerations for LFAA deployment and maintenance.
Rainfall	The deployed antennas have not exhibited any negative response or issue arising from rainfall.
Water flow	The deployed antennas have not exhibited any negative response or issue arising from water flow.
Flora	The deployed antennas have not exhibited any negative response or issue arising from flora in the vicinity of the FN, nor the regrowth of minor vegetation through the prepared FN surface. Management of regrowth must form part of the LFAA routine preventative maintenance regime in order to ensure that vegetation cannot reach sufficient size as to mechanically or electro-magnetically impact the antenna.
Fauna	The deployed antennas have not exhibited any negative response or issue arising from animals on the MRO. However, a number of minor termite mounds have begun to develop within the FN. This is common on the MRO where the ground surface has been disturbed. If left unchecked, these have the potential to mechanically impact the antenna.
Radio Frequency	The deployed antennas have not exhibited any unanticipated negative response or issue arising from the radio-frequency environment at the MRO.

Table 3: Environmental impacts and issues associated with the AAVS Antennas

Table 4 summarises environmental impacts and issues associated with the AAVS Antenna Power Interface Unit.

Environmental factor	**Impacts and issues**
Solar insolation	The AAVS APIU has not exhibited any negative response or issue arising from solar insolation.
Temperature	The AAVS APIU has not exhibited any negative response or issue arising from the ambient temperature.
Wind	The AAVS APIU has not exhibited any negative response or issue arising from the wind.
Particulate matter	The AAVS APIU has not exhibited any negative response or issue arising from the ingress of particulate matter. However, the exposure of the LC/APC optical connection points to the risk of ingress by dust, dirt and other particulate matter carried by the wind/rain when the lid of the APIU is removed for installation and/or maintenance activities has been identified for remediation in subsequent versions of the APIU design.
Rainfall	The AAVS APIU has not exhibited any negative response or issue arising from rainfall.
Water flow	The AAVS APIU has not exhibited any negative response or issue arising from water flow.
Flora	The AAVS APIU has not exhibited any negative response or issue arising from flora.
Fauna	The AAVS APIU has not exhibited any negative response or issue arising from fauna. However, a number of systems deployed to the MRO for MWA and the EDA have been negatively impacted by ants and spiders that nest inside electronics enclosures and cause shorts. These instruments have implemented minor fixes to make them less susceptible. Future designs, including for LFAA, must consider this when doing board layouts (placing components to reduce the risk of shorting by small fauna like ants and spiders); by minimising ingress points and implementing barriers to entry where possible; and in the formulation of preventative maintenance regimes. The area underneath the APIU, provided to allow water to flow, provides a potential habitat for local fauna, including snakes. Maintenance procedures will need to include careful inspection/clearance of this area.
Radio Frequency	The AAVS APIU has not exhibited any negative response or issue arising from the radio frequency environment at the MRO.

Table 4: Environmental impacts and issues associated with the AAVS APIU

Table 5 summarises environmental impacts and issues associated with the AAVS Fibre Cable Assembly (FCA)

Environmental factor	**Impacts and issues**
Solar insolation	The jacketing and construction of the AAVS FCA was specified to be tolerant of high solar insolation loads and to protect the optical fibre within the cable. To this point, the AAVS FCA has not exhibited any negative response or issue arising from solar insolation.
Temperature	To this point, the AAVS FCA has not exhibited any unanticipated negative response or issue arising from solar insolation. See section 5.2 for further relevant discussion.
Wind	To this point, the AAVS FCA has not exhibited any unanticipated negative response or issue arising from wind. See section 5.2 for further relevant discussion.
Particulate matter	The AAVS FCA has not exhibited any negative response or issue arising from ingress of particulate matter.
Rainfall	The AAVS FCA has not exhibited any negative response or issue arising from ingress of rainfall.
Water flow	The AAVS FCA has not exhibited any negative response or issue arising from ingress of water flow. However, in general, the flow of surface water at the MRO can produce significant strain on the end-points/connections/terminations of cables laid on the surface of the ground as the AAVS FCA is. For example, every MWA tile is supported by a surface laid cables between 90m and 1600m in length. The slack in these cables can be moved tens of meters by water flows, often in different directions at different points along their length. They can also become snagged on flora and collect debris. Surface laying cables over any distance greater than a few tens of meters represents a considerable risk of damage and should be avoided in SKA_LOW.
Flora	The AAVS FCA has not exhibited any negative response or issue arising from ingress of flora.
Fauna	Noting that its jacketing and construction were specified to prevent damage by mastication by large fauna such as feral goats, camels and kangaroos, and small fauna such as termites, the AAVS FCA has not exhibited any negative response or issue arising from interaction with fauna on the MRO.
Radio Frequency	The AAVS FCA has not exhibited any negative response or issue arising from the radio frequency environment at the MRO.

Table 5: Environmental impacts and issues associated with the AAVS Fibre Cable Assembly

Table 6 summarises environmental impacts and issues associated with the AAVS Field Node (FN) surface and Ground Plane (GP)

Environmental factor	**Impacts and issues**
Solar insolation	The AAVS FN surface and GP have not exhibited any negative response or issue arising from solar insolation.
Temperature	The AAVS FN surface and GP have not exhibited any negative response or issue arising from changes in the ambient temperature at the MRO.
Wind	The AAVS FN surface and GP have not exhibited any negative response or issue arising from the wind.
Particulate matter	The AAVS FN surface and GP have not exhibited any negative response or issue arising from the ingress of particulate matter.
Rainfall	The AAVS FN surface and GP have not exhibited any negative response or issue arising from rainfall.
Water flow	The AAVS FN surface and GP have not exhibited any negative response or issue arising from the flow of water. In AAVS (and also MWA and EDA) moving water periodically results in very minor (>0.05sqm), localised undermining of the GP. This generally results from a specific perturbation of flow by an impediment such as a rock embedded in the ground surface. Even with the 200mm x 200mm pitch of the AAVS GP, the mesh is sufficiently robust to support the antennas and foot traffic over this scale of unsupported area. The surface can be easily restored by placing fill through the GP mesh. The siting-in-detail of LFAA FNs will need to carefully consider water flow in order to ensure that damage associated with it is limited to the minor, localised, repairable scale experienced in AAVS. Major undermining of an LFAA FN would require the entire installation to be removed, and the ground surface restored.
Flora	Vegetation regrowth in areas where the ground surface has been disturbed is common at the MRO and has been experienced in AAVS. This regrowth is relatively easy to control but must be actively monitored and managed to prevent negative mechanical and electron-magnetic impacts on antennas and supporting equipment.
Fauna	The AAVS FN surface and GP have not exhibited any negative response or issue arising from interaction with fauna at the MRO. However, a number of minor termite mounds have begun to develop within the FN. This is common on the MRO where the ground surface has been disturbed. If left unchecked, these have the potential to mechanically impact the antenna.
Radio Frequency	The AAVS FN surface and GP have not exhibited any negative response or issue arising from the radio frequency environment at the MRO.

Table 6: Environmental impacts and issues associated with the AAVS Field Node surface and Ground Plane

4 Calibration of AAVS and risks for LFAA

This section presents calibration results obtained to date, and addresses issues identified about station beam calibration. These are discussed at length in Section 4.4 and Appendix A.1.

4.1 Background

During work towards CDR, concerns were raised regarding calibrating the AAVS [RD32]. The key issue is that the individual antennas have quite different patterns due to mutual coupling and the quasi-random layout; using the average element pattern to calibrate the station may not result in a sufficiently accurate calibration solution. In the language of calibration, the station has both direction dependence and baseline (specific antenna) dependence.

This issue is discussed in some detail in this section. Whilst it has proven possible to obtain a calibration solution using an approximation of the patterns of each antenna in the station, it is not anticipated that a measurement of the accuracy and stability of this approximation will be available by CDR, nor will a detailed simulation. Similarly, the computational cost of a calibration scheme using the individual elemental patterns is also still to be determined.

It should be noted that work undertaken independently has arrived at similar preliminary conclusions [RD38], incorporated in this report as Appendix A.1. This is discussed further in Section 4.6.

4.2 Initial calibration results

4.2.1 Sun-based calibration

Initial calibration and imaging was performed on 2.26s raw voltage data for a single coarse channel centred around 159 MHz. The initial effort focussed on resolving the inevitable issues with metadata: time formats, data formats, antenna to correlator mapping, frequency offsets, polarisation labels and so on. This test provided the initial "bootstrap" such that the end-to-end signal path was fully understood. Prior to this test, correlated data had been captured with the GPU-based correlator in the LMC system of AAVS, but the data had not been successfully calibrated or imaged. The main results of this test were:

- Confirmed/updated antenna and polarisation mappings through the various connections and data re-ordering in the data files
- Confirmed known dead/disconnected antennas
- Identified unintended polarisation swaps on some antennas
- Confirmed that there were no large uncorrected delays between antennas

- Confirmed that data can be calibrated from a short (2 second) datablock with a strong calibration source in the data (in this case the sun)

Subsequent imaging was performed on visibilities generated with the GPU-based correlator in the LMC system. Details of this are described in Table 7, and results are shown in Figure 8 and Figure 9.

Dataset	correlation_204_20180405_12105_0.hdf5
Date	2018-04-05
Frequency:	159.4 MHz
Frequency channels:	1 (approx 0.9 MHz BW)
Time resolution:	0.849 s averaged to 8.49 seconds
Flagged antennas:	3, 26, 128, 120, 121,12, 38, 41
Time range:	UTC at start of observation: 03:21:40. (Local time: 11:21:40 AM)
Duration:	Just under 2 hours.
LST at start of observation:	approx 00:02 hours

Table 7: Details of AAVS dataset

The dataset has no spectral resolution but runs for almost 2 hours with good time resolution. The sun was used as a calibrator to solve for antenna-based gains on roughly 5 minute intervals. It was assumed that all the individual antenna patterns (embedded element patterns, EEPs) are the same. In the classification scheme of Appendix A.1.2, this would be a Class 1 calibration scheme; calibration on one bright source, assuming identical EEPs. The main results of this test were:

- Antenna gain solutions are generally well behaved on 10 minute time scales, with some significant gain amplitude changes due to unmodelled sources in the sky. In this case, the setting galactic plane affected data
- Antenna phase solutions show 10-20 degree variations on ~15 minute timescales

Full-sky images made with the sun at the phase centre show the sun and some other strong radio sources at their known (correct) locations in the sky. In Figure 8 below, the sun and radio sources Fornax A and Tau A are clear in the image. The oval shape of the sky is due to the slant orthographic projection.

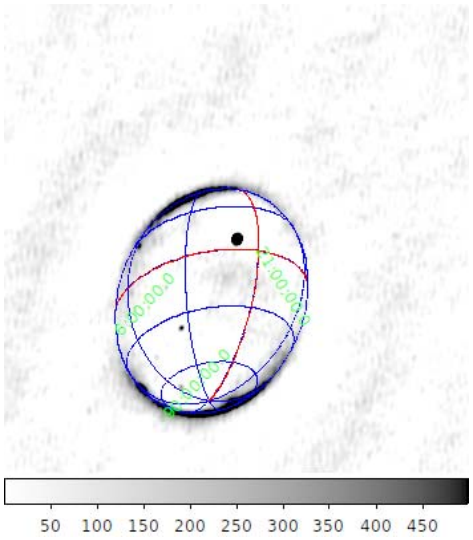

Figure 8: XX polarisation images of the sky from 2018-04-05 with the sun at the phase centre.

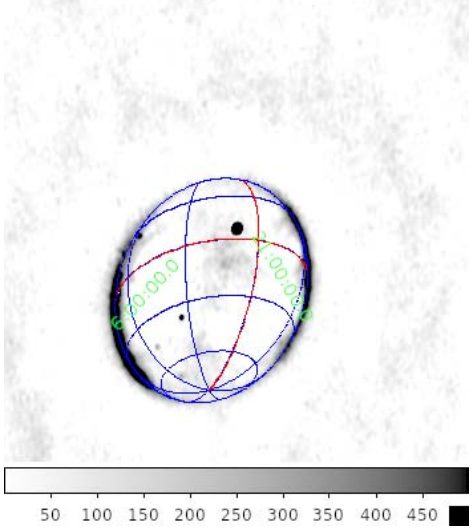

Figure 9: YY polarisation images of the sky from 2018-04-05 with the sun at the phase centre.

Using data from 2018-07-11, another ~2 hour dataset centred on solar transit was calibrated as described above. The results confirmed the general behaviour seen in the April data, and did not have any ambiguity due to the Galactic plane setting during the observations.

Figure 10 shows example gain phase solutions from the solar observations for a subset of 16 antennas. Antenna 2 was used as the phase reference. The phase solutions are generally well behaved and have similar variations with time similar to previous observations we have analysed. There are slow variations over the two-hour scan with changes of order 10-20 degrees over tens of minutes.

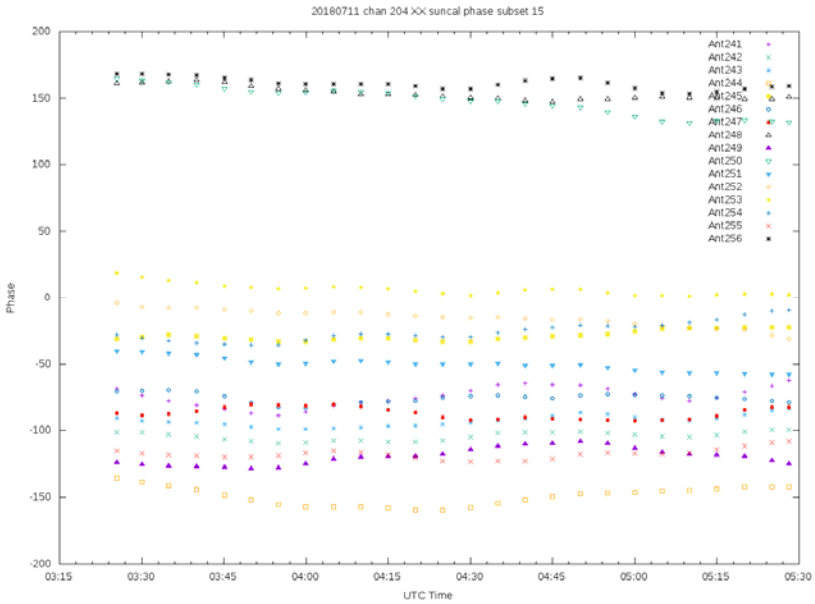

Figure 10: Example antenna-based calibration phase for a selection of 16 antennas from 2018-07-11 solar observations

Based on the specified 10 minute calibration timescale of LFAA, the data were examined for their variability within a 10 minute interval. To calculate the variability, all gains were divided into 10 minute bins and the variation relative to the gain at the start of the bin was calculated. In Figure 11 the phase was calculated as the difference between the antenna phase at any time vs the phase from 10 minutes prior.

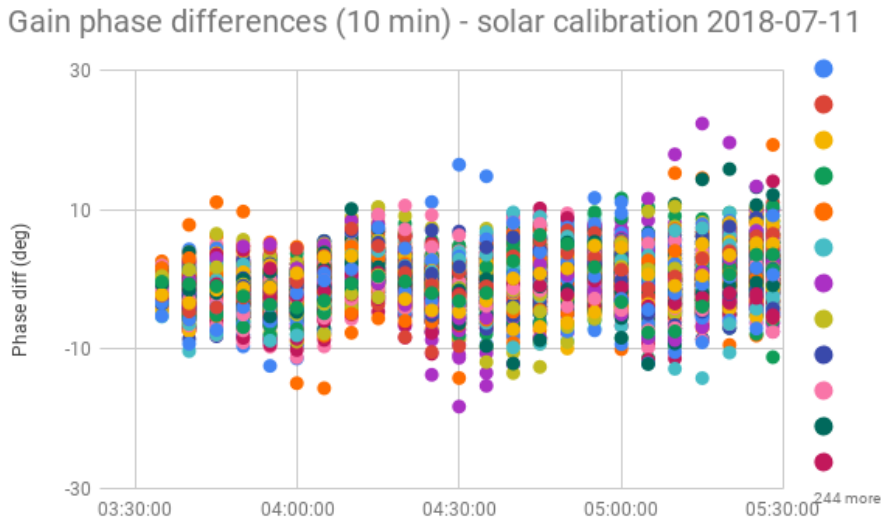

Figure 11: The phase difference of the gain calibration for all antennas between successive 10-minute calibration intervals (contains all 256 antennas). Time stamp is UTC.

4.2.2 Sky-based calibration

The LFAA calibration plan (SKA-TEL-LFAA-0200006) proposed a method for station calibration based on forming correlation products (visibilities) between all pairs of antennas within the station, using a full diffuse sky model. The plan included simulations to test the calibratability of the station at different frequencies at different LSTs and concluded that there is sufficient signal in the diffuse Galactic sky emission at most LSTs to self-calibrate the station. *The only caveat to the conclusion was that the simulations assumed each element (dipole) in the array has an identical pattern on the sky*. In the case of the simulations, this was a simple average dipole pattern. In the classification scheme of Appendix A.1.2, this would be a Class 2 calibration scheme; calibrating on a diffuse sky, assuming identical EEPs. (We know from simulations that the SKALA2 dipoles in AAVS have very dissimilar element patterns, a topic that will be addressed in detail in the next section).

For an initial test of the method, we used the same data from 2018-07-11 but this time using the full 24 hours of data, phased at the zenith. The data were split into 1-minute chunks and for each chunk a sky model was generated based on a scaled version of the Haslam 408 MHz sky map. The sky model was multiplied by the average embedded element power pattern (one each for X and Y polarisations).

An example sky model is shown below in Figure 12, including the Y polarisation average antenna power pattern at 160 MHz (Figure 13). Two sky models are generated (one each for X and Y pols) and each polarisation is independently calibrated.

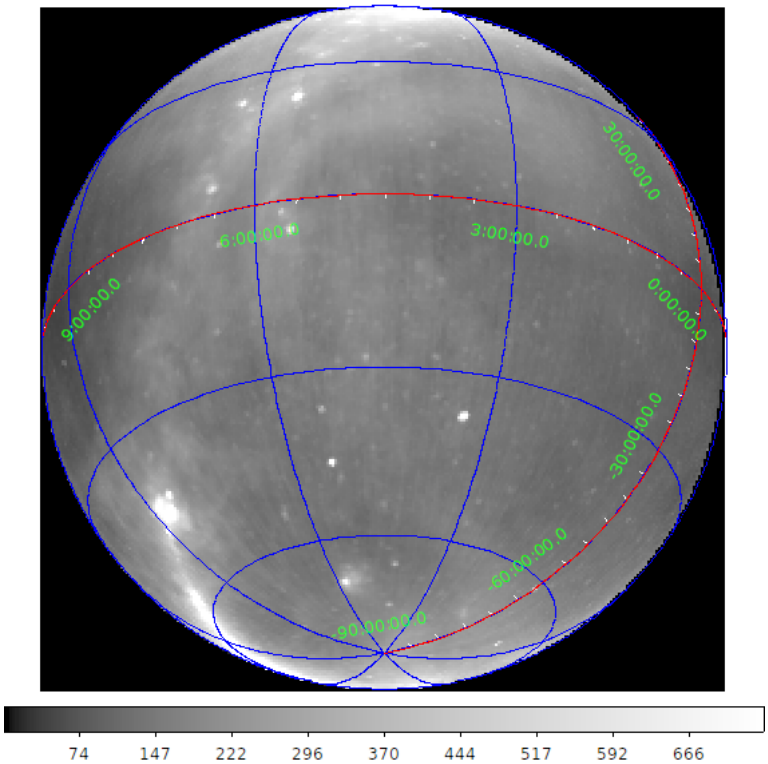

Figure 12: Sky model used for calibration around LST = 4.5 hours. This image includes the average embedded element pattern shown in Figure 13.

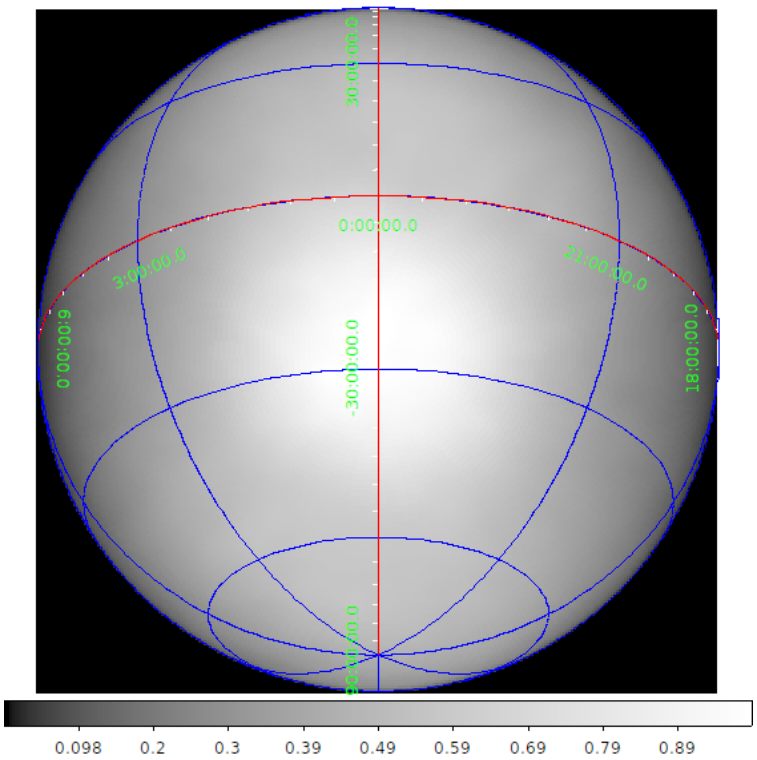

Figure 13: Average embedded element pattern for the Y polarisation.

A subset of data that used sky-based calibration during the night was examined in more detail. This dataset is most useful because it is night-time (hence the sun does not need to be included in the model) and the Galactic plane was rising, hence there is good signal to calibrate on. In Figure 14 the antenna gain solutions were calculated on more frequent intervals (approximately 1 minute) and the difference of a solution to the start of a 10 minute bin is shown.

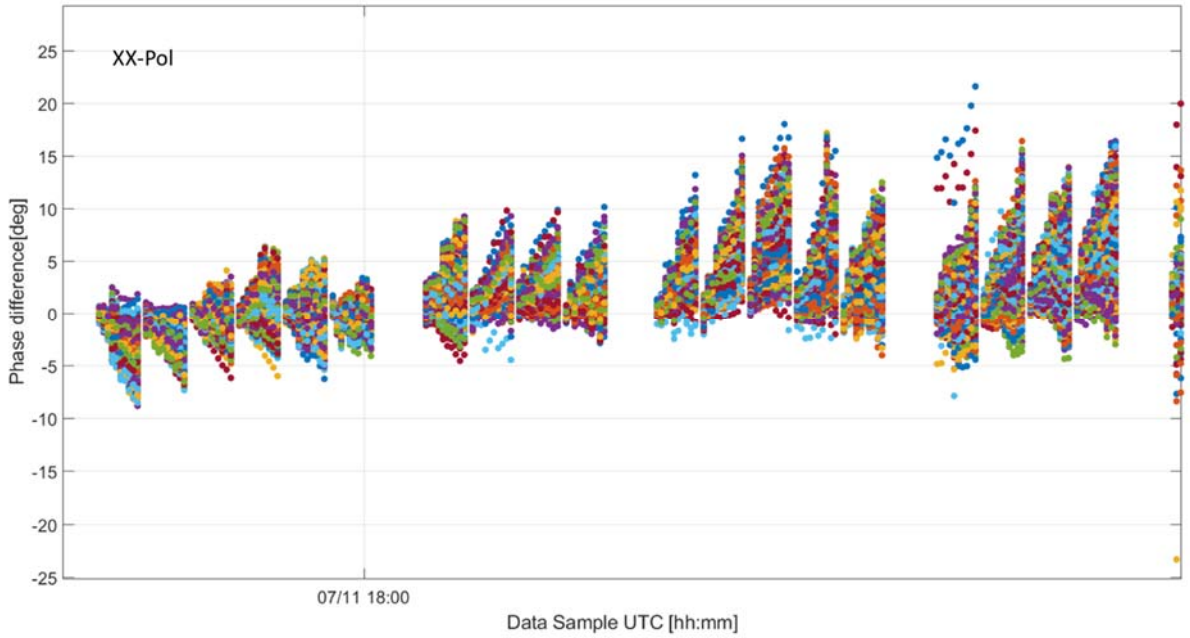

Figure 14: Further analysis of antenna calibration phase drift for the 2018-07-11 sky-based calibration during night-time

Both calibration methods show variations substantially larger than several degrees over 10-minute timescales on a per antenna basis.

A detailed investigation into the statistics of the phase solutions is provided in Appendix A.8.

4.3 Analysis of initial calibration results

These results caused us concern, as initially, requirement SKA1-LFAA-133 (0.1% maximum RMS between the parametrised station beam and the actual station beam) was taken as a motivation for the exploration of issues of station calibration. Subsequent clarification with SKAO pointed to [RD33], identifying a working assumption that the station beam provided by LFAA should be accurate to 1%. %. SKA1-LFAA-228 now specifies relative gain tolerances, varying across the frequency bands, but the 1% working assumption is representative for the following.

Using this working assumption of 1% beam stability error, a simple argument based on the standard array tolerance formula can be applied [RD34] and [RD37]:

$$\frac{D}{D_0} = \mathrm{e}^{-(\sigma_p^2+\sigma_a^2)} \approx 1 - (\sigma_p^2 + \sigma_a^2)$$

Here, D is the directivity with error, and D_0 is the ideal directivity, i.e. no error. (This formula is related, but not identical to, the Ruze formula for dish surface errors). The approximation applies for small errors. σ_a and σ_p are the errors on the amplitude and phase of the input signal. The biggest degradation to directivity (which is proportional to sensitivity, and hence deviation from the ideal beam) will come from uncorrected phase variations per antenna. A

1% phase-only error would correspond to $D/D_0 = 0.99$. Hence this RMS phase variation cannot be more than approximately 5.7 degrees over the 600 second calibration interval.

4.4 Electromagnetic simulations and array theory: embedded element patterns

Motivated by our initial analysis, we further investigated station calibration via electromagnetic simulations and contemporary array theory. The AAVS calibration plan [RD34] proposed a method for sky-based station calibration based on forming correlation products (visibilities) between all pairs of antennas within the station, using a full diffuse sky model. The plan included simulations to test the calibration of the station at different frequencies, and at different local sidereal times (LSTs), and concluded that there is sufficient signal in the diffuse Galactic emission at most LSTs to self-calibrate the station. However, that plan specifically noted the assumptions of no mutual coupling, and that all station antenna elements have the same radiation pattern. That document showed early results for element patterns, and already raised concerns (in 2015) about these assumptions of identical patterns, which if not valid (as will be shown here) would result in systematic errors in the calibration solutions.

The AAVS calibration outlined above and applied in 4.2 requires a beam (pattern) model for each antenna within the station. As described in Section 7.2, [RD31], the calibration system documented for the AAVS station envisages the use of the interferometer simulation tool OSKAR2.7. Using a global sky model, updated in real-time to include sources rising and setting, this should produce the required visibilities for the sky dependent calibration. However, recent tests have demonstrated that OSKAR is unable to ingest the element patterns, for reasons to be described. At the time of writing, OSKAR will only be able to handle average element patterns.

In array theory, the term “embedded element pattern” (EEP) denotes the radiation pattern of an individual element embedded in the array, with all the other elements terminated. Appendix A.2 discusses the conventions used regarding the choice of terminating impedance for these non-fed elements. It is noted there that EEPs computed for different loading conditions may appear quite different; however, when correctly combined (usually requiring the array mutual impedance matrix), the final station beam will be the same.

Figure 15 shows the embedded element patterns for antennas 1-15, as predicted by computational simulation at 160 MHz. The measured LNA input impedance at the relevant frequency was used as the loading condition in the simulation; note that this is frequency dependent. (Results have been computed for all 256 elements, but only 16 antennas are shown here). The key point here is the fine structure visible in the pattern. (Y here refers to the North-South antenna arms; X, not shown, in East-West).

Note that these patterns were computed using the array as a transmitter; reciprocity permits the use of these results on receive. (A summary of the important results in this context may be found in Chapters 2 and 5 of [RD27]).

This structure is on the scale of several degrees, consistent with significant electromagnetic interaction (i.e. mutual coupling) across much of station. It is this pattern which OSKAR is presently unable to handle; the simulator was designed for smooth beams, and applies spatial interpolation to model the beam. The average embedded element pattern does smooth out these variations. However, to fully calibrate the station, *each* element pattern would need to be modelled using some type of reduced-order model (not a full computational

electromagnetic model as this would be too costly), and this fine structure will be computationally costly to model. This computational cost will be greatly increased by the current requirement to have different random layouts for each station. (This requirement arises from considerations regarding the sidelobe noise of the overall synthesized beam).

Also evident in Figure 15 is the relatively strong pattern on the horizon (on the circumference of the patterns). This has not been fully explained at the time of writing.

An analysis of the RMS deviation between computed embedded element patterns and the average pattern for the AAVS and EDA (the latter, using a simpler bow-tie element) is shown in Figure 19, computed over a hemisphere. The computations show the RMS difference between each embedded element pattern and the patterns averaged for that that element. (This is only one of several metrics which could be used). The largest variations are demonstrated by AAVS at 160 MHz. (Note that in the lower figure, the x-axis is essentially arbitrary).

Results from an initial calibration solution, also at 160 MHz, are shown in Figure 17 and Figure 18. These used the sun as source (treated as 100 000 Jy source), and solutions were computed using the visibilities. The gain solutions from the calibration are essentially pattern cuts over a restricted angular range in Figure 15. For comparison, the corresponding pattern cuts from those simulations are also shown on the figures. A variety of effects can be noted. For some antennas, for example Ant004, the correlation between the shape of the curves is good. For some others, the curves appear to be anti-correlated. Some dead elements (e.g. Ant003) can also be observed. Work on this is currently in progress. The key point here is that the gain solutions demonstrate rates of changes similar to the pattern cuts. Figure 18 also shows an attempt to use knowledge of the EEPs to correct the phase of the calibration solution. The procedure involves subtracting the mean phase from both the calibration solutions and the phase variations predicted by the beam model and then adding the two phases (since they are anti-correlated). The aim is to flatten out the phase solutions – ideally, with a flat line. However, the results are mixed; for some antennas, the models flatten out the phase solutions well, but for many, the beam model greatly over-predicts the magnitude of the phase variation. Further investigations on this continue. A comparison of measured data for the 16-element AAVS0.5 is available approach in [RD43] and may present a path for further studies.

Computer simulations for the overall AAVS station beam, with the array beamformed for a zenith pointing, are shown in a 3D visualization in Figure 20, and as a contour plot Figure 21. In the computer model, the individual embedded element patterns using the actual terminating impedance can simply be appropriately combined as noted in Appendix A.2, and the station beam appears reasonable. (The station beam computed at 110 MHz, shown in Appendix A.7, shows better main beam and first side lobe formation, no doubt due to the lower frequency). It is important to emphasize that this simulation assumes a perfectly-calibrated RF chain; in the real AAVS, this will require sufficiently accurate calibration of each element, as outlined above, to create this beam. As noted elsewhere, due to hardware problems, it has not been possible to form and test an AAVS station beam to date.

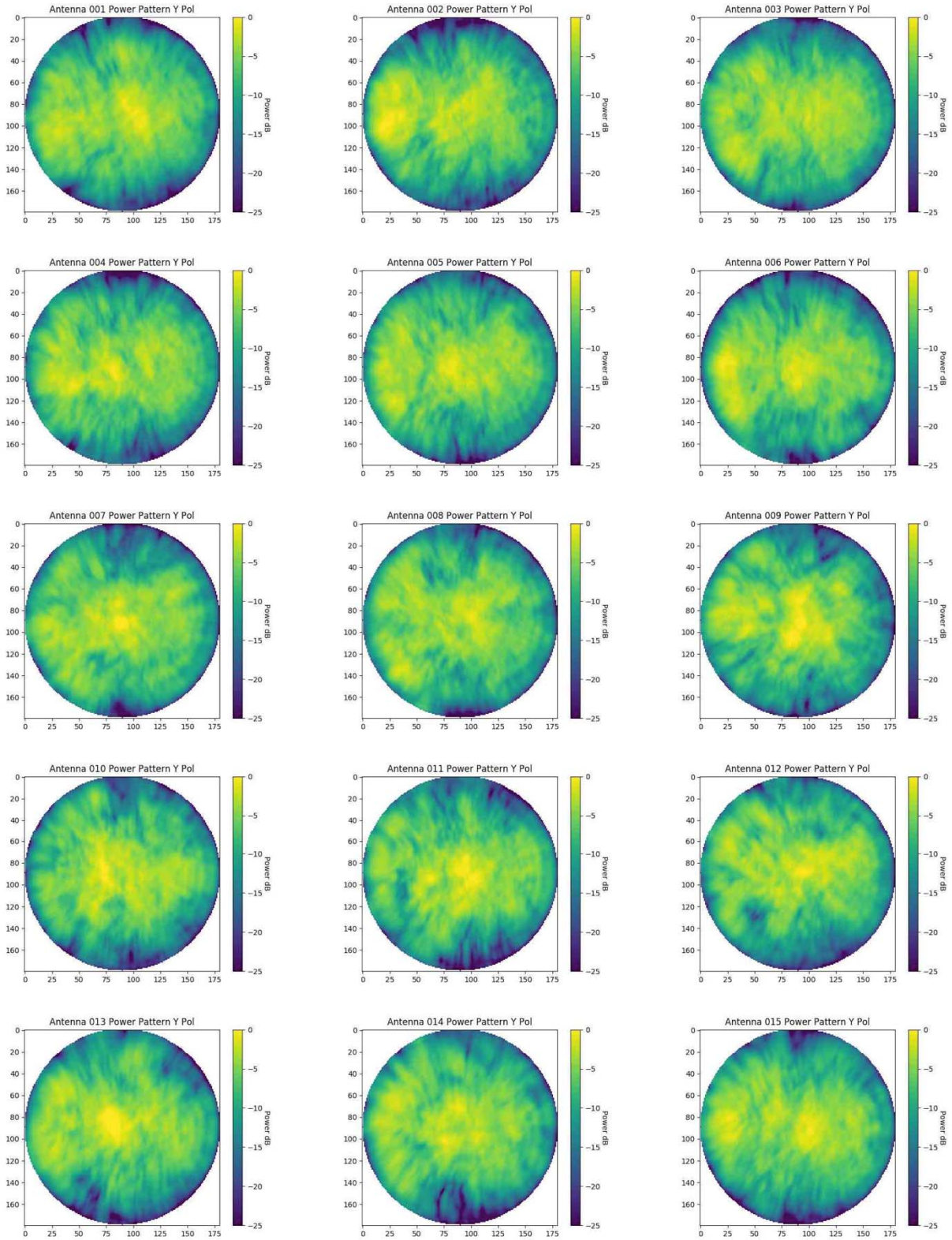

Figure 15: Embedded element patterns, amplitude, at 160 MHz, as predicted by computational simulation.

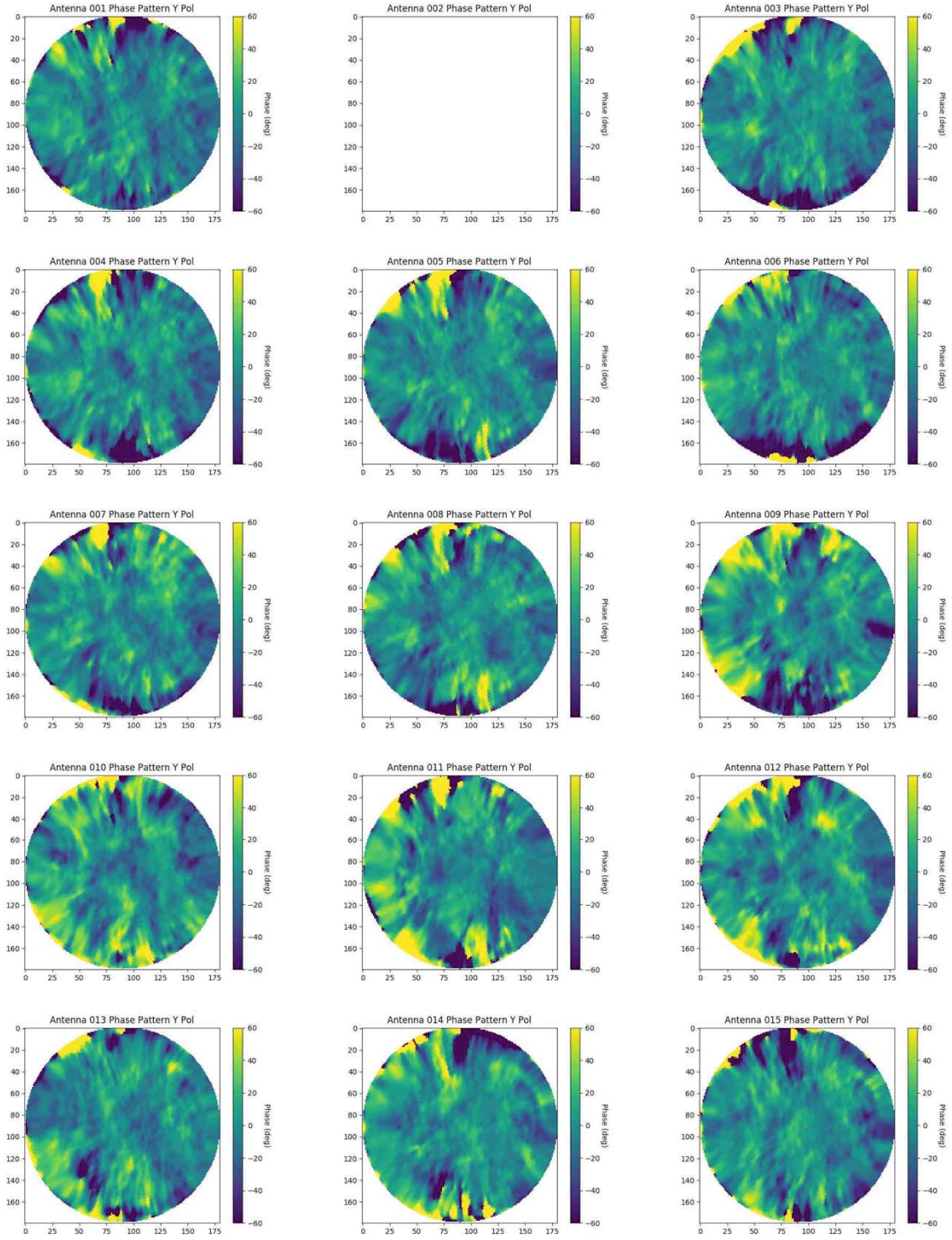

Figure 16: Embedded element patterns, phase, at 160 MHz, as predicted by computational simulation.

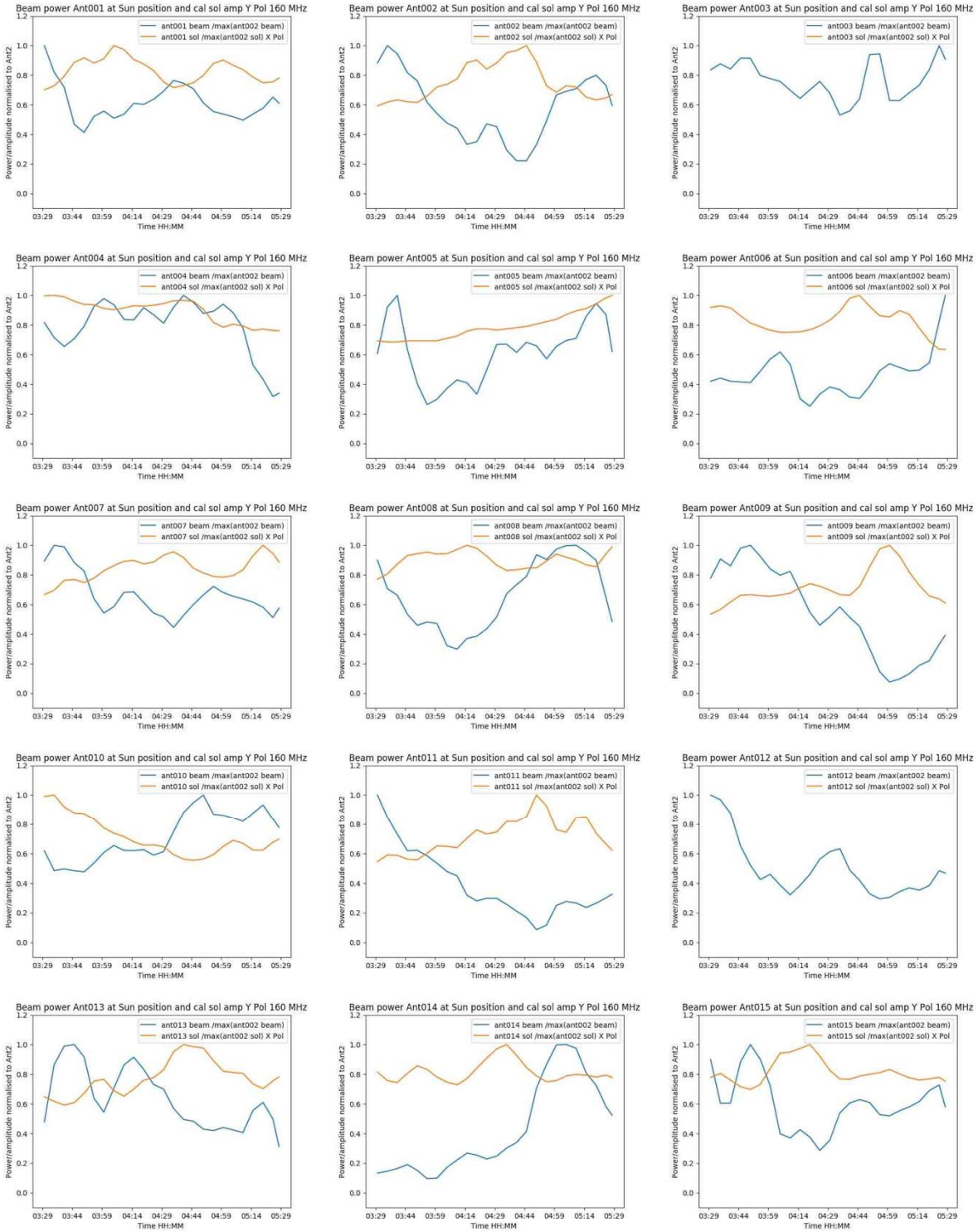

Figure 17: Initial calibration results, amplitude, for AAVS, antennas 1 to 15. Orange: calibration solution. Blue: beam simulation. Frequency 160 MHz.

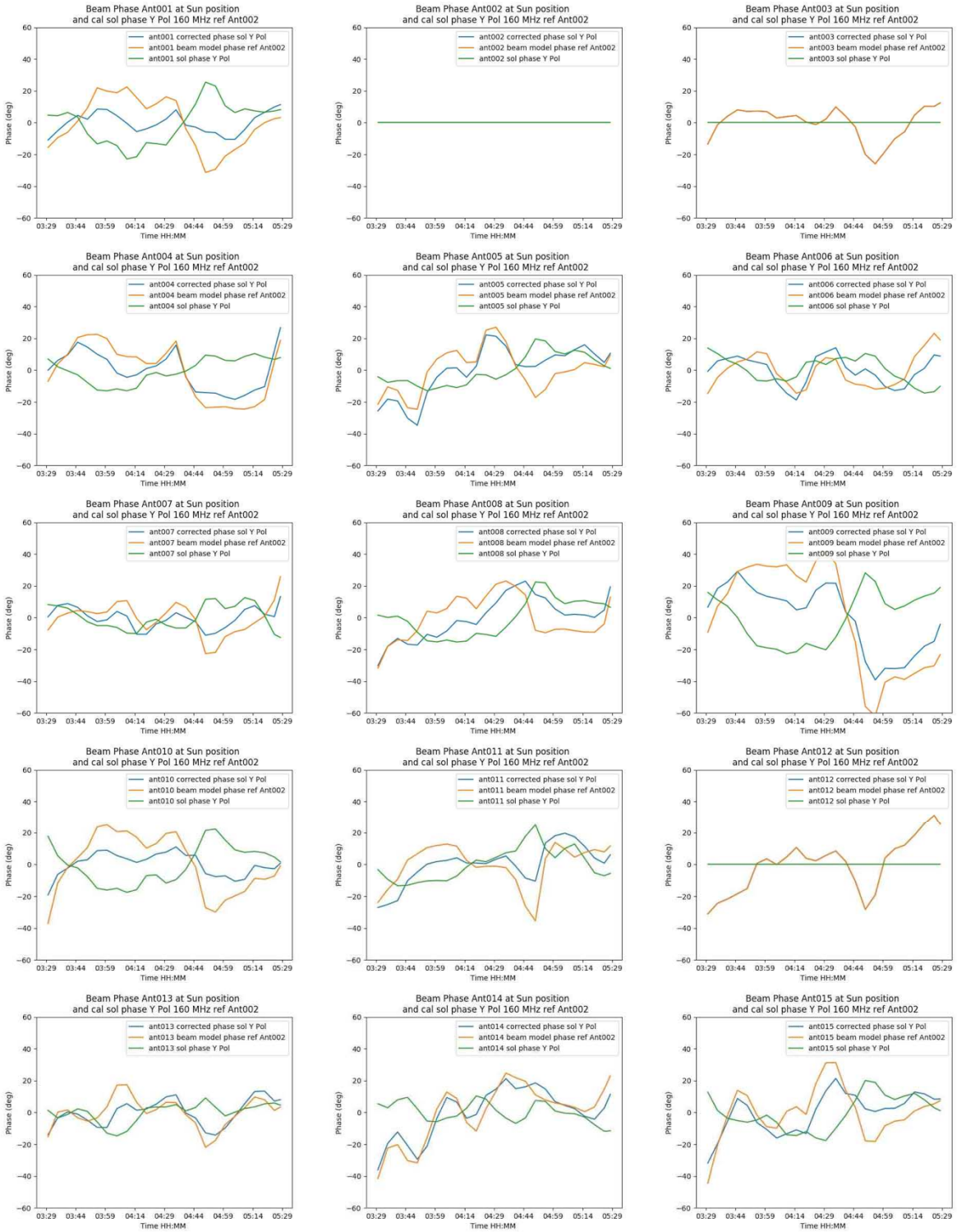

Figure 18: Further calibration results for AAVS, phase, antennas 1 to 15. Green: calibration solution. Orange: beam simulation. Blue: including phase correction from EEP. Frequency 160 MHz.

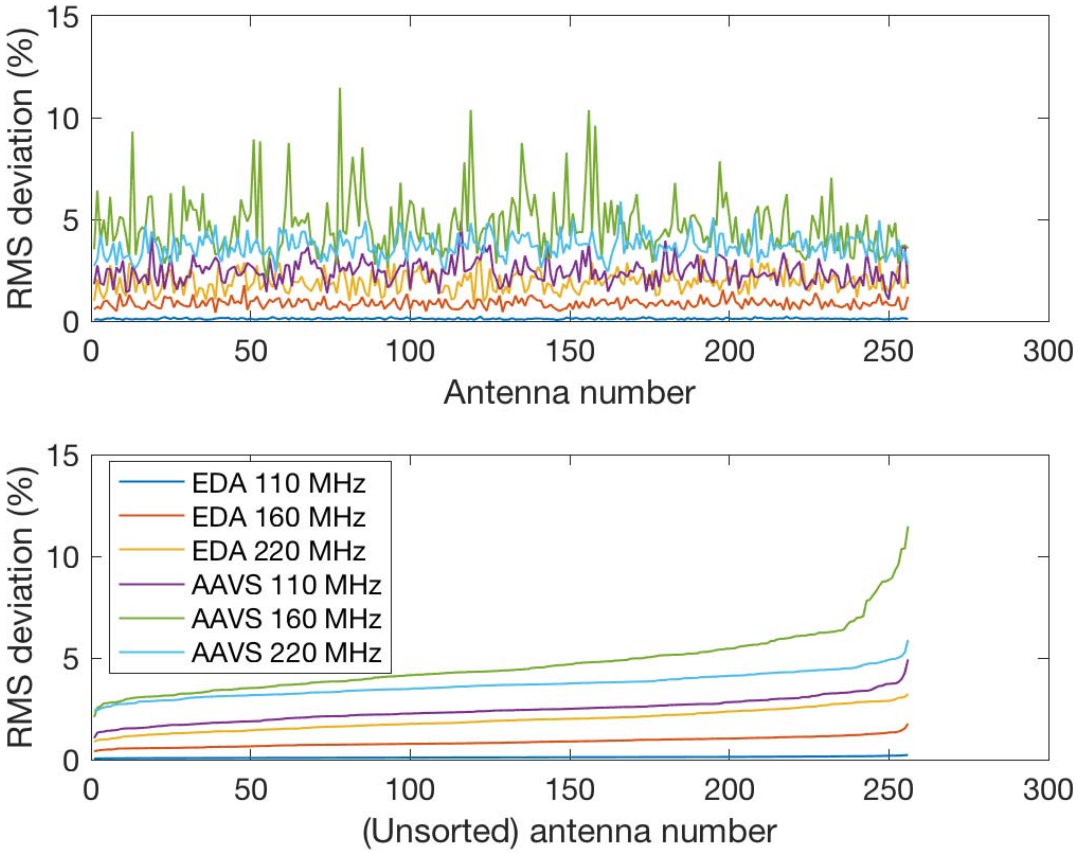

Figure 19: An analysis of the RMS deviation of embedded element patterns from average element patterns for two arrays. The top figure shows the RMS deviation per antenna number; the lower figure the same information, but with this sorted from smallest to largest. The legend is the same in both figures.

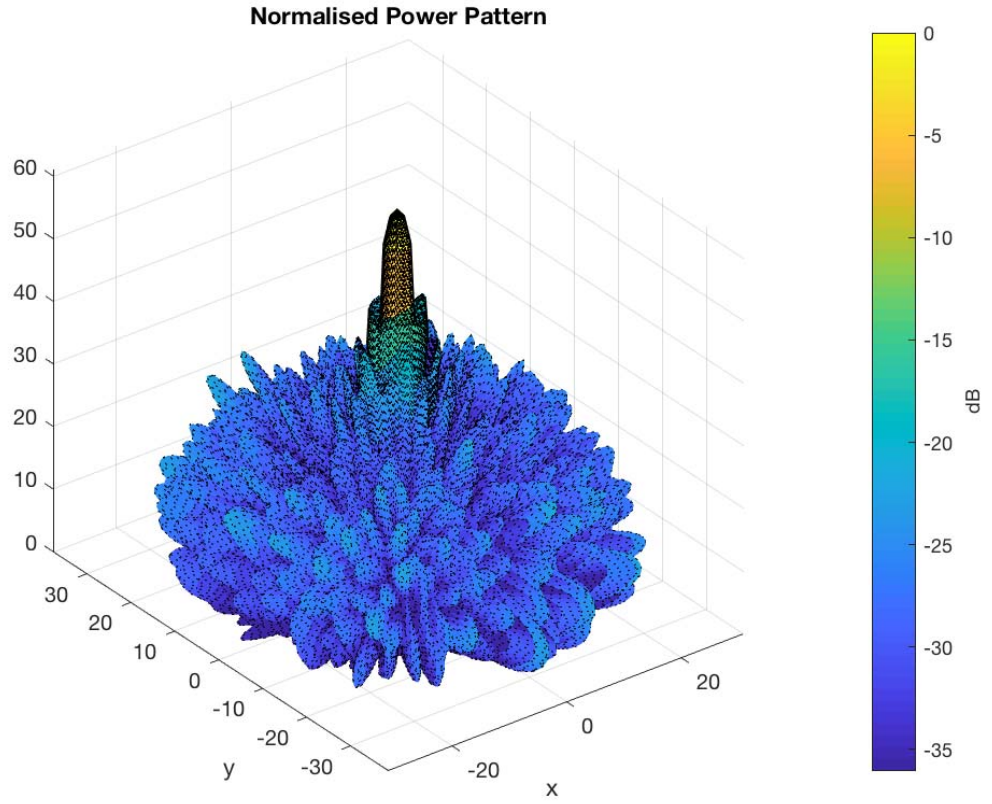

Figure 20: AAVS station pattern, 160 MHz, zenith pointing.

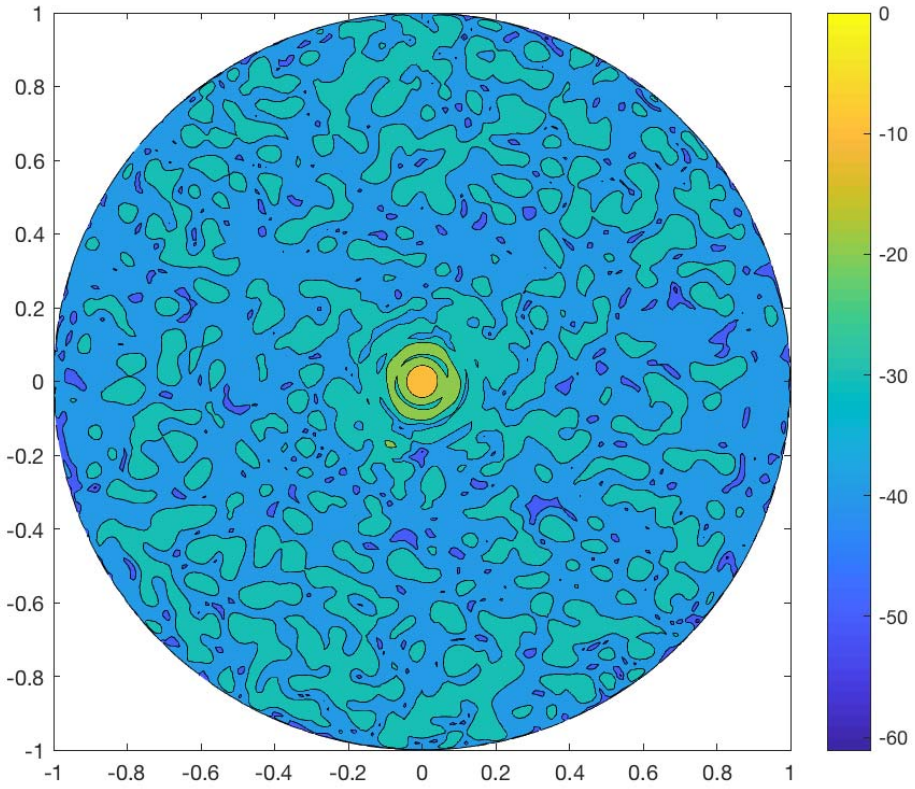

Figure 21: A contour plot of the same beam.

4.5 Further AAVS calibration results: frequency dependence of antenna-based phase

4.5.1 Background

During September 2018, AAVS was run in a mode whereby short dumps (approximately 2 seconds) of correlated data, for each coarse channel over the full frequency band between 0 and 400 MHz, were written to disk at the start of each hour. This procedure was run over several days.

These datasets are representative of what is envisioned to be available to the LFAA LMC/station calibration system during normal operations, where each station is calibrated with an approximate 10 minute cadence.

The goal of this investigation is to build an understanding of the important physical parameters that will be required for a station calibration model.

4.5.2 Data processing

This initial investigation only used daytime data between roughly 9am and 3pm local time, so that the Sun could be used as a calibration source, and the data processing was simplified.

The high-level processing steps consist of, for each coarse channel data file:

- Converting the raw data to uvfits files, including phasing the data towards the sun after extracting relevant time/frequency info
- Loading the data into miriad and splitting the XX and YY data into separate units
- Performing self-calibration with the sun as a 100000 Jy source at the phase centre using antenna 2 as the reference, excluding baselines shorter than 5 wavelengths
- Extracting the calibration solutions and inserting them into the AAVS calibration database

This basic procedure is very similar to that used in previous AAVS data processing where the Sun was used as a strong compact source. Note that by September when these data were taken, the Sun is at RA approximately 12 hours, and the Galactic Centre rises in the second half of the day. This makes the assumption that the sun is a dominant source potentially invalid during the latter part of the day.

4.5.3 Data extraction and results

Data from all coarse channels within the ~10 minute calibration window were associated as a single calibration solution and examined for all antennas. An example of the antenna phase solutions for a group of 16 antennas is shown in Figure 22. This example is generally indicative of all the solutions and exhibits the following characteristics:

- Phase solutions generally follow a linear phase ramp, consistent with the bulk of uncalibrated phase being due to uncorrected delays in the system (no solution was generated for frequencies below 50 MHz)
- Variations in phase around the linear slope are generally 10 degrees or less (except in problem frequency ranges obviously). At this point it is not clear if the variations are due to antenna or incomplete sky model, but the incomplete sky model is likely to be the cause of the bulk of variation given the Sun's current position in the sky.
- X and Y phase are generally very similar, but there are some exceptions (not shown in the example below are antennas 5, 17, 152, 203)
- Solutions at low frequency (below approximately 100 MHz) and in the known RFI bands do not follow the general pattern, hence are not reliable using this method of calibration
- Most of the solutions have a phase slope that appears to intersect with zero phase at zero Hz, however a small number of solutions (e.g. Ant 40 in the figure below, also Ant 105) appear to have 180 degrees of phase at zero Hz. This would indicate that either the entire trumpet assembly or entire antenna has been rotated by 180 degrees.

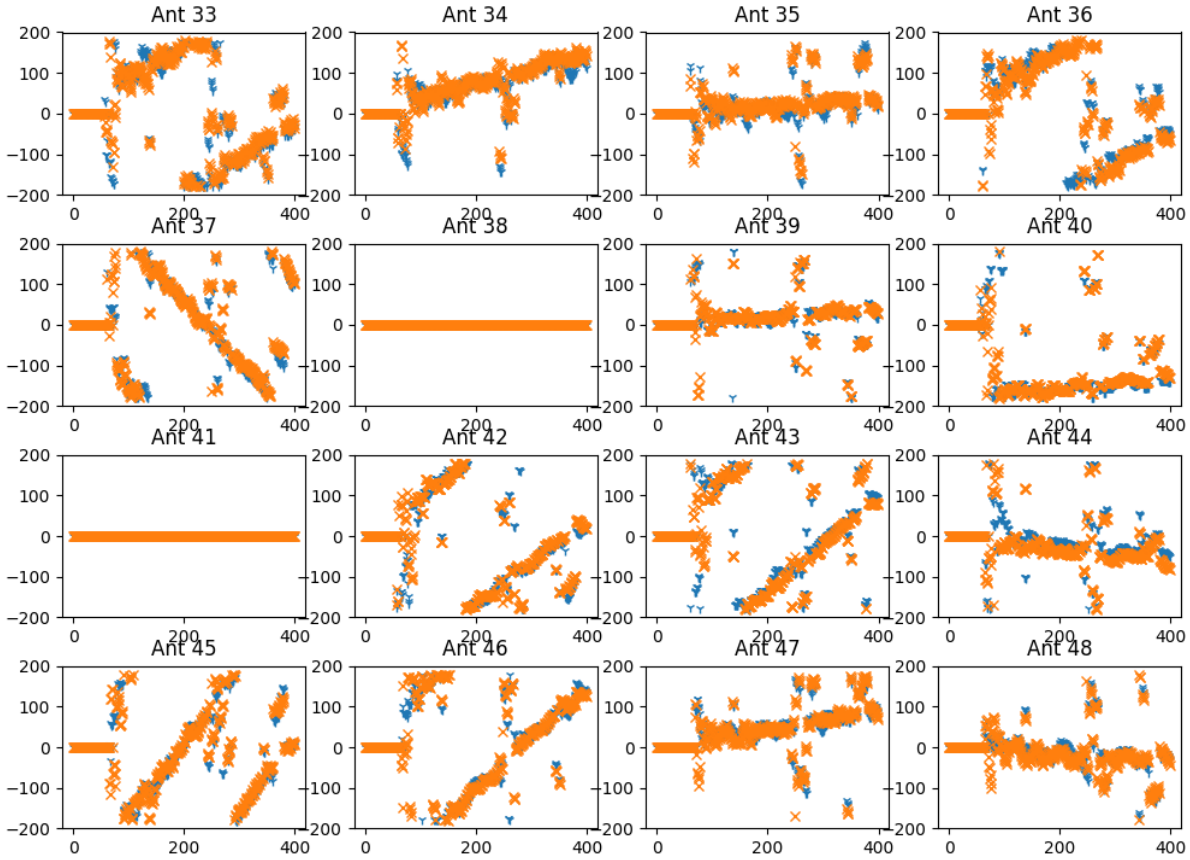

Figure 22: Example antenna phase solutions vs frequency for a group of 16 antennas on 2018_09_18 14:00 AWST.

Generally, the solutions show less than 2 turns of phase over the full 400 MHz, but a small number of antennas (e.g. antennas 240, 254) have 4 turns of phase over the frequency range, corresponding to roughly 3 meters of differential delay, presumably due to cable length differences.

Initial inspection also shows that the solutions do not change significantly within a day.

4.5.4 Conclusions and next steps

Based on this initial inspection of data, we can devise a physically-motivated calibration model for the antennas in a station, based on the following observations:

- The large-scale phase behaviour of the calibration is consistent with a phase ramp that intersects with either 0 or 180 degrees at zero Hz frequency.
- This phase ramp can thus be represented by two numbers for each polarisation, the excess delay, and the zero Hz intercept. (Calibration code may optionally force the intercept to be 0 or 180 degrees.)
- It is therefore not necessary to measure the antenna phase at all frequencies to determine the excess delay, but using a range of frequencies to get a good lever-arm, and to average over small-scale variations, would be appropriate.

Next steps:

- Understand the cause of differential delay between the polarisations on antennas 5, 17, 152, 203. Is this a sign of a problem, or is it to be expected in the real system?
- Solve for the delay for each polarisation for each antenna for each calibration interval and plot the delay solutions vs time.
- Understand if the variation of the phase solution with frequency is due to incomplete sky model or other physical factors

4.6 Towards a station calibration model

The work reported here is currently in progress, and definitive conclusions cannot presently be drawn. Independent work - undertaken in parallel with this work - at ASTRON by S Wijholds [RD38], indicates that an LFAA station comprising SKALA antennas is likely to require calibration on a complete sky model that includes diffuse emission from the Galactic plane, taking into account that the EEPs may be different for different elements (classified as a Class 4 calibration scheme in that work), which echoes the concerns raised in this section. [RD38] is incorporated in this report as Appendix A.1, with very minor edits. Note that the simulation results presented in Appendix A.1 indicate that stations comprising either SKALA2 or SKALA4 antennas exhibit similar calibration behavior, which is to be expected given that both are fundamentally log-periodic antennas, with comparable inter-element spacings.

Another point which has emerged from this work is that OSKAR cannot presently ingest complex EEPs as computed for SKALA2 (and by extension, SKALA4).

These caveats notwithstanding, we have been able to demonstrate calibration using AAVS in correlation mode. It should be re-iterated that the issue is not whether the station can be calibrated, but rather how accurate, stable and computationally costly this calibration procedure will be.

5 Sub-system maturity

The intent of this section it to provide an objective assessment of the maturity of a number of elements of the LFAA design—technical and procedural—that are perceived to be high-risk. Key outcomes and conclusions arising from AAVS are presented along with references to other relevant analyses and reports.

5.1 Antenna system

AAVS has borne out the basic feasibility of a SKA LFAA station. Regarding system risks and maturity, it is important to note firstly, that there are still some unanswered questions relating to full impact of selecting a log-periodic antenna, specifically on the element patterns and of course the station beams. The computational cost associated with simulating the station beams is highlighted below. Initial simulations and calibration results indicate that the SKALA2 (and by extension SKALA4) has fine angular structure in the element patterns, which may require a complex and computationally costly calibration scheme to properly form station beams. The challenges this issue raises for calibration models have been addressed at length in Section 4. Initial data also indicates that the element pattern may be stronger towards the horizon than expected, which raises other issues. Secondly, the marginal electronic stability of the entire SKALA2 RF front-end system has also been discussed.

As well as the electromagnetic performance of the antenna, some non-functional consequences of antenna choice have also been exposed. These are noted in section 5.3 and detailed in [RD7].

5.2 Radio-Frequency over Fibre

The performance of RFoF in the demanding environment of the MRO was a key risk flagged early in the SKA preconstruction phase. The key findings of a number of analyses of the effect of environmental temperature fluctuations on RF performance of the Receiver Front-end are summarised in Appendix A.3.

The combination of lab and MRO based testing and analysis conducted as part of the AAVS program has demonstrated that RFoF is a viable technology for LFAA. It should be noted that the AAVS implementation of the analogue chain, where the trunk fibre carrying the analogue signals between the Field Node and the processing facility is surface laid, represents a worst-case scenario, giving confidence that the implementation that will feature in SKA will be robust. Overall phase calculations were discussed in Section 3.2, supporting this conclusion.

AAVS has addressed one of the critical risks associated with the use of RFoF and thus contributed to the improved maturity of the LFAA design. Another key risk flagged in association with RFoF is longevity in the field environment. This question has been the subject of work in Italy.

5.3 Deployment and installation

The cost and schedule associated with the deployment and installation of the LFAA was flagged as a key risk by the SKA Office early in preconstruction phase. Considerable work

has been invested in demonstrating that these activities can be completed within realistic cost and schedule bounds.

[RD22] and [RD23] present a detailed and highly parameterised deployment plan and costing of the LFAA deployment and installation activities. These documents have been informed and refined by evidence and experience gleaned from the AAVS program, and in turn have informed evolution of the LFAA design from the AAVS implementation.

Among other things, AAVS represents an important transition from small scale, institute-based production and quality control to a regime that is more applicable to SKA. The kinds production, transport, assembly and installation procedures and techniques that will be required for SKA were exercised for the first time. It is not surprising then that a variety of issues emerged.

The deployment, installation and commissioning of AAVS clearly bore out the significant drivers of the LFAA deployment cost and schedule; and identified a variety of issues arising from preliminary activities including procurement, manufacture and transport.

[RD7] documents myriad practical lessons learned through the deployment of AAVS.

The complementary and mutually supporting development of [RD22], [RD23], [RD7] and AAVS have comprehensively addressed the project-level uncertainty associated with LFAA deployment and refined the risk profile associated with it.

5.4 Models and simulations

This section addresses the validity of models and simulations being used to support LFAA maturity assessment(s) based on AAVS measurements and simulations. However, since these are yet to be fully demonstrated on AAVS, the application to LFAA must also be viewed as provisional.

From an electromagnetic modelling viewpoint, the computational simulation methods applied to SKALA2 are equally applicable to SKALA4, but at rather higher computational cost, as discussed below. This has used commercial simulation codes, in particular using the method of moments. As such, the methods applied to element and station beam simulation, documented in RD4, can equally be applied to LFAA using SKALA4. Additionally, the validation performed on numerical models of AAVS0.5 (which used a pre-SKALA2 version of the antenna) provided excellent agreement for the main lobe of the element pattern as reported in RD9, although the sidelobes showed more variation.

As computational electromagnetic simulation plays an important role here, the following should be noted. Whilst the full 256 element AAVS station can also be simulated, the 16-fold increase in element numbers from AAVS0.5 to AAVS results in a very much larger computational problem. The method of moments simulation algorithm in its basic form scales as the third power of problem size; more advanced versions of the algorithm have better scaling properties but are still computationally expensive. Similar comments apply to other computational methods, such as the finite difference time domain method; the scaling properties with problem size differ but are not fundamentally better.

It should also be noted that limitations of the computational model (in particular, the challenges involved with incorporating both the finite ground plane and the real ground) may result in uncertainties regarding element patterns towards the horizon. This is so for both SKALA2 and SKALA4 elements (ie both AAVS and an LFAA station). Initial data processed from AAVS indicates that the element pattern does indeed not cut off a sharply as intended in this direction.

Clearly, many aspects of LFAA which involve multiple stations cannot be tested on the single LFAA station as deployed.

5.5 Radio Frequency Interference

All equipment deployed to the MRO must comply with the extant MRO radio-frequency emission management regime. The emission limits applicable under this regime are provided in [RD11]. All equipment fielded as part of the AAVS program was subjected to pre-deployment testing to ensure compliance with these standards.

The existing MRO RFI emission limits are not as demanding as those specified in [RD12] for SKA_LOW and as such equipment that is compliant with the current regime will not necessarily be so under the SKA regime. However, the emission characteristics and effectiveness of the mitigations applied for AAVS equipment provide an indication of the feasibility of meeting the SKA requirement(s). This is further addressed in Section A.6.

[RD40] provides an extensive set of radiated and conducted emission tests for the APIU. For the case of radiated emissions in the lower measurement bands (20-200 MHB and 200-600 MHz), the synchronous rectifier did not meet the relevant MIL-SDT-4621F standard, and 20dB of shielding was recommended. An example, measured under full load conditions, is shown in Figure 23. (This is Fig 8 in [RD40]; note that this used same antenna over the full band, and as such it is not a true MIL-STD-461F measurement, which is given in Appendix A.6). In [RD41], a number of COTS power supplies were measured for EMC compliance for LFAA, with similar findings. That report also provides details of average shielding effectiveness for a pre-qualified shielding solution.

EMC compliance for the TPM is addressed in [RD42]. Since the TPM is installed in the MRO control room, the limits are less stringent, as discussed in Section A.6.

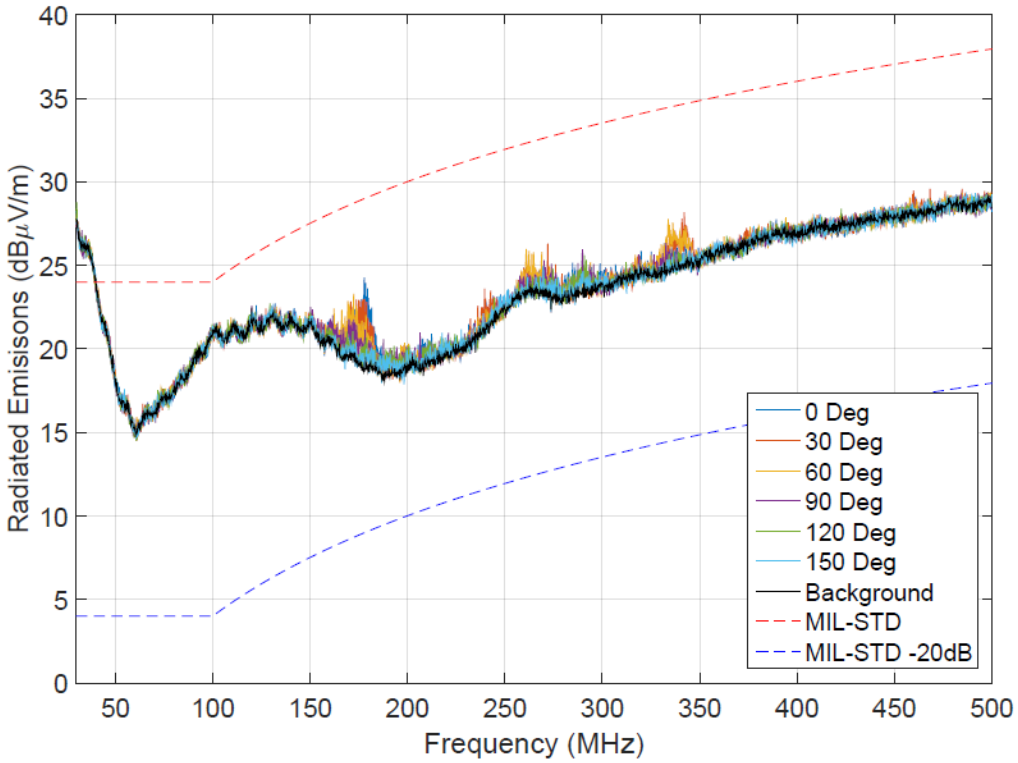

Figure 23: Radiated emissions results from 30-500 MHz for full load conditions. Orientations are from 0° to 150° degrees in 30 degree increments. The background trace, Mil-Std and Mil-Std minus 20 dB are shown as black, red and blue traces respectively.

6 Progress towards compliance

Note: the L2 specifications listed below were originally exported from JAMA 2018-06-25, updated as per 2018-09-40 export, and updated again 2018-09-12. Two particularly relevant specifications (SKA1-LFAA-106 and SKA1-LFAA-133) were updated further following feedback from SKAO to align with the baseline as of 2018-10-31; also at the same time, SKA1-LFAA-228 was added.

ID	Requirement	Description	Verification	Allocation
SKA-LFAA-XXX	Requirement short name	Requirement description	Prescribed verification method	L3 internal allocation (not definitive - refer to JAMA).
Requirement validation		This fields comments on/discussed the requirement itself. This is the place to record concerns related to the interpretation, intent, provenance etc of the requirement, strictly constrained to objective statements of issue/concerns.		
L2 compliance impact		Section 1 makes it clear that AAVS is a demonstration/test system applicable at the single station level only. This field should briefly state how the demonstration system test(s) does/does not and/or can/cannot contribute to **compliance at L2** (LFAA).		
Current compliance status		This field should start with a standard compliance classification (Compliant, Partially-compliant, Non-compliant); followed by should a short statement/summary of the Current compliance status of the requirement at the **individual station level**. Cross-reference the analysis contained in the appendix as appropriate.		
Next steps		This field should flow directly from the last. Where 'partial' or 'non' compliance is stated in the previous field, this field should start with a statement as to whether further work will/could lead to compliance or not. Where it is likely that compliance will/could be demonstrated with further work, that work should be briefly outlined here. This should include discussion about extrapolation/extension to L2 (LFAA) compliance.		

Comments and recommendations		Use this field to document any concluding statements and/or recommendations. In particular, this is where we include commentary on the relevance and criticality of each requirement at CDR.		
SKA1-FLD-4241	Telescope			
SKA1-FLD-4251	Configuration and performance			
SKA1-LFAA-103	Receptor type	The LFAA shall be implemented with dual, orthogonally polarised antenna elements.	Analysis	LFAA.FN
Requirement validation		The SKALA2 and SKALA4 elements are both compliant.		
L2 compliance impact		AAVS used the SKALA2 element, rather than the current SKALA4.		
Current compliance status		Compliant		
Next steps				
Comments and recommendations		The choice of element was specified in the requirement.		
SKA1-LFAA-104	Antenna spacing	The average spacing between antenna elements within a Field Station shall be the same for each of the LFAA Field Stations.	Inspection	LFAA.FN
Requirement validation				
L2 compliance impact		As AAVS consists of one FN only, AAVS cannot contribute to L2 compliance on this requirement.		
Current compliance status		Not compliant		
Next steps		This can only be evaluated on a larger prototype or on the full system.		
Comments and recommendations				
SKA1-LFAA-105	Normalisation of station gains	The LFAA shall match station beam power as a function of frequency across stations within a margin of TBD %.	Analysis	LFAA.MCCS
Requirement validation		AAVS can inform this requirement, via station- level simulations and measurements.		
L2 compliance impact		As AAVS consists of one FN only, AAVS can only contribute partially to L2 compliance on this requirement.		
Current compliance status		Partially compliant		
Next steps		Full validation requires at least an array-level simulation		

Comments and recommendations		This specification was changed substantively on 05/09/2018.		
SKA1-LFAA-106	Station beam bandpass stability	On a maximum time scale of 600 seconds, and within the envelope of the listed spline points with TBD frequency smoothness, SKA1_Low shall have a station beam bandpass stability, post calibration and RFI mitigation, of · 0.05 % at 50 MHz · 0.02 % at 110 MHz · 0.03 % at 160 MHz · 0.03 % at 220 MHz · 0.05 % at 280 MHz · 0.08 % at 350 MHz compared to the full polarization parameterized beam model.	Test	LFAA.FN, LFAA.SPS, LFAA.MCCS
Requirement validation		This requirement has been substantially updated following input.		
L2 compliance impact		AAVS is in a good position to contribute to this, since it is a specification at station level.		
Current compliance status		Unknown		
Next steps		Both analysis and test work on the calibration of AAVS should proceed.		
Comments and recommendations		This is a key specification, correctly posed after the July 2018 bridging meeting in Manchester. (As noted, this was updated to the 2018-10-31 baseline, following input from SKAO).		
SKA1-LFAA-107	Beam pointing angle range	The LFAA shall accept commands to steer and form beams at all possible azimuth and elevation angles.	Test	LFAA.MCCS, LFAA.SPS
Requirement validation		This requirement is supported by design in the LFAA station digital systems.		
L2 compliance impact		It can be verified at the station level by pointing a station beam on a strong source at various elevation/azimuthal angles and checking the station beam power levels compared to "cold sky".		
Current compliance status		Not yet tested on AAVS. Station beamforming for LFAA is still a WIP.		
Next steps		Work is ongoing to verify the AAVS1 station beam.		
Comments and recommendations				

SKA1-LFAA-108	Support for sub-stations	The LFAA shall be configurable for the control and monitoring of up to 2048 sub-stations, configured within the limits set out in section 5.7.1 of [AD18]. Representative cases include but are not limited to the following (see document for further explanation: a. 1024 sub-stations randomly distributed within field nodes. i. Stations are populated with 4 randomly-located sub-stations in the core and 4 randomly-located sub-stations in one of the 6 field nodes at each cluster location. ii. 75 MHz of bandwidth is available. b. 1024 sub-stations regularly distributed within field nodes. i. Stations are populated with 6 sub-stations in the core and 4 sub-stations in one of the 6 field nodes at each cluster location. ii. 75 MHz of bandwidth is available c. 2048 sub-stations randomly distributed within field nodes. i. Stations are populated with 4 randomly located sub-stations in all of the 512 field nodes. ii. 19 MHz of bandwidth is available. d. 2048 sub-stations regularly distributed within field nodes.	Test	LFAA.MCCS, LFAA.SPS

		i. Stations are populated with 6 sub-stations in the core and 6 sub-stations in 3 of the 6 field nodes at each cluster location. ii. 19 MHz of bandwidth is available."		
Requirement validation		The requirement is clear, but can only be tested on the full system, or a substantial part thereof.		
L2 compliance impact		As a full system level specification, AAVS cannot address this at station level.		
Current compliance status		Cannot be fully verified with AAVS1. As above, this is a overall SKA1_Low requirement, and station level tests are of limited utility.		
Next steps		Key advances in support of this will be testing multiple beams.		
Comments and recommendations				
SKA1-LFAA-109	Sub-station beams	The LFAA, when commanded, shall form dual polarisation beams from up to six sub-stations for any station.	Test	LFAA.SPS, LFAA.MCCS
Requirement validation		This is closely linked to SKA1-LFAA-108, with the additional requirement of forming dual polarized beams.		
L2 compliance impact		This is dependent on the firmware available for AAVS.		
Current compliance status		Cannot be fully verified with AAVS1		
Next steps		Testing at station level via AAVS, provided the firmware permits this.		
Comments and recommendations				
SKA1-LFAA-110	Cross polarisation purity	The LFAA intrinsic cross polarisation ratio shall be at least 15 dB over the whole observing band within the half power beam width up to observing angles of 45 degrees from the zenith.	Test	LFAA.FN, LFAA.SPS, LFAA.MCCS
Requirement validation				
L2 compliance impact				
Current compliance status		Not known.		
Next steps		We are working on AAVS1 simulation at 160, 110, 220, 50, 300 MHz. Each frequency point takes 2-3 days. We will produce intrinsic cross-pol. ratio plots at certain example pointings at those freqs.		

Comments and recommendations				
SKA1-LFAA-111	Array sensitivity	Assuming a sky noise temperature defined in the definitions section of the system requirements specification document [AD1], the LFAA shall have sensitivity per polarisation at zenith corresponding to the following values interpolated by a 'not-a-knot' cubic spline function and not deviating by more than ±5% from the spline interpolation spanning the following points: a. 68 m 2 K -1 at 50 MHz b. 70 m 2 K -1 at 55 MHz c. 232 m 2 K -1 at 80 MHz d. 531 m 2 K -1 at 110 MHz e. 588 m 2 K -1 at 140 MHz f. 610 m 2 K -1 at 160 MHz g. 614 m 2 K -1 at 220 MHz h. 576m 2 K -1 at 280 MHz i. 522 m 2 K -1 at 340 MHz j. 515 m 2 K -1 at 345 MHz k. 516 m 2 K -1 at 350 MHz	Analysis	LFAA.FN, LFAA. SPS
Requirement validation				
L2 compliance impact				
Current compliance status		Cannot be verified with AAVS1		
Next steps				
Comments and recommendations				
SKA1-LFAA-112	Sensitivity for off zenith angles	The sensitivity of the LFAA shall not degrade by more than 30% at local elevation angle of 60 degrees and not by more than 50% at local elevation angle of 45 degrees for all local azimuthal angles between 0 and 360 degrees, compared to the peak sensitivity at zenith.	Test	LFAA.FN, LFAA.SPS
Requirement validation				
L2 compliance impact				

Current compliance status		Not known. This can potentially be tested on AAVS, depending on firmware.		
Next steps				
Comments and recommendations				
SKA1-LFAA-113	Distribution of collecting area within field nodes	Placement of antennas within each field node shall be independently randomised in two dimensions (within the constraints of antenna and station size) so as not to form a regular grid.	Analysis, Inspection	LFAA.FN
Requirement validation		AAVS1 has a pseudo-random antenna distribution within the station. This requirement is at array level, however, and cannot be addressed by AAVS1 except to say that pseudo-random layouts are feasible.		
L2 compliance impact				
Current compliance status		Compliant		
Next steps		N/A		
Comments and recommendations				
SKA1-LFAA-114	Alignment of antennas	Polarisations of antenna elements should be aligned for all the antennas, with the following tolerances: - between antennas belonging to the same Field Node: TBD - between antenna elements belonging to different Field Nodes: TBD.	Inspection	LFAA.FN
Requirement validation		Specifications are TBD, so this cannot be quantified. AAVS1 antennas are bolted to concrete bases, which in turn are aligned to the wire ground mesh. The mesh was laid down using survey equipment to align it to the cardinal directions with sub-degree precision. The overall alignment uncertainty is estimated to be approximately 1 degree.		
L2 compliance impact				
Current compliance status		Not possible to comply with TBD requirement		
Next steps				
Comments and recommendations				
SKA1-LFAA-115	Antennas per field node	Each field node shall be populated with 256 antennas.	Analysis	LFAA.FN
Requirement validation		This is a specified requirement. Verification is by inspection. AAVS1 has 256 antenna pads, although two were not populated.		

L2 compliance impact				
Current compliance status		Compliant		
Next steps				
Comments and recommendations				
SKA1-LFAA-116	Field Station diameter	Each Field Station shall have a maximum "Effective Station Diameter" as defined in [AD8] of 38 metres.	Inspection	LFAA.FN
Requirement validation		AAVS1 was deployed with maximum distance between centres of antennas to be 35 metres. The groundscreen is larger to accommodate longer wavelengths.		
L2 compliance impact				
Current compliance status		AAVS was compliant with the original specification. LFAA will deploy a larger field station for LFAA.		
Next steps				
Comments and recommendations				
SKA1-LFAA-117	Ground plane diameter	The "Ground-plane Station diameter" as defined in [AD8] shall be 42mt (-0+1mt).	Inspection	LFAA.FN
Requirement validation				
L2 compliance impact				
Current compliance status		As for LFAA-116.		
Next steps				
Comments and recommendations				
SKA1-LFAA-118	Number of stations	LFAA shall be composed of 512 stations	Inspection	LFAA.FN, LFAA.MCCS, LFAA.SPS
Requirement validation		Not relevant to AAVS1		
L2 compliance impact				
Current compliance status		Cannot be verified with AAVS1		
Next steps				

Comments and recommendations				
SKA1-LFAA-119	Field node coordinates	The coordinates of the LFAA field node centers shall be as specified in the SKA1_Low Configuration coordinates document [AD8]	Inspection	LFAA.FN
Requirement validation		Not relevant to AAVS1		
L2 compliance impact				
Current compliance status		Cannot be verified with AAVS1		
Next steps				
Comments and recommendations				
SKA1-LFAA-120	Antenna coordinates	The coordinates of the antennas and equipment of each Field Station centers shall be as specified in the TBD [TBD]	Inspection	LFAA.FN
Requirement validation		AAVS1 has demonstrated that antennas can be deployed with cm level precision using standard surveying tools and techniques.		
L2 compliance impact		Based on the observing frequencies, accuracy better than 1cm is not required for placement of dipoles in a station.		
Current compliance status		Likely to be compliant		
Next steps				
Comments and recommendations				
SKA1-LFAA-121	Station identification	Each station of the LFAA shall be uniquely identifiable. This will include both the identity of the cluster and the individual station as defined in SKA-TEL-SKO-0000422 SKA1_Low Configuration Co-ordinates document [AD8]. The identification shall be according to the Identification and Marking Standard document (number TBD).	Inspection	LFAA.FN, LFAA.MCCS, LFAA.SPS
Requirement validation		AAVS1 antenna bases were uniquely labelled and this could be carried in to LFAA. However, at station level,this is not relevant to AAVS1.		
L2 compliance impact				
Current compliance status		Cannot be verified with AAVS1		
Next steps				
Comments and recommendations				

SKA1-LFAA-122	Maximum baseline length between stations	The maximum distance between station centres shall be 65 km.	Inspection	LFAA.FN
Requirement validation		Not relevant for AAVS1		
L2 compliance impact				
Current compliance status		Will be compliant		
Next steps				
Comments and recommendations				
SKA1-LFAA-123	Instantaneous bandwidth	LFAA, when commanded by the telescope manager, TM, shall process 300 MHz of aggregate bandwidth per polarisation for a given observation period or until commanded to stop.	Test	LFAA.FN, LFAA.SPS, LFAA.MCCS
Requirement validation		LFAA/AAVS1 digital systems meet this requirement by design.		
L2 compliance impact				
Current compliance status		Compliant, station beamforming tests still in progress		
Next steps				
Comments and recommendations				
SKA1-LFAA-124	Digitisation	Digitisation of LFAA antenna signals shall be to at least 7.8 ENOB (equivalent number of bits).	Demonstration	LFAA.SPS
Requirement validation		Digital systems in AAVS1/LFAA meet this requirement by design. Data generated by the station beamfomer is 8 bits real+imag.		
L2 compliance impact				
Current compliance status		Compliant		
Next steps				
Comments and recommendations				

SKA1-LFAA-125	Clipping	The amplitude dynamic range of the system shall be such that the system remains linear according to the linearity requirement for the 95% percentile of the RFI use cases as provided by the SKAO (see [RDxx])	Test	LFAA.FN, LFAA.SPS
Requirement validation		RFI handling specifications are still being reviewed at the system level. At the station level, the clipping behaviour of the digital hardware is fully controllable by adjusting the analogue and digital gains within the system.		
L2 compliance impact				
Current compliance status		Compliant by flexibility and adjustability of analogue and digital design		
Next steps		This is verifiable with AAVS1 in the future		
Comments and recommendations				
SKA1-LFAA-126	Clipped data flagging	LFAA shall flag saturated data within the data stream.	Demonstration	LFAA.SPS
Requirement validation		The method of flagging bad/clipped data is still being finalised at the system level.		
L2 compliance impact		This is a firmware change in the future. Low risk.		
Current compliance status		Not currently implemented but potentially testable in the future with AAVS1		
Next steps				
Comments and recommendations				
SKA1-LFAA-127	Linearity	The level of spurious products generated by LFAA, in the presence of signals representative of the expected RFI [AD9] environment shall not degrade the expected thermal noise floor by more than 10% over an integration period of 1000 hours.	Analysis	LFAA.FN, LFAA.SPS
Requirement validation		This is a system level requirement and cannot be directly verified by AAVS1.		
L2 compliance impact				
Current compliance status		Cannot be verified with AAVS1		
Next steps				
Comments and recommendations				

SKA1-LFAA-128	Direct sun observation	The response of LFAA shall be linear when the sun is in the antennas field of view, for solar activity up to TBD times the quiet sun emission in the SKA-LOW band.	Test	LFAA.FN, LFAA.SPS
Requirement validation		This is a system level requirement and cannot be directly verified by AAVS1, although AAVS1 could inform this.		
L2 compliance impact				
Current compliance status		Cannot be verified with AAVS1		
Next steps				
Comments and recommendations				
SKA1-LFAA-129	Polarisation dynamic range - Imaging	The system shall provide a 45 dB polarisation dynamic range for imaging, after calibration, at all spatial and at all fractional bandwidths across the full band.	Analysis	LFAA.SPS
Requirement validation		This is a system level requirement and cannot be directly verified by AAVS1.		
L2 compliance impact				
Current compliance status		Cannot be verified with AAVS1		
Next steps				
Comments and recommendations				
SKA1-LFAA-130	Polarisation dynamic range - Pulsar Search	The system, when performing calibration imaging in support of Pulsar Search, shall provide better than 25 dB polarisation dynamic range for the configured bandwidth.	Test	LFAA.DS
Requirement validation		This is a system level requirement and cannot be directly verified by AAVS1.		
L2 compliance impact				
Current compliance status		Cannot be verified with AAVS1		
Next steps				
Comments and recommendations				

<table>
<tr><td>SKA1-LFAA-131</td><td>Polarisation dynamic range - Pulsar Timing</td><td>The system, when performing Pulsar Timing, shall provide better than 40 dB polarisation dynamic range across each Pulsar Timing tied array at their bore sight for the configured bandwidth/ time resolution. This implies 40 dB out to the half power bandwidth (HPBW) for the station primary beam as a pulsar timing tied array beam can be located anywhere in that area.</td><td>Test</td><td>LFAA.SPS, LFAA.MCCS</td></tr>
<tr><td colspan="2">Requirement validation</td><td colspan="3">This is a system level requirement and cannot be directly verified by AAVS1.</td></tr>
<tr><td colspan="2">L2 compliance impact</td><td colspan="3"></td></tr>
<tr><td colspan="2">Current compliance status</td><td colspan="3">Cannot be verified with AAVS1</td></tr>
<tr><td colspan="2">Next steps</td><td colspan="3"></td></tr>
<tr><td colspan="2">Comments and recommendations</td><td colspan="3"></td></tr>
<tr><td>SKA1-LFAA-132</td><td>Brightness dynamic range</td><td>The brightness dynamic range of the LFAA shall be at least 50 dB for a spatial resolution of 300 arcsec and 1 MHz spectral resolution.</td><td>Test</td><td>LFAA.FN, LFAA.SPS, LFAA.MCCS</td></tr>
<tr><td colspan="2">Requirement validation</td><td colspan="3">This is a system level requirement and cannot be directly verified by AAVS1.</td></tr>
<tr><td colspan="2">L2 compliance impact</td><td colspan="3"></td></tr>
<tr><td colspan="2">Current compliance status</td><td colspan="3">Cannot be verified with AAVS1</td></tr>
<tr><td colspan="2">Next steps</td><td colspan="3"></td></tr>
<tr><td colspan="2">Comments and recommendations</td><td colspan="3"></td></tr>
<tr><td>SKA1-FLD-4252</td><td>Station beamforming</td><td></td><td></td><td></td></tr>
<tr><td>SKA1-LFAA-133</td><td>Receive path stability</td><td>The receive paths (all analog electronics from antenna to ADC) shall have RMS amplitude variations and RMS phase variations over a 600 second interval better than:
<table>
<tr><td>Frequency (MHz)</td><td>50</td><td>80</td><td>110</td><td>160</td><td>220</td><td>280</td><td>340</td><td>350</td></tr>
</table>
</td><td>Test</td><td>LFAA.FN, LFAA.SPS, LFAA.MCCS</td></tr>
</table>

		Constr. Rel. gain tolerance RX path (%)	8.45	4.68	3.18	4.78	7.76	12.36	14	14	
		RMS amplitude tolerance (dB)	0.70	0.39	0.27	0.40	0.64	1.00	1.15	1.15	
		RMS phase tolerance (deg)	4.85	2.68	1.82	2.74	4.46	7.13	8.1	8.1	
Requirement validation		As originally specified ("Station beam spatial stability"), this should have been assigned to the CSP consortium. This was confirmed at the July 2018 bridging meeting. This has now been updated to the above specification on receive path stability (as of 2018-10-31 baseline).									
L2 compliance impact		Given that AAVS used surface laid cable, using buried cable should substantially improve receive path stability (at least as a result of temperature).									
Current compliance status		AAVS is marginally compliant as regards of phase tolerance (at 160 MHz).									
Next steps		Evaluate compliance across the frequency band.									
Comments and recommendations		Refer to Section 3.2.									
SKA1-LFAA-134	Multi-beam capability	LFAA shall control and monitor up to 8 beams (dual polarization) from each station within a sub-array, which can be independently and individually pointed.							Test	LFAA.SPS, LFAA.MCS S	
Requirement validation		Functionality provided by digital firmware.									
L2 compliance impact											
Current compliance status		Not yet tested									
Next steps											
Comments and recommendations											

SKA1-LFAA-135	Beam pointing accuracy	LFAA shall steer each station beam independently in both azimuth and elevation with an accuracy of better than 1/1000 of the half power beam width, for source velocities up to TBD times the sidereal rate.	Demonstration	LFAA.SPS, LFAA.MCCS
Requirement validation		AAVS1 cannot verify pointing accuracy to 1/1000 of the FWHM.		
L2 compliance impact				
Current compliance status		Unknown.		
Next steps				
Comments and recommendations				
SKA1-LFAA-136	Multiple beam widths	LFAA shall control and monitor beams that have different frequency and channel selections independent of each other (where independence allows identical, overlapping or non-overlapping). The independence allows each of one of the beams to have a non-contiguous bandwidth.	Demonstration	LFAA.SPS, LFAA.MCSS
Requirement validation		Functionality provided by digital firmware.		
L2 compliance impact				
Current compliance status		Not yet tested		
Next steps				
Comments and recommendations				
SKA1-LFAA-137	Synchronous Time Stamping	Each station beam shall provide to the correlator-beamformer a data block time stamps, synchronous with and locked to the sample clock and deterministically related to 1PPS, within the accuracy of the 1PPS distribution.	Test	LFAA.SPS, LFAA.MCSS
Requirement validation		This is a system-level specification.		
L2 compliance impact				
Current compliance status		Cannot be verified with AAVS1		
Next steps				
Comments and recommendations				

SKA1-FLD-4253	Correlation			
SKA1-LFAA-138	Autocorrelation spectra	For all stations belonging to a given subarray, LFAA shall deliver data in order for SKA1-Low to deliver full-polarisation auto-correlated spectra, with frequency coverage, spectral resolution, and spectral and temporal response matching that of the cross-correlation spectra from that sub-array.	Demonstration	LFAA.SPS, LFSS.MCCS
Requirement validation		This requirement is not clear, but appears to be a CSP requirement not an LFAA requirement. The station beams from LFAA can be processed by CSP to meet this requirement.		
L2 compliance impact				
Current compliance status		Not applicable to AAVS1		
Next steps				
Comments and recommendations				
SKA1-LFAA-139	Channelisation transition band for adjacent frequency channels	The transition band between the LFAA coarse frequency channels shall be monotonically decreasing starting from the coarse channel edge plus 1/128th of a coarse channel, to -60 dB or better at the nominal coarse channel edge as aliased in the oversampled channelizer.	Test	LFAA.SPS
Requirement validation		This can be validated in the laboratory; AAVS1 is not needed for this.		
L2 compliance impact				
Current compliance status		Not known.		
Next steps				
Comments and recommendations				
SKA1-LFAA-140	Channelisation maximum leakage for non-adjacent	The upper envelope of the power of noise leaking for non-adjacent coarse frequency channels shall fall off as 1/f or better as a function of frequency offset from the centre of a given frequency channel, for frequency offsets from one coarse channel up to half the input bandwidth.	Test	LFAA.SPS

	frequency channels			
Requirement validation		As for LFAA-139		
L2 compliance impact				
Current compliance status		Not known.		
Next steps				
Comments and recommendations				
SKA1-LFAA-141	Channelisation frequency channel amplitude response	The amplitude response of the LFAA telescope shall have a spectral slope of less than 0.005 dB per imaging zoom frequency channel across each LFAA channel passband. This includes the uncalibrated amplitude gain response in the analog chain and the frequency response of the LFAA channelizer. If the response interests more than one imaging zoom channel (overlapping region) the requirement applies to the sum of the power responses of the overlapping channels.	Test	LFAA.FN, LFAA.SPS, LFAA.MCCS
Requirement validation		This is an array-level requirement for SDP.		
L2 compliance impact				
Current compliance status		Cannot be verified with AAVS1		
Next steps				
Comments and recommendations				
SKA1-LFAA-142	Channelisation configuration	LFAA shall produce station and sub-station beams, as commanded, to allow the rest of the SKA1_Low telescope to produce for each sub-array correlated visibilities and auto correlations for all polarization products, at either the full bandwidth resolution or a higher spectral resolution over limited bandwidth in accordance with the configuration definition.	Dem	LFAA.SPS
Requirement validation		This is a duplication of the sub-arraying requirement at the station level.		
L2 compliance impact				
Current compliance status		Cannot be verified with AAVS1		

	Next steps			
	Comments and recommendations			
SKA1-LFAA-144	Zoom window noise leakage power	The maximum noise leaked from a non-adjacent channel into SKA1_Low zoom window channels from all frequencies outside the window shall be less than 60 dB.	Test	LFAA.SPS
	Requirement validation	This should be a CSP requirement, not LFAA.		
	L2 compliance impact			
	Current compliance status	N/A – this should not be an LFAA specification.		
	Next steps			
	Comments and recommendations			
SKA1-LFAA-145	Overlapped window amplitude response	The SKA1_Low post-calibration amplitude response variation across the full (concatenated) frequency range covered by overlapped zoom windows of the same frequency resolution shall be within +/-0.01 dB of the nominal.	Test	LFAA.SPS
	Requirement validation	This is an SDP requirement. If no error budget has been assigned to LFAA for this, then it is a duplicate of the station beam calibration requirement.		
	L2 compliance impact			
	Current compliance status	N/A – this should not be an LFAA specification.		
	Next steps			
	Comments and recommendations			
SKA1-FLD-4254	Tied array or Pulsars, transients and VLBI			
SKA1-LFAA-148	Absolute timing time stamping	For critical timing and dynamic spectrum measurements, the LFAA shall time stamp each station beam with an accuracy of 1.5 ns (1σ) referenced to the common delay centre of the SKA1_Low.	Dem	LFAA.SPS
	Requirement validation	This is an array-level requirement.		

L2 compliance impact				
Current compliance status		Cannot be verified with AAVS1		
Next steps				
Comments and recommendations				
SKA1-LFAA-150	Transient buffer	LFAA, when configured, shall store digitized beamformed voltage data, with 2-bit or better sampling, for at least 150 MHz of continuous or non-continuous frequency range within the observed frequency range, in both polarizations, from a configurable subset up to all of the station/sub-station beams, covering at least 900 seconds.	Dem	LFAA.SPS, MCCS
Requirement validation		This is an array-level requirement.		
L2 compliance impact				
Current compliance status		Cannot be verified with AAVS1		
Next steps				
Comments and recommendations				
SKA1-LFAA-151	LFAA to CSP latency	The LFAA shall have latency of at most 1 second from the time that a signal arrives at the antenna to the time when the beamformed signal is forwarded to CSP for further processing.	Dem	LFAA.FN, LFAA.SPS, LFAA.MCCS
Requirement validation		This is an array-level requirement.		
L2 compliance impact				
Current compliance status		Cannot be verified with AAVS1		
Next steps				
Comments and recommendations				
SKA1-LFAA-152	Transient buffer transfer	When commanded by TM, LFAA shall transfer transient buffer data to SDP via SADT, independently for each sub-array, and according to the configuration set by TM.	Dem	LFAA.MCCS

Requirement validation		This is an array-level requirement.		
L2 compliance impact				
Current compliance status		Cannot be verified with AAVS1		
Next steps				
Comments and recommendations				
SKA1-LFAA-153	VLBI time stamping	Each SKA1_Low VLBI data sample shall be directly traceable to the time at the common delay centre of the SKA1_Low telescope, with an accuracy of better than 2 nanoseconds (1σ).	Dem	LFAA.SPS, LFAA,MCCS
Requirement validation		This is an array-level requirement.		
L2 compliance impact				
Current compliance status		Cannot be verified with AAVS1		
Next steps				
Comments and recommendations				
SKA1-FLD-4244	Synchronization and Timing			
SKA1-LFAA-100	LFAA coherence losses 1s	The LFAA shall provide a 0.1% maximum coherence loss within a maximum integration period of 1 second and up to an operating frequency of 350 MHz	Test	LFAA.FN, LFAA.SPS
Requirement validation		This is not testable with AAVS1. This requirement can only be verified by analysis.		
L2 compliance impact				
Current compliance status		Cannot be verified with AAVS1		
Next steps				
Comments and recommendations				
SKA1-LFAA-101	LFAA coherence losses 1 minute	The LFAA shall provide a 0.1% maximum coherence loss for interval of 1 minute and up to an operating frequency of 350 MHz	Test	LFAA.FN, LFAA.SPS
Requirement validation		As for SKA1-LFAA-100.		
L2 compliance impact				
Current compliance status		Cannot be verified with AAVS1		

Next steps				
Comments and recommendations				
SKA1-LFAA-102	Network Time Protocol	All client devices and applications that require synchronised telescope network time shall comply with the Network Time Protocol version 4 standard, RFC 5905.	Dem	LFAA.DS
Requirement validation		AAVS LMC servers and all MWA servers are synchronised with observatory NTP system.		
L2 compliance impact				
Current compliance status		Compliant		
Next steps				
Comments and recommendations				
SKA1-FLD-4232	Calibration	This section contains requirements related to calibration.		
SKA1-LFAA-44	SKA1_Low Glass Box Calibration: parameter application	LFAA shall apply calibration correction parameters in a manner that they can be reconstructed.	Dem	LFAA.SPS, LFAA.MCCS
Requirement validation		Calibration parameters are applied as complex gains, one for each antenna, polarisation and coarse channel.		
L2 compliance impact				
Current compliance status		Compliant		
Next steps				
Comments and recommendations				
SKA1-LFAA-45	SKA1_Low Glass Box Calibration: parameter storage	LFAA shall provide necessary information to TM for storage such that calibration correction parameters can be reconstructed.	Dem	LFAA.SPS, LFAA.MCCS
Requirement validation		Calibration parameters are applied as complex gains, one for each antenna, polarisation and coarse channel.		

L2 compliance impact				
Current compliance status		Compliant		
Next steps				
Comments and recommendations				
SKA1-LFAA-47	Calibration transfer	When commanded, changes in frequency, band and/or sources shall not affect the calibrated beams generated by LFAA by more by 0.1% in amplitude or 0.001 radians in phase due to the applying of LFAA specific calibration corrections.	Test	LFAA.SPS, LFAA.MCCS
Requirement validation		This is effectively a duplicate of the bandpass stability requirement and pointing correctness requirement. AAVS1 cannot demonstrate this level of accuracy.		
L2 compliance impact				
Current compliance status		Cannot be verified with AAVS1		
Next steps				
Comments and recommendations				
SKA1-LFAA-48	Global sky model	LFAA shall utilize a Local Sky Model for internal calculations (calibration) which is derived from the SKA-Low Global Sky Model as described in the SDP-LFAA ICD [AD15]	Dem	LFAA.MCCS
Requirement validation		This is a system-level requirement.		
L2 compliance impact				
Current compliance status		Cannot be verified with AAVS1		
Next steps				
Comments and recommendations		The local sky model is extracted from the global sky model which lives within Telescope Manager.		
SKA1-LFAA-49	Calibration update period	LFAA shall provide updated calibration calculations up to once every correlator dump time	Dem	LFAA.SPS
Requirement validation		This requirement is poorly worded. AAVS1 can self-calibrate on timescales that are determined by how often intra-station correlation products are formed.		
L2 compliance impact				
Current compliance status		Compliant		

Next steps				
Comments and recommendations				
SKA1-LFAA-50	Real time calibration	LFAA shall provide on-line station beam calibration functions with an update period of not more than 10 minutes	Dem	LFAA.MCS S
Requirement validation		Not relevant for AAVS1. Station calibration can be performed in these timescales for the full SKA-Low		
L2 compliance impact				
Current compliance status		Cannot be demonstrated with AAVS1		
Next steps				
Comments and recommendations				
SKA1-LFAA-178	Absolute flux density scale	LFAA shall contribute to the calibration of SKA1_Low in order to achieve an absolute flux density scale with an accuracy of better than 5% across the band.	Analysis and Test	LFAA.SPS, LFAA.MCC S
Requirement validation		This is a system-level requirement and ambiguous. Overall flux scale calibration occurs in SDP. The key requirement for LFAA is to have a linear response.		
L2 compliance impact				
Current compliance status		Cannot be verified with AAVS1. AAVS1 analogue gain level are adjusted so that ADCs are run at the target level for good linearity.		
Next steps				
Comments and recommendations				
SKA1-FLD-4242	Observing/operational			
SKA1-FLD-4255	Operational modes			
SKA1-LFAA-154	Mode transition	The LFAA shall complete all internal reconfiguration to support any observing mode changes in less than 30 seconds.	Test	LFAA.MCC S, LFAA.SPS
Requirement validation		This is a system-level requirement.		
L2 compliance impact		Cannot be fully verified with AAVS1.		

Current compliance status		Not yet tested.		
Next steps				
Comments and recommendations				
SKA1-FLD-4256	Sub arrays			
SKA1-LFAA-155	Subarraying	LFAA, when commanded, shall assign station/sub-station resources as independent groups (sub-arrays) that can be configured and operated independently of each other as described in the TM-LFAA ICD [AD7].	Dem, Test	LFAA.MCCS
Requirement validation		This is effectively a duplicate of the sub-arraying requirement.		
L2 compliance impact		Cannot be fully verified with AAVS1.		
Current compliance status		Not yet tested		
Next steps				
Comments and recommendations				
SKA1-LFAA-156	Subarray membership	Any LFAA beam shall be assigned independently to one sub-array at a time.	Dem	LFAA. MCCS
Requirement validation		This requirement has been updated and reads more clearly.		
L2 compliance impact		Could potentially be tested on AAVS1.		
Current compliance status		Not yet tested.		
Next steps				
Comments and recommendations				
SKA1-LFAA-157	Subarray granularity	LFAA shall support sub-arrays containing an integer number of stations between 0 (none) and all 512 stations.	Dem	LFAA. MCCS
Requirement validation		Array-level requirement.		
L2 compliance impact				
Current compliance status		Cannot be verified with AAVS1		
Next steps				
Comments and recommendations				

SKA1-LFAA-158	Subarray independence	LFAA shall accept and execute commands for, and process data from, each sub-array independently of, and concurrently with all others.	Dem	LFAA.MCCS
Requirement validation		Effectively a duplicate. This is the same requirement as being able to form sub-arrays.		
L2 compliance impact				
Current compliance status		Cannot be verified with AAVS1		
Next steps				
Comments and recommendations				
SKA1-LFAA-159	Subarray configuration	LFAA stations within the same subarray shall be configured according to the Scheduling Block controlling that sub-array.	Dem	LFAA.MCCS
Requirement validation		Not relevant to AAVS1. System level requirement.		
L2 compliance impact				
Current compliance status		Cannot be verified with AAVS1		
Next steps				
Comments and recommendations				
SKA1-LFAA-160	Subarray station allocation	The LFAA, when performing observations, shall allocate stations to sub-arrays at Scheduling Block boundaries only.	Dem	LFAA.MCCS
Requirement validation		Not relevant to AAVS1. System level requirement.		
L2 compliance impact				
Current compliance status		Cannot be verified with AAVS1		
Next steps				
Comments and recommendations				
SKA1-LFAA-161	Subarray station failure flagging	When performing observations, LFAA shall detect and report to TM failed stations immediately after detection of the failure.	Dem	LFAA.MCCS
Requirement validation		Not relevant to AAVS1. System level requirement.		
L2 compliance impact				
Current compliance status		Cannot be verified with AAVS1		
Next steps				
Comments and recommendations				

SKA1-LFAA-162	Unique resource allocation	Each LFAA schedulable resource shall be allocated to no more than one sub-array at a time.	Dem	LFAA.MCCS
Requirement validation		Not relevant to AAVS1.		
L2 compliance impact				
Current compliance status		Cannot be verified with AAVS1		
Next steps				
Comments and recommendations				
SKA1-LFAA-163	Subarray pointings	The LFAA logical station beams for each SKA1_Low subarray shall be individually and independently pointed.	Dem	LFAA.MCCS
Requirement validation		This is a duplicate requirement of the ability to form sub-arrays. Not relevant to AAVS1.		
L2 compliance impact				
Current compliance status		Cannot be verified with AAVS1		
Next steps				
Comments and recommendations				
SKA1-LFAA-164	Subarray independence	LFAA shall support the independent logical control and monitoring of each instantiated sub-array.	Dem	LFAA.MCCS
Requirement validation		Primarily a system level requirement.		
L2 compliance impact				
Current compliance status		Not yet tested.		
Next steps				
Comments and recommendations				
SKA1-LFAA-165	Scheduling block set-up time	On receiving a subarray configuration request from TM, the time to complete configuration of LFAA resources to be ready for an observation shall be less than a TBD subset of 30 seconds**.**	Dem	LFAA.MCCS
Requirement validation		A system level requirement.		
L2 compliance impact				
Current compliance status		Cannot be verified with AAVS1		

Next steps				
Comments and recommendations				
SKA1-FLD-4257	Telescope Management			
SKA1-LFAA-166	Sky mapping	The LFFA, when commanded by TM, shall acquire data for imaging while the telescope is either (a) driven by TM across a region of sky defined in (Az, El), (RA, Dec), or Galactic coordinates to build a map of the sky, or (b) at a fixed (Az, El) position.	Dem	LFAA.MCCS
Requirement validation		This is a duplicate requirement that is the same as requiring sub-arrays and for sub-arrays to point in the same place. Again, this is system level requirement.		
L2 compliance impact				
Current compliance status		Cannot be verified with AAVS1		
Next steps				
Comments and recommendations				
SKA1-LFAA-167	Beam pointing model	LFAA shall implement a model which translates from topocentric Az, El to the delay corrections required to steer the beam. This model must include any known imperfections in the geometry of the station (e.g. orientation) and any other effects that can be reproducibly corrected in software. Parameters of the model will be stored by and downloaded from TM, but the calculation happens in LFAA..	Dem	LFAA.MCCS, LFAA.SPS
Requirement validation		Not an LFAA or AAVS1 requirement. Station beams will point to whatever az/el they are instructed to and LMC/TM should provide pointing corrections. Corrections like polarisation and refraction are not known at the station level.		
L2 compliance impact				
Current compliance status		Cannot be verified with AAVS1.		
Next steps				
Comments and recommendations				

SKA1-LFAA-168	Alarm latency	Latency from the time a measurement crosses an alarm set-point until the time it is reported by LFAA to TM shall be no more than 0.8 seconds	Test	LFAA.MCCS, LFAA.SPS, LFAA.FN
Requirement validation		Not relevant for AAVS1, which does not have a full TM system.		
L2 compliance impact				
Current compliance status		Cannot be verified with AAVS1		
Next steps				
Comments and recommendations				
SKA1-FLD-4258	Science data processing			
SKA1-LFAA-169	Correction of pointing errors	The LFAA, when commanded, shall correct pointing errors as a function of both time and station, which will be provided by SDP and/or TM.	Dem	LFAA.DS
Requirement validation		This is an array-level requirement, not station-level. Not relevant for AAVS1.		
L2 compliance impact				
Current compliance status		Cannot be verified with AAVS1		
Next steps				
Comments and recommendations				
SKA1-LFAA-170	Aperture Array DDE	The LFAA shall have direction dependent models for the station beams for each station with an accuracy of 35 dB at the half-power points to be used in calibration and imaging.	Test	LFAA.SPS, LFAA.MCCS
Requirement validation		This is a closely related to the requirement for station beam model accuracy. AAVS1 can inform on the accuracy of the DDE models for its station beam.		
L2 compliance impact				
Current compliance status		Unknown – still to be tested on AAVS1.		
Next steps				
Comments and recommendations		This specification is awaiting modification.		

SKA1-LFAA-171	Faraday rotation DDE	The LFAA shall have an initial direction dependent Faraday Rotation model for ionospheric contributions that can be used in calibration and imaging at SDP, in support of the polarisation dynamic range performance.	Test	LFAA.SPS, LFAA.MCCS
Requirement validation		Not a station-level requirement. This is a system-level requirement.		
L2 compliance impact				
Current compliance status		Cannot be verified with AAVS1		
Next steps				
Comments and recommendations				
SKA1-FLD-4259	RFI mitigation			
SKA1-LFAA-172	RFI masking	LFAA, on the request of TM, shall flag beamformed data according to the mask provided by TM, with a time resolution defined by TM and a frequency resolution of one coarse channel.	Test	LFAA.SPS, LFAA.MCCS
Requirement validation		This is possible but meaningless at the station level. Coarse channels with known RFI can be avoided by not observing them in the first place. This should not be an LFAA requirement.		
L2 compliance impact				
Current compliance status		Unknown.		
Next steps				
Comments and recommendations				
SKA1-LFAA-173	RFI flagging	LFAA shall flag data according to a pre-selected RFI Mask to assist the SKA1_Low to automatically flag frequency data with a resolution of one channel and time data to the resolution of the integration unit if the data is corrupted by RFI.	Dem	LFAA.SPS, LFAA.MCCS
Requirement validation		This is not an LFAA requirement. Pre-defined RFI masks can be given to CSP or SDP. Known RFI frequencies can be avoided in TM by not observing those frequencies.		
L2 compliance impact				

Current compliance status	Cannot be verified with AAVS1
Next steps	
Comments and recommendations	

SKA1-LFAA-288	Relative gain tolerance	The station beam accuracy for LFAA over a 10-minute interval shall have a relative gain tolerance of better than: *Frequency (MHz)* | *50* | *80* | *110* | *160* | *220* | *280* | *340* | *350* Rel. gain tolerance (%) | 1.05 | 0.58 | 0.39 | 0.59 | 0.97 | 1.54 | 2.39 | 2.55		

Requirement validation	This can be evaluated using AAVS.
L2 compliance impact	AAVS can contribute directly to LFAA compliance.
Current compliance status	Unknown.
Next steps	This can be evaluated using AAVS once the beamformer is operational.
Comments and recommendations	This specification was added subsequent to the JAMA export of 2018-06-25, hence is listed here separately, as per the 2018-10-31 baseline.

7 Summary and Future Work

This report has discussed the Aperture Array Verification System (AAVS), evaluating work done and results achieved against the aim of this demonstrator, namely to provide a full-scale Low Frequency Aperture Array (LFAA) station prototype deployed on the Australian SKA site. This was specifically done to permit the design team to investigate, mitigate and retire key risks.

Much of practical value was learned from the AAVS deployment, including the challenges of transporting substantial amounts of electronic equipment to a remote site, the vulnerability of items to damage during transport, and of course the problems of working on such a remote site at a time of year with an inhospitable climate. Issues regarding the electronic instability (resulting in highly undesirable oscillations in the RF band) of the front end as installed were also only exposed during installation and operation on site. Although a satisfactory work-around has been found, it remains a risk for the current design.

It is important to highlight a number of potentially challenging places where good results have been obtained. As expected from laboratory and field tests on the relevant subsystems, the RFoF system appears to be working well. The TPMs are largely working as planned, at least to the beamforming stage. The electrical reticulation is functioning. The AAVS is sufficiently RFI compliant that it can operate on the MRO without interfering with the operation of either the MWA or ASKAP. (In this regard, note that the RFI compliance for AAVS is rather less stringent than that intended for SKA_LOW.)

One of the main risks exposed during evaluation of the AAVS has been station-level calibration. As highlighted in Section 4 of this report, reinforced by an independent analysis in Appendix A, the current design poses significant calibration challenges. The work to date indicates that the required calibration scheme will need calibration on a complete sky model that includes diffuse emission from the Galactic plane, taking into account that the EEPs differ from element to element. It should be re-iterated that the issue is not whether the station can be calibrated, but rather how accurate, stable and computationally costly this calibration procedure will be. Calibration has been demonstrated using AAVS in correlation mode, but the source of residual time variability in calibration solutions has not yet been apportioned between true (instrumental) variability and incomplete calibration model due to instrumental and/or sky complexity.

Future work needs to urgently address a number of threads highlighted above. Some of these relate specifically to AAVS, but most address the larger issue of the LFAA station design. A detailed statement of this work is contained in the pre-EPA bridging project proposal [RD45] which has been developed in parallel with the completion of this document. This is summarised very briefly here. The most pressing item is to resolve the highest priority technical risk in the SKA-LOW station reference design identified at CDR, namely station calibratability. This should be addressed firstly, with the deployment of a mini-station comprising at least 16 (preferably 32) SKALA4 antennas, including drone measurements; and secondly, with the deployment of the second version of the Engineering Development Array (EDA2) as a further risk mitigation strategy. (The EDA2 is an LFAA station consisting of bow-tie dipole elements). Electromagnetic simulation work on the station embedded element patterns and beams should continue, with a focus on SKALA4 elements.

Astronomical measurements to evaluate the performance against LFAA requirements should also be undertaken. Additionally, further digital backends should be deployed on-site. In parallel with this work, the calibration and commissioning of AAVS should progress as rapidly as possible, in particular regarding beamforming and the testing of sub-station capability. A detailed list of steps relating to ongoing calibration work has been presented in Section 4.5.4.

This page intentionally left blank

Appendices

A.1 Complexity of LFAA station calibration

A.1.1 Introduction

Initial results from the AAVS 1.0 prototype station indicate that station calibration for LFAA may become a challenging and resource consuming task due to the limited stability of the receive paths and the large differences between the embedded element patterns. In this note, a brief overview of station calibration classes is given and their implications for development and commissioning of the LFAA system. Simulation results are also presented to assess which station calibration class best matches the needs of LFAA based on currently available knowledge of the expected instrument response and demonstrate the impact of large inter-element variations.

A.1.2 Station calibration classes

In order of increasing complexity, methods for station calibration can be subdivided in the following classes:

- Class 1: calibration on one or a few bright calibration sources assuming that all embedded element patterns (EEPs) are the same;
- Class 2: calibration on a complete sky model that includes diffuse emission from the Galactic plane assuming that all EEPs are the same;
- Class 3: calibration on one or a few bright calibration sources taking into account that the EEPs may be different for different elements;
- Class 4: calibration on a complete sky model that includes diffuse emission from the Galactic plane taking into account that the EEPs may be different for different elements.

Below, each class is discussed in more detail.

Class 1: few calibration sources, identical EEPs

As all EEPs are identical, the direction dependent gain of the elements can be absorbed in the source flux estimates, making the calibration algorithm solve for the apparent fluxes of the sources. The calibration algorithm thus only has to solve for the direction independent gain of each receive path and the apparent source fluxes. As a method of this class is used for the station calibration of LOFAR, this algorithm is well understood and demonstrated in practice. As the source model is very simple, the computational resources required to construct a visibility model are very low.

Class 2: complete sky model, identical EEPs

To get away with a simple sky model consisting of only a few point sources, LOFAR station calibration uses a baseline restriction to ensure that accurate visibility modelling on the shortest baselines is not required. The signal measured on the short baselines represents the flux on large spatial scales. Removing the short baselines thus effectively implements a spatial filter removing the diffuse emission from the Galactic plane. If there is an insufficient number of long baselines (long being defined as longer than the baseline restriction) to successfully calibrate the station, a visibility model for the short baselines is required which, in turn, requires a sky model that includes the diffuse emission from the Galactic plane. This brightness map needs to be weighted by the common EEP. As there are simply not enough degrees of freedom in the data of a single snapshot to solve for a direction dependent gain towards each patch of the brightness map, the common EEP should be a priori known. The common EEP may be established using (astronomical) calibrator sources that drift through the EEP during commissioning.

Calibration methods in this class require a brightness map of diffuse emission that needs to be projected to a horizon coordinate system at the appropriate sidereal time with a resolution that ensures at least 3 resolution elements within the HPBW of the station. The map in local coordinates then needs to be weighted by the common EEP and Fourier transformed to produce model visibilities.

Class 3: few calibration sources, different EEPs

LOFAR LBA actually requires a method from this class. The small differences between the EEPs in the LBA outer array cause small systematic errors in the LOFAR station calibration caused by the violation of the assumption that all EEPs are the same. Due to the very good stability of LOFAR, this is solved by producing calibration tables based on the average gain solutions found over one sidereal day. This effectively averages out the errors caused by this bias. If the EEPs are known, the direction dependent gains of the individual elements can be taken into account during construction of the visibility model. The EEPs can be predicted by a validated EM model. The validation of the EM model can be done using, e.g., drone measurements. As a result, taking into account the differences between the respective EEPs thus translates into a significant effort to validate the EM model and significant resources to store the EEPs of all elements with sufficient spatial and spectral resolution.

Class 4: complete sky model, different EEPs

If a valid visibility model is needed on the shortest baselines, diffuse emission with large spatial scales needs to be taken into account. This requires a brightness map of the sky that needs to be projected to the local horizon system. As the EEPs are different for each element, each element sees a different apparent sky, meaning that a copy of the projected brightness map needs to be weighted by the EEP of each element before the contribution of that element to the visibilities involving that element can be predicted. This class thus involves the most elaborate visibility modelling procedure. Just like class-3 methods, class-4 methods require validation of an EM model to predict the EEPs and storage of the EEPs of all elements with sufficient spatial and spectral resolution.

A.1.3 Simulations

Using EEPs obtained from EM simulations for a 256-element station with proposed SKA-low layout kindly provided by ICRAR-Curtin (Daniel Ung, EDA) and Cambridge University (Eloy de Lera-Acedo and Hardie Pienaar, SKALA2 and SKALA4), a simulation was set up to assess the needs of LFAA station calibration. In these simulations, mock intra-station visibilities were generated using a detailed model and calibrated using a visibility model that was simplified in one way or the other. The visibility data were noise-free such that all calibration errors can be attributed to the bias caused by the simplification in the model visibilities. This was done for the following scenarios:

- Station calibration of an array of isotropic radiators observing a full brightness model of the sky (noise sources and extended emission) using a calibration model containing only the brightest point sources.
- Station calibration of an array of SKALA2 antennas observing a full brightness model of the sky using a calibration model based on the same full brightness model but assuming that all EEPs are identical to the average EEP of the 256 SKALA2 antennas;
- Station calibration of an array of SKALA4 antennas observing a full brightness model of the sky using a calibration model based on the same full brightness model but assuming that all EEPs are identical to the average EEP of the 256 SKALA4 antennas;
- Station calibration of an array of bowtie antennas observing a full brightness model of the sky using a calibration model based on the same full brightness model but assuming that all EEPs are identical to the average EEP of the 256 bowtie antennas.

For all scenarios, the simulation is done for 20 instances spread across a sidereal day as it is expected that the outcome of the simulation will depend on the exact geometry of the array and the brightness distribution on the sky, in particular the rise and set of the Galactic plane. To simulate a realistic brightness distribution, the Haslam map is used. The simulated station is located at the AAVS site. The assumed observing frequency is 160 MHz as this is the only frequency simulated for both EDA and SKALA2 / SKALA4. Some other frequencies are almost common but, strictly speaking, require a little interpolation in frequency.

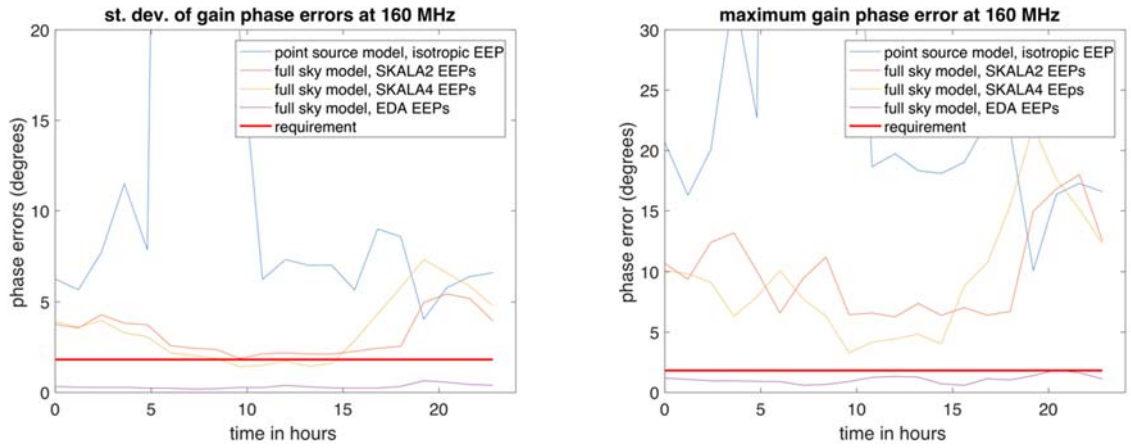

Figure 24: Standard deviation of the phase errors (left) and maximum phase error (right) at different sidereal times of the 256 receive paths within a station at the AAVS site. The thick red line indicates the accuracy needed to meet the receive path stability requirement.

Figure 24 shows the standard deviation of the 256 phase errors for the four scenarios simulated as well as the maximum phase error found during a single sidereal day. The thick red line shows the station calibration accuracy required to meet the stability requirement imposed on the individual receive paths within a station. These results indicate that

- Calibration of the LFAA stations will require careful modelling of the visibilities on the short baselines, i.e., a calibration model purely based on the brightest point sources will lead to poor calibration results. This confirms an earlier analysis by Tim Colegate, Randall Wayth and the author (Wijnholds) as can be explained by the fact that the LFAA stations are so compact that spatial filtering as used in LOFAR will effectively flag all data. This implies that LFAA requires a class-2 or class-4 method for station calibration.
- The inter-element variations of both SKALA2 and SKALA4 are so large, that the required station calibration accuracy cannot be attained while assuming that all EEPs are equal. This implies that LFAA stations composed of SKALA2 or SKALA4 antennas will require a class-4 station calibration method that knows the response of each individual antenna within a station.
- Considering the particular aspect of achievable station calibration accuracy only, there is not much difference between SKALA2 and SKALA4.
- The inter-element variations of the bowtie antennas currently used in EDA are sufficiently small to attain the required station calibration accuracy while assuming that all their element radiation patterns are identical. This implies that if an LFAA station would consist of bowtie-antennas, a class-2 station calibration method might be sufficient.

A.1.4 Conclusions

The simulations presented here indicate that stations consisting of SKALA2 or SKALA4 antennas require a station calibration method from class 4 introduced above. As far as the author is aware, such a station calibration method has not been demonstrated on an actual system yet. Although one may argue that LOFAR's LBA inner arrays also fall in this category, the LOFAR system is sufficiently stable to work with calibration tables valid for

extended periods of time (several months). LOFAR can therefore average the errors over a sidereal day to largely remove the bias caused by using a simplified method. As the LFAA system will not have this stability, gain variations of the individual receive paths need to be tracked during an observation. Implementation of a class-4 station calibration method will require:

- A validated EM model. This can be done using detailed drone measurements on a single station. Once the EM model is validated, the response of individual LFAA stations can be simulated based on their respective station configurations. The resulting tables are likely valid for a long period assuming that the input impedance of the LNA connected to the antenna ports hardly changes with time. Also, the production tolerances need to be sufficiently small to ensure validity of the EM simulations when applied to stations that are not measured in detail. The feasibility of this validation procedure has been demonstrated on LOFAR. However, that campaign also demonstrated that measurement preparation, measurement execution and measurement analysis requires several man years of work.
- Once the EM simulation has been validated, the element response for ***all*** antennas in the LFAA system will need to be tabulated in full polarization with sufficiently high spectral and spatial resolution to allow interpolation to the desired position on the sky and observing frequency. It has been proposed to tabulate coefficients of adequately chosen basis functions instead. This may reduce storage / memory requirements for the antenna response tables at the cost of a higher compute load to evaluate the superposition of basis functions.
- Creation of a sky model describing the brightness distribution across the visible sky with resolution elements that are 3 to 5 times as small as the HPBW of the station. At the highest LFAA operating frequency (350 MHz) this corresponds to $\sim 10^5$ image elements. For the simulation at 160 MHz, there were $\sim 3 \times 10^4$ image elements, for which visibility modeling for the full 256-element station with different EEPs per element took about 5 seconds in Matlab for a single time and frequency slot on the author's laptop (MacBook Pro 2017 with 2.9 GHz Intel Core i7 and 16 HB 2133 MHz LPDDR3 RAM).

If one can assume that all EEPs are identical, this average EEP can be established using measurements on astronomical sources using regular self-calibration techniques. This does not only save (a lot of) work during the commissioning phase to validate the EM model and simulate all EEPs, but also reduces the risk of not achieving or retaining (due to deterioration of components and an increasing number of defective antennas in the course of time) sufficient accuracy of the EM model. This risk may be quite significant given the extreme inter-element variations of SKALA2 and SKALA4 indicating a high sensitivity to the EEP to the precise loading condition of the antenna. This does not only make the validation of the EM simulation a challenging task, but also increases the likelihood of EEP changes over time if the loading conditions change due to aging of the components or antenna failures. The simulations presented in this note indicate that replacing the SKALA antennas by bowtie antennas in the design of the LFAA station may offer these advantages.

A.2 Embedded element patterns

In array theory, the term “embedded element pattern” denotes the radiation pattern of an individual element embedded in the array, with all the other elements terminated. The choice of terminating impedance for those elements is arbitrary, but certain choices greatly simplify further analysis. (This should not be confused with the active impedance at an antenna port, which is the impedance seen at that port including mutual coupling from the other array elements). The most widely used choices of terminating impedance are short-circuit, open-circuit, matched, and actual loading conditions. Open-circuit loading is widely used in the literature [RD27]; match loading is attractive for well-matched antennas. However, for the typical impedance presented by the AAVS LNA - which is not well matched - actual loading conditions are the most convenient to use. For this case, the array (station) mutual impedance is already captured in the patterns and the overall station pattern is the sum of the individual embedded element patterns, weighted by the beamformer weights. Open-circuit loaded patterns can similarly be summed, but the resultant open-circuit voltages at the input ports must then be weighted by the array mutual impedance matrix to determine the actual system response. EEPs computed with matched loads must be similarly transformed to the actual terminating impedances when the antenna and LNA (for instance) are not impedance matched. It is important to note that the EEPs computed for different loading conditions may look quite different. An example is shown in Figure 25, where the open- and short-circuit EEPs for one element of a very simple two-element array of half-wavelength dipoles, a half wavelength apart, are shown. These patterns are quite different. However, when correctly combined (usually requiring the array mutual impedance matrix), the final station beam will be the same.

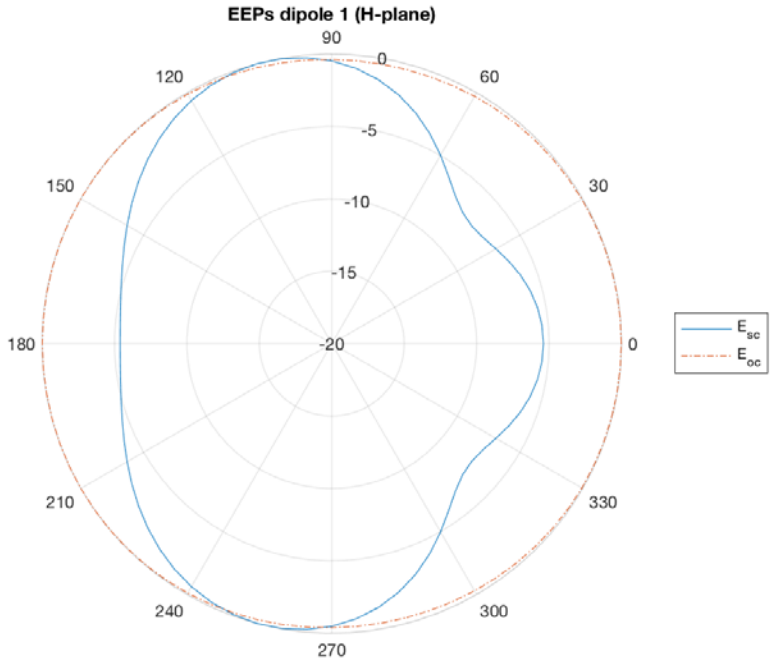

Figure 25: Comparison of embedded element patterns (dB scale) for short-circuit (SC - blue) and open-circuit (OC - red) loading conditions.

A.3 Optical fibre and power stability

Statistics on the measured optical path lengths of the two 576-core cables.

- G.652.D standard cable was adopted for the AAVS project, as the cable has a Zero Dispersion Wavelength (ZDW of around 1310 nm) near the operating wavelength of the Wavelength Division Multiplex (WDM) laser used in the front-end module (FEM) AAVS antenna (at 1270nm and 1330nm). The specifications for AAVS FO cable therefore follow closely the G.652.D standard as follow in Table 8 [RD25]:

Table 8: Specification for AAVS FO cable

Transmission wavelength	1260 nm to 1625 nm	
Mode field diameter	8.6 – 9.2 μm ± 0.4 μm, at 1310 nm wavelength, *compatible for splicing with ITU-T G.652.D cable.*	
Attenuation	1310 nm – 1625 nm: 0.4 dB/km	
	1260 nm – 1309 nm: 0.47 dB/km	
Point discontinuity	< 0.05 dB in the specified transmission wavelength	
Cable cut-off wavelength	< 1260 nm	
Zero dispersion slope:	At 1310 nm	Min: 0.073 ps/(nm^2 .km) Max: 0.092 ps/(nm^2 .km)
	At 1550 nm	Min: 13.3 ps/(nm^2 .km) Max: 18.6ps/(nm^2 .km)
Zero dispersion wavelength	Min: 1300 nm Max: 1324 nm	
Dispersion coefficient between 1285 nm to 1330 nm	≤ |3| ps/nm.km	
Optical cladding diameter	125 ± 0.7 μm	

- Following the measurement methods as documented in [RD26], Optical Time-Domain Reflectometry (OTDR) measurements were performed on all AAVS fibre cores after installation by the cable installer (Mitchel & Brown). OTDR is measured at 3 different wavelengths (1310 nm, 1550 nm, and 1625 nm), with measurement time of 30.2 sec for each wavelength. Individual OTDR raw data of each fibre core are available. Table 9 summarises the statistics of the fibre optic cables post-installation. In that table, AFL refers to the Spider Web Ribbon (SWR) cable that is sourced from Fujikura (parent company of ALCOA Fujikura Limited – AFL). SDGI refers to the conventional ribbon fibre inside loose tubes that is sourced from Shenzhen SDG Information Co. Ltd. Both have been deployed as part the AAVS system. ORL is (optical) Output Return Loss'.

Table 9: Statistics from the OTDR results of the AAVS FO cables

Wavelength:		**1310 nm (n=1.468)**			
Statistics (576 cores)		**Loss (dB)**	**ORL (dB)**	**Length (km)**	**Delay (μsec)**
AFL	**Max**	2.281	34.790	5.216	25.541
	Avg.	1.578	33.082	5.213	25.528
	Std. dev	0.231	0.300	0.001	0.006
SDGI	**Max**	2.258	37.650	5.357	26.232
	Avg.	1.718	33.573	5.291	25.908
	Std. dev	0.071	0.370	0.001	0.007

Wavelength:		1550 nm (n=1.4686)			
Statistics (576 cores)		Loss (dB)	ORL (dB)	Length (km)	Delay (µsec)
AFL	Max	1.580	36.140	5.217	25.557
	Avg.	0.930	34.441	5.214	25.540
	Std. dev	0.217	0.302	0.001	0.006
SDGI	Max	1.577	38.260	5.356	26.238
	Avg.	1.033	34.927	5.289	25.910
	Std. dev	0.068	0.376	0.002	0.008
Wavelength:		1625 nm (n=1.4691)			
Statistics (576 cores)		Loss (dB)	ORL (dB)	Length (km)	Delay (µsec)
AFL	Max	1.617	36.000	5.216	25.560
	Avg	1.012	34.474	5.214	25.548
	Std. dev	0.233	0.281	0.001	0.006
SDGI	Max	2.544	38.140	5.355	26.242
	Avg	1.109	35.012	5.287	25.908
	Std. dev	0.106	0.546	0.002	0.008

- The length information in Table 2 is rounded-up to the nearest meter (1 m resolution). For higher length resolution, the raw *.msor files cm resolution (with an estimated accuracy of around 20 cm).
- Note that the OTDR data is provided to record the performance and the spread of the fibre optic cable post installation, as well as a mean to assess degradation later over a certain period, in the future.
- Note also that has been discussed in [RD19] **fibre core length difference has a much smaller effect on the relative phase variation**, if the length difference is relatively small compared to the total length of the cable. Rather, a simple physical model relating expansion coefficient, fibre length tolerance, optical index variation and temperature change suggests **that temperature difference among the fibre cores** significantly influence the phase variations.

Optical power measurements

- Pre-deployment, the AADCC ran a series of measurements on the front-end modules (FEMs), where among other parameters, the optical power of each wavelength was recorded. The measurement was repeated in the field at the MRO, to ensure that there was no significant degradation in the RFoF module. The statistics for the RF-over-Fibre (RFoF) module is given in Table 10.

  These power optical measurements were made for the record only, at constant ambient temperature. One use has been as a means to screen SKALA trumpets after transporting and unpacking. Other uses are for RF chain budget analysis and also so that in the future we could track any (optical performance) degradation. Currently there are no specifications for the RFoF module optical power level; differences in the optical power level across the array is inherently captured as absolute gain variations from one RF chain (link) to another RF

chain (link) in an array. However, this should be budgeted for in the overall RF chain analysis.

The conclusion is that with array calibration, the optical power variation across different RFoF modules (at constant ambient temperature) is not affecting spectral stability, or relative gain variation of the array. In the RFoF TX, an automatic power control circuit is present which should keep the emitted optical power constant. (What changes with temperature is the efficiency of the DFB laser, which means different gains - and noise figure - of the RFoF links with temperature, even if the emitted optical power is the same.) Nonetheless, it is useful to also assess the RF performance of the laser module (RFoF Tx) with varying operating temperature, to ensure that the performance - as installed in the field - is meeting the specifications with respect to temperature fluctuation as well as within the allocated optical power budget in the RFoF link chain.

Table 10: Statistics of the AAAVS1 front-end module (FEM) optical power output level measured at the end of the Hybrid Cable.

AAVS WDM		Power [dBm(o)]
1270 nm	Max	5.800
	Min	3.230
	Avg.	4.498
	Std. dev	0.494
1330 nm	Max	5.880
	Min	3.140
	Avg.	4.414
	Std. dev	0.458

A.4 Temperature Effects on the Radio Frequency Front-end Chain (LNA and RF Over Fibre)

A.4.1 Introduction

This appendix presents results for the RFoF system. Key points from the measurements are summarised at the end of the appendix.

A.4.2 Measurements

Thermal contribution from solar loading, as well as any internal heat-dissipation of the electronics components/ sub-assembly should be considered when assessing the reliability of equipment under LFAA L3 non-operating temperature (Req. R131) and operating ambient temperature (Req. R132) as specified in [RD13]. As such, the upper limit of the requirements should reflect these contributions, besides just considering the environmental ambient temperature condition as described in the requirements.

Measurements using empty SKALA trumpet in the field at the MRO indicates that non-operating temperature inside the enclosure could reach up to 11°C higher than the ambient or air temperature RD14. The temperature rise contribution from solar loading is a function of the dimension, material and colour of the enclosure.

Furthermore, when the equipment is in operation, the effect of internal heat dissipation contribution must be included together in the operating ambient temperature and contribution from solar loading [RD14]. When evaluating thermal dissipation of the device, care must be taken to ensure that the temperature of the device-under-test (DUT) reaches steady-state. Based on the measured and calculated data, for AAVS electronics, it is reasonable to test the operating temperature from -10 °C to 70 °C (or higher).

Ambient temperature records at the MRO are available from the CSIRO weather database. However, the database only provides measurement at a single location, and does not provide the spread of relative temperature difference across a specified area in the field. This information is critical to gauge the impact of temperature difference on RF front-end stability of the array across the LFAA stations [RD15].

The relative temperature difference information can be employed to estimate the relative elongation (expansion or contraction) on the antenna structures, cables and connectors, as well as the stability of active electronics (e.g.: LNA, RFoF and biasing/ power supply modules). Thus, from these measurement data, we could infer the RF gain and phase variations due to temperature gradients across the station at any instantaneous time, as well continuously over time [RD15].

Based on the measurement at AAVS location performed in July 2015, we calculated the maximum relative temperature difference that could occur at two locations in an area within 35 m diameter is 1.1° C in any 10-min window (std. dev. of 0.72° C). The maximum rate of change of the temperature is 0.2° C/ minute and 75th percentile rate of change of 0.1° C/ minute [RD15]. This information is the basis to simulate outdoor temperature conditions in the lab, when assessing the performance of the RF electronics over the expected operating temperature in the field.

Of particular importance is evaluating the extent of the maximum relative gain and phase variation along RF receiver front-end chain over a 10-minute window, as this defines the accuracy and validity of instrumental calibration at the beginning of the 10-min window [RD13], as well as impact on the V-leakage, U-leakage and Q-leakage performance.

These magnitude and phase variations of the RF front-end chain due to temperature consist of contributions from:

1. **LNA and RF-over-fibre transmitter (RFoF Tx) electronics** [RD16], [RD17]
    a. Measured gain and phase variation of the CCL SKALA LNA (10-min Window) is estimated to be ±0.043dB±0.28° [RD16].
    b. Measurement of max. gain and phase variation of RFoF Tx (based on ASTRON RFoF solutions), (10-min Window) is [RD15], [RD18]:
        i. Between: -10° C to 35° C: 0.05dB, 0.25° (phase) @ 160 MHz
        ii. Between 40° C to 49° C: 0.5 dB, 0.75° (phase) @ 160 MHz

2. **Dispersion-induced relative phase variation** [RD15], [RD17], [RD18]
   This is due to the effect of laser diode wavelength shift over temperature when the light is propagating over dispersive media. Estimates assuming 2 km G.652.D fibre core is used and that the wavelength is 1310 nm (relatively around the Zero Dispersion Wavelength) [RD18]:
    a. From -10° C to 50° C, (10-min window): max. 0.013° (phase), 300 MHz
    b. From -10° C to 50° C, (24-hour period) max. 0.24° (phase), 300 MHz

3. **Thermal effect on Fibre Optic (FO) cable** [RD19], [RD20], [RD21]
   Solar and wind exposure, as well as temperature difference between the surface of the cable that makes contact into soil surface and ambient air interface along Fibre Optic (FO) cable result in:
    a. Physical expansion or contraction (length variation) of the fibre optic
    b. Change in refractive index of the media (due to strain).
    c. Temperature gradient across cross-section of the FO cable.
    d. Variations mainly in the phase of the transmitted RF signal.

Measurement results of the FO cable from the field (MRO) suggest the following:

- Relative phase variation is influenced predominantly by the temperature difference across each fibre cores inside the cable assembly [RD19].

- The relative phase variation, calibration intervals, as well as deployment strategies (burying vs surface, maximum length of the cable that can be deployed, etc.) could be estimated from measurement results [RD19], [RD20].

- We could minimise the temperature gradient effect by carefully select the cable construction as well as the way it is routed (underground or above ground on the surface) [RD20],[RD21].

If we directly impose the LFAA L3 phase limit (as of 2015, when AAVS was conceptualised) as a basis for fibre optic phase stability assessment, based on the actual measurement on FO cables that are used for AAVS project (5.2-km surface laid cable) [RD21], the following phase results pertain:

- On AFL Spider Web Ribbon type cable, we estimate max relative phase variation of [0.78° (phase)/ km] @ 160 MHz in any 10-min window (assuming linear scaling).

- On SDGI loose tube cable, we estimate max relative phase variation of [~1.5° (phase)/ km] @ 160 MHz in any 10-min win.

- Note that this is the worst-case scenario that could possible occur (as per AAVS deployment), where the FO cables are routed 5.2 km on the surface above the ground exposed to the elements, and that the phase variations were measured relative to two different WDM laser wavelengths & fibre core 'bunching' inside the cable.

We also reported measurement for MWA implementation, where the FO cable (5.5 km) is buried underground. We estimate max relative phase variation of [0.013° (phase)/ km] @ 160 MHz in any 10-min win, and that it is relatively stable/not affected by ambient temperature fluctuations [RD20].

A.4.3 Summary

For surface laid cable, in any 10-minute window at 160 MHz RF frequency, a maximum relative phase variation of 0.78°/ km for the AFL Spider Web Ribbon type cable and 1.5°/ km for SDGI loose tube cable are predicted (both cables were deployed as part of AAVS). With the AAVS deployment, the fibre optic cable runs 5.2 km on the surface. By comparison, for an MWA implementation on the MRO where the cable (5.5 km) is buried underground, the figure is 0.013°/ km. The RF-over-fibre transmitter has a phase variation of 0.75°, and the LNA around 0.28°.

A.5 Laboratory measurement procedure for AAVS LNA temperature stability

This appendix reviews a laboratory measurement at Curtin University of the AAVS LNA.A measurement using a simulated temperature cycle and a thermal plate. The temperature was ramped at 0.1^{O} C/minute, simulating MRO conditions, and data was processed using the approach described in [RD39]. The LNA tested LNA has relatively good temperature stability, and a good margin with regards to the LFAA L3 requirement of stability of 10 minute intervals. The test set-up in shown in Figure 26 and the temperature profiles of the plate and DUT are shown in Figure 27 and Figure 28. Results are shown in Figure 29 and Figure 30.

These tests were run over a -10ºC to +70 ºC temperature range; some tests on the MRO indicated a maximum daily temperature variation of around 20ºC [RD39].

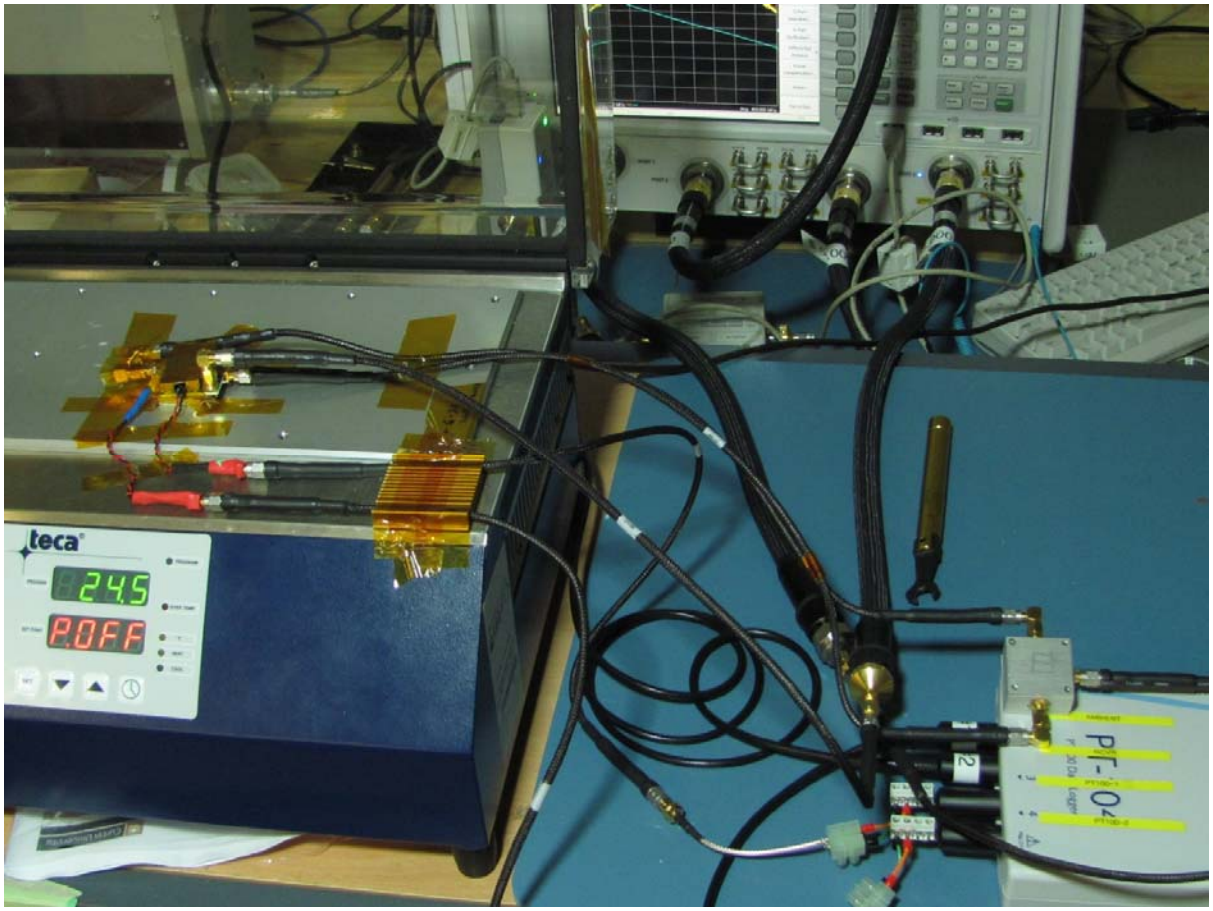

Figure 26: Test set-up for measuring temperature effects in the ICRAR-Curtin laboratory using a thermal plate.

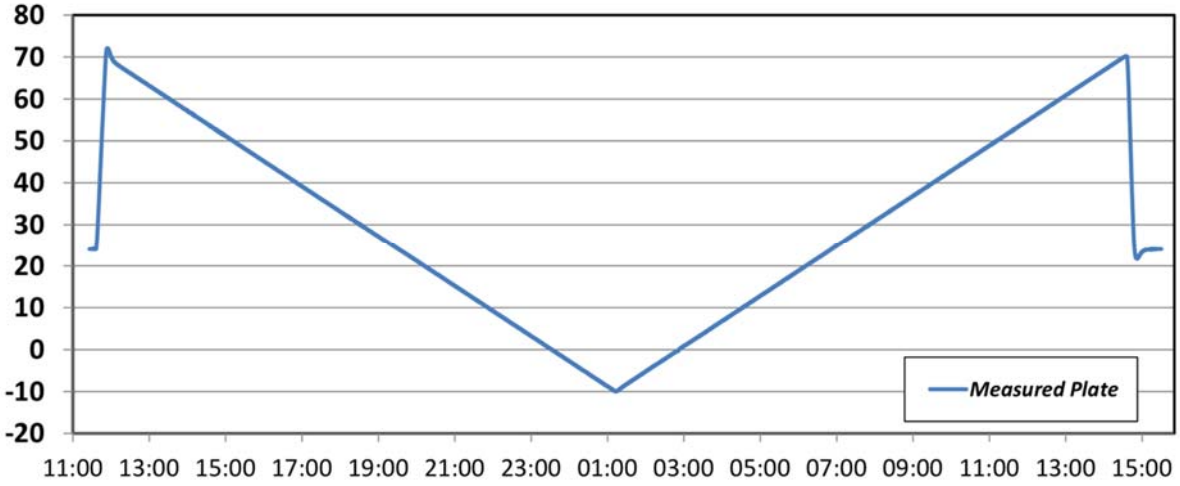

Figure 27: Temperature of thermal plate.

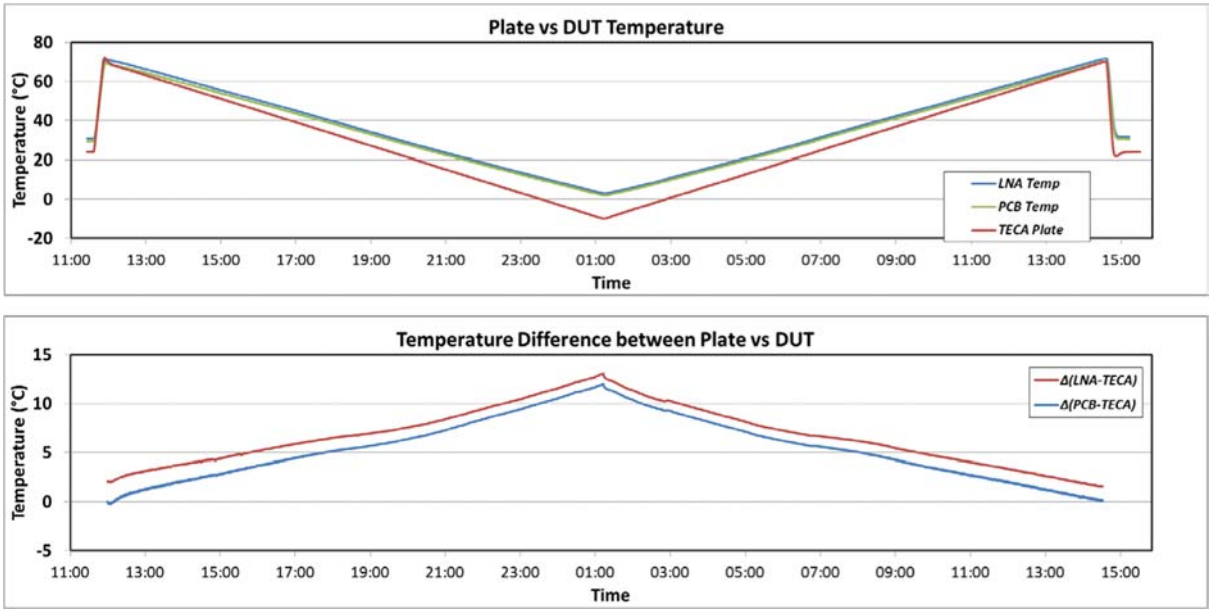

Figure 28:Temperature of plate vs DUT.

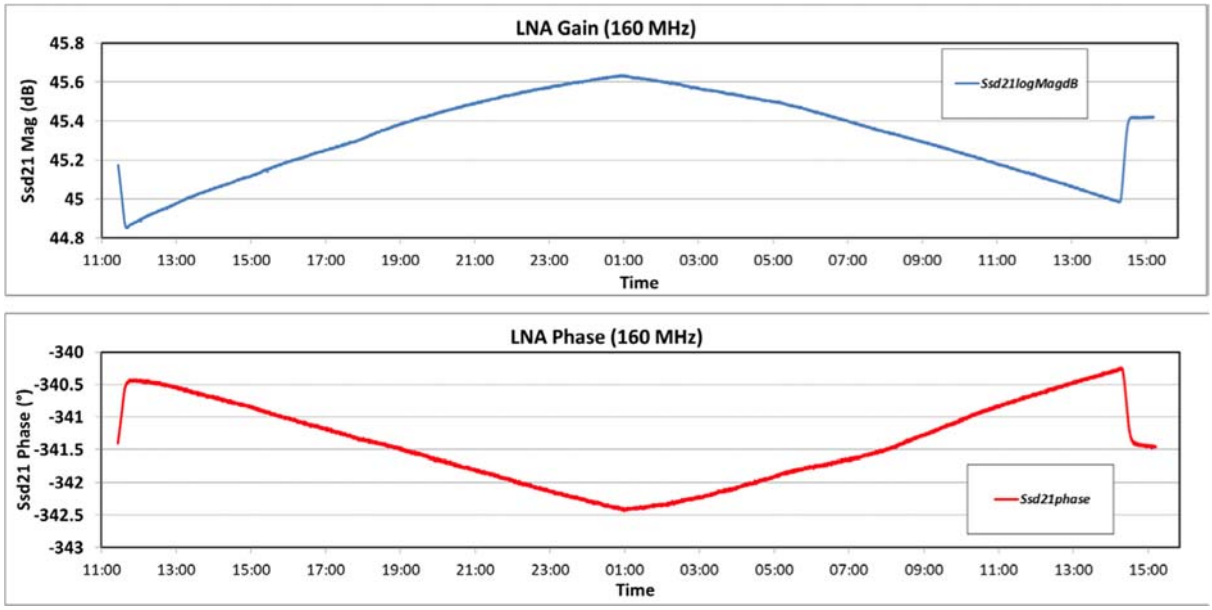

Figure 29: Measured gain and phase of the AAVS LNA on in laboratory conditions.

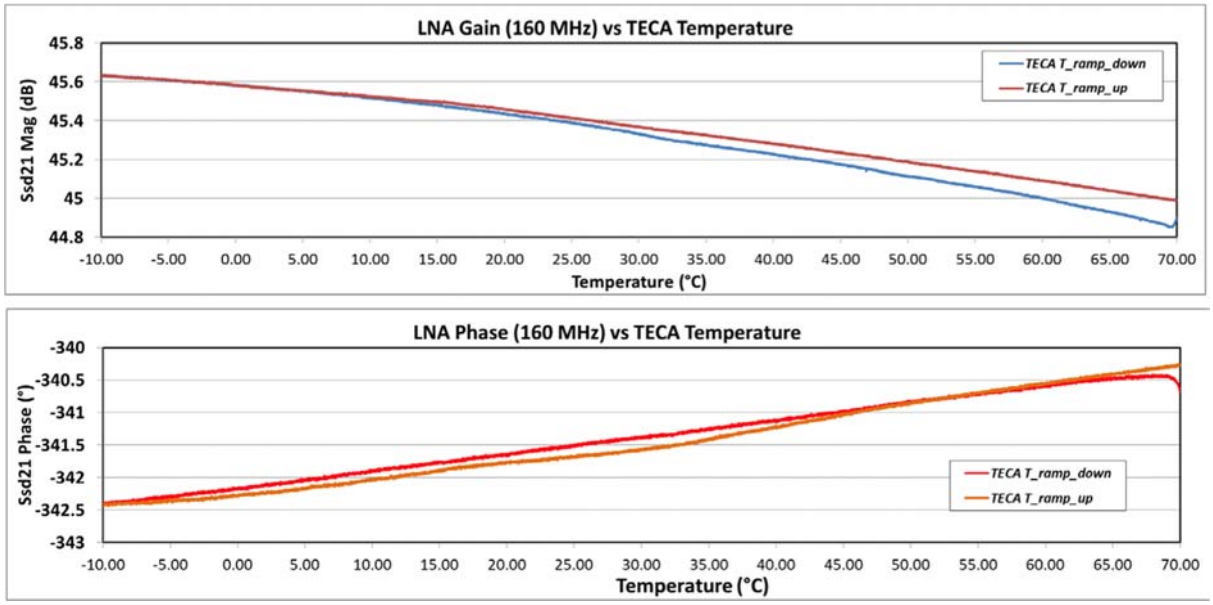

Figure 30: Measured gain and phase of the AAVS LNA versus temperature, for ramping up (-10°C to +70 °C) and ramping down (+70 °C to -10°C).

A.6 EMC/RFI and AAVS

This appendix presents some general comments on the current (measured) state of the EMI characteristics of AAVS components and their compliance with applicable SKA limits.

The EMI limit values for equipment deployed at the MRO for AAVS project were divided into two categories:

- **Equipment for the correlator room**
  For AAVS 1, equipment must meet CISPR B (CISPR- 11 class B, CISPR-22 class B, CSIRP-32 Class B, IEC 61000-6-3/ equivalent). Assuming that shielding effectiveness of the enclosures for both the correlator room and the MRO control building provide a total of more than 160 dB of RF attenuation (an assumption which is not universally accepted), and accounting for the quasi peak detection factor as well different measurement distance, a *CISPR B compliant devices* should comply with *80 dB below the limit of MIL-STD-461F* as required in [RD11]. See also [RD29].
- **Equipment for the AAVS 1.0 Station**
  The limit values are: 20 dB below MIL-STD-461F (RE102-4, Army, Mobile, Navy). In terms of field strength, this is 4 dBµV/m up to 100 MHz, then increasing linearly over a logarithmic frequency to 49 dBµV/m at 18 GHz. This is derived from the fact that AAVS is located 5 km away from the ASKAP dish as per CSIRO RFI requirements [RD11].

CSIRO requirements specify a frequency range at least covering 70 MHz to 5 GHz [RD11]. For AAVS, the approach ICRAR/Curtin currently adopt is to directly measure the device-under test down to the sensitivity as required according to the EMC target emissions level of MIL-STD-461F – 20 dB. (Another approach is to measure the device-under-test (e.g. APIU) to MIL-STD-461F and then assume that a shielding enclosure will provide sufficient additional shielding to meet the specification). An example of results from a test set-up complying with MIL-STD-461F (in this case for the APIU discussed in Section 5.5) is shown in Figure 31, Figure 32, and Figure 33. (Note that the device under test in this case does not meet the MIL-STD-461F – 20 dB specification in the two lower bands, also as noted in Section 5.5).

Based on current instrumentation set-up and capabilities, for equipment deployed at the AAVS.0 Station in the field, ICRAR-Curtin typically measure radiated emission from 30 MHz - 3 GHz. This is performed over 3 frequency bands:

- 30 MHz – 200 MHz: good sensitivity down to 10dB below MIL-STD-461F.
- 200 MHz – 1 GHz: good sensitivity at 20 dB below MIL-STD-461F
- 1 GHz – 3 GHz: good sensitivity only at MIL-STD-461F level.

These are shown in Figure 34.

As we do not have sufficient sensitivity on two frequency bands, we often have to perform additional assessments for EMC compliance. These have included include post-processing of the data; injecting known RF signal level into electrical cabling/ connectors to determine the shielding effectiveness of the enclosure of the equipment-under-test, and improving the shielding effectiveness and EMI filtering.
According to SKA EMC guidelines [RD12], EMI performance measurement must cover the entire range of frequencies and applicable bandwidth, which in Australian Radio Quiet Zone (RQZ) legislation covers a range from 70 MHz to 25.25 GHz, while recognising that it is often impractical to cover the entire band. Therefore, the range can be appropriately limited if suitably justified.

The EMC guidelines document [RD12] also establishes the SKA thresholds of harmful interference for Continuum and Spectral Line measurements as follow:

- Continuum, with bandwidth ratio of 1% of observing the frequency:
  (dBm/Hz)=−17log(f)−192 for f < 2 GHz.
  $P(dBmHz)$=−249 for f ≥ 2 GHz.
- Spectral Line, with bandwidth ratio of 0.001% of the observing frequency:
  $P(dBmHz)$=−17log(f)−177 for f < 2 GHz.
  $P(dBmHz)$=−234 for f ≥ 2 GHz.

It is expected that verification procedures must ensure that peak EMI emissions, including impulsive RFI, are lower than the limits, at the distance of the nearest receiver input from the source of the emission over the frequency range of 50 MHz to 20 GHz.

Currently there is a difference of 60 - 80 dB between the sensitivity of the instrument used to conform to MIL-STD-461F standard, and the Continuum and Spectral Line threshold limit given in [RD12]. It is worth noting that the bandwidth requirements for MIL-STD-461F and the SKA threshold limits are different, therefore correction factors need to be considered, which have not been established yet. In practice, it is often challenging to strike a balance between providing sufficient sensitivity, having reasonable measurement time and capturing transient/ impulsive RFI-type emission over a wide frequency range. Furthermore, we often have to customise measurement methods to verify the shielding effectiveness of enclosures used to house equipment once the enclosure is populated with connectors, cabling, holes, grounding connection and active electronics. (These might compromise the integrity and effectiveness of the shield).

Experience has shown that some clarification on the frequency range and bandwidth requirements would be useful, given that there are several different frequency range requirements (i.e. 70 MHz to 5 GHz [RD11], 70 MHz to 25.25 GHz and 50 MHz to 20 GHz [RD12]), and that of the established standards (e.g. 30 MHz to 18 GHz for MIL-STD-461F under specific measurement bandwidth).

Finally, it is often the case that equipment has to be placed directly next to, or in the near proximity of the antenna in the field, in which aggressive shielding and filtering solutions would probably be the approach adopted to conform to the SKA threshold requirements [RD35].

Recent work has included revisiting the EMC characterisation set-up, with a view to further verification, and potentially repeating some measurements.

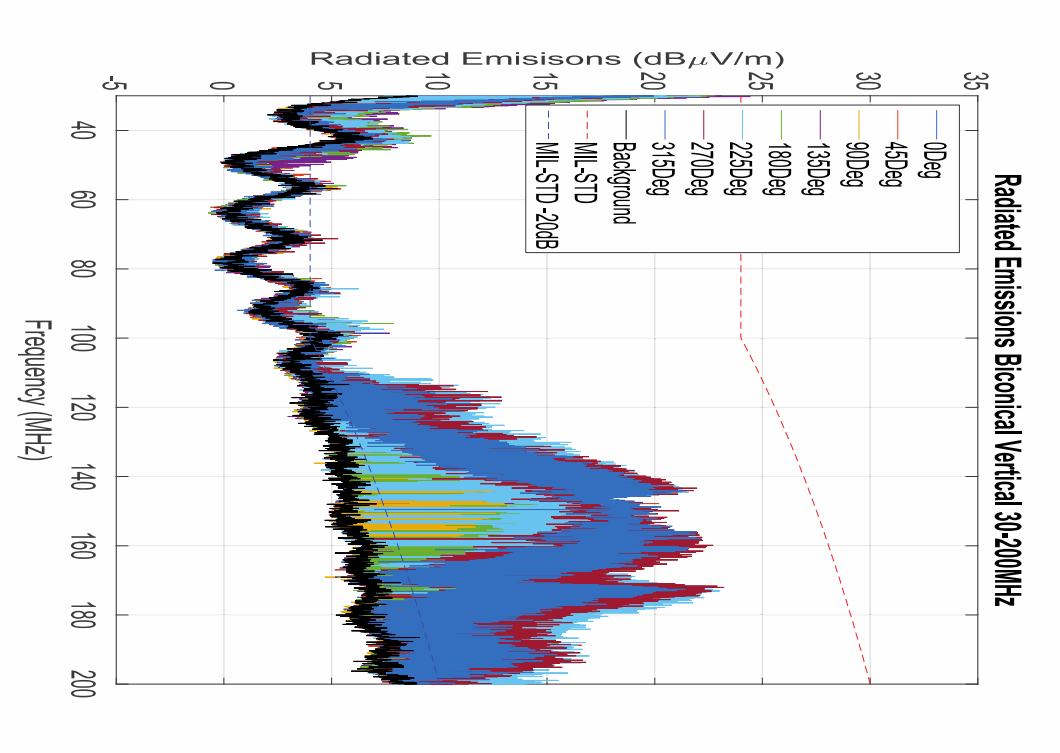

Figure 31: APIU EMC Radiated emissions results, 30-200 MHz.

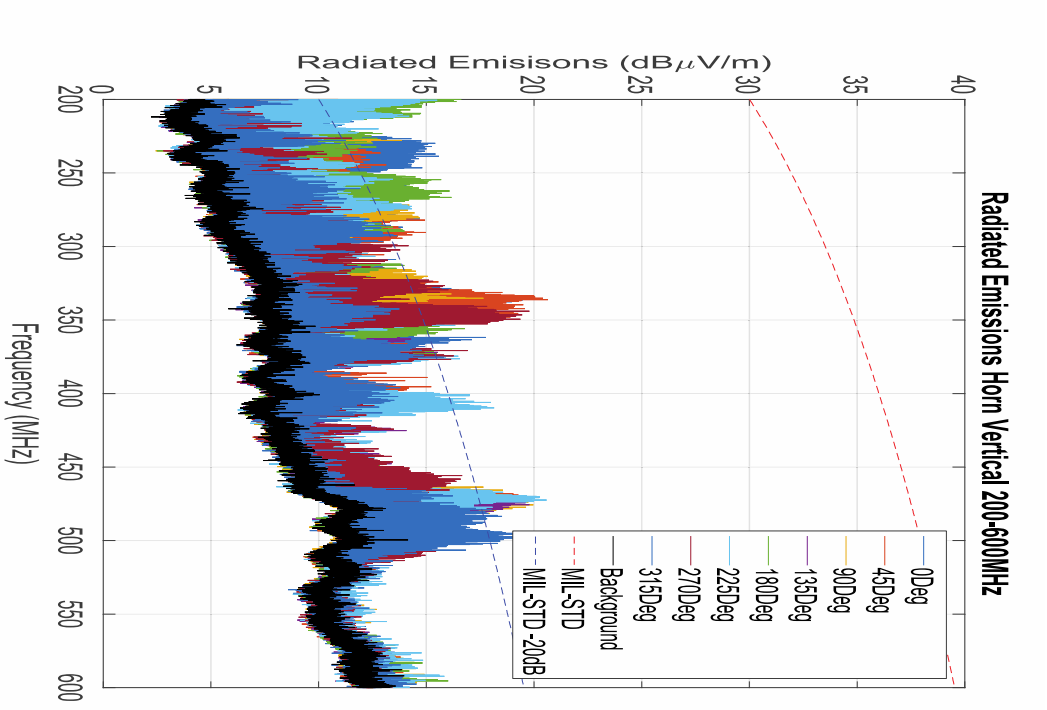

Figure 32: APIU EMC Radiated emissions results, 200-600 MHz

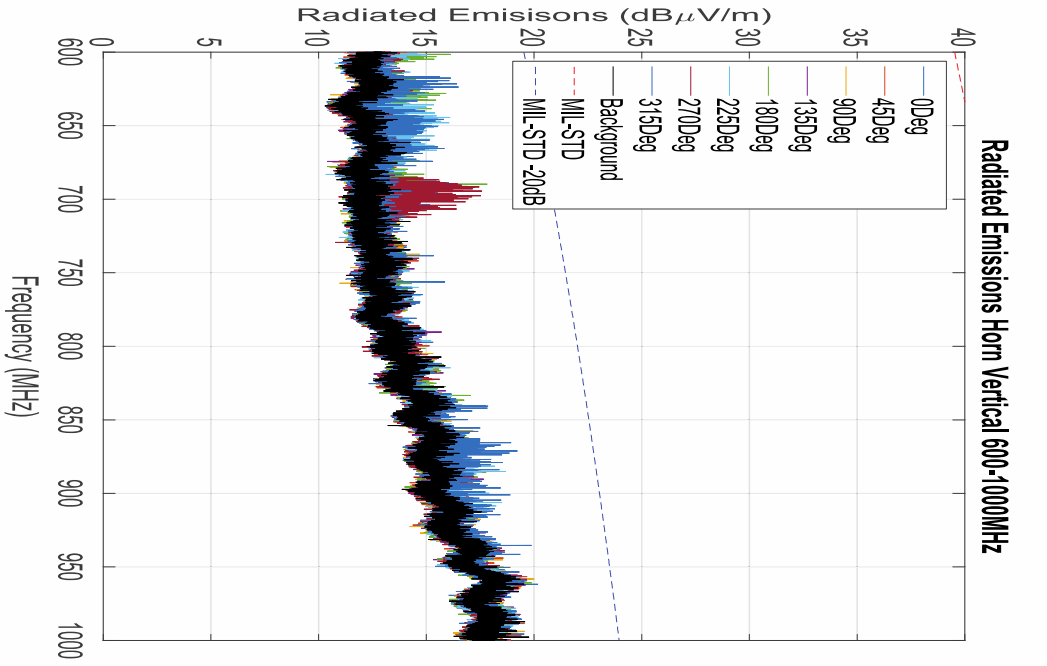

Figure 33: APIU EMC Radiated emissions results, 600-1000 MHz

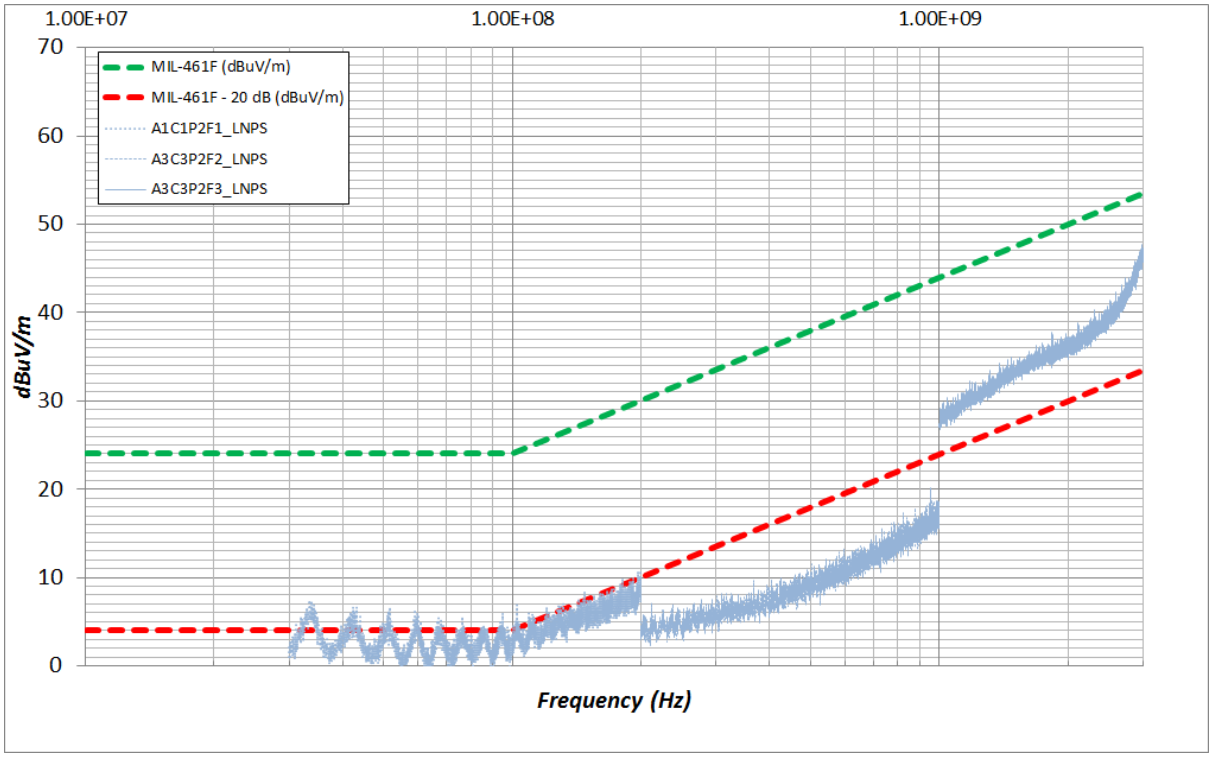

Figure 34: Measurement capabilities in ICRAR-Curtin laboratory. The green and red lines show the target emission thresholds; the blue curves show the measurement noise floor.

A.7 Simulated AAVS station beams at 110 MHz

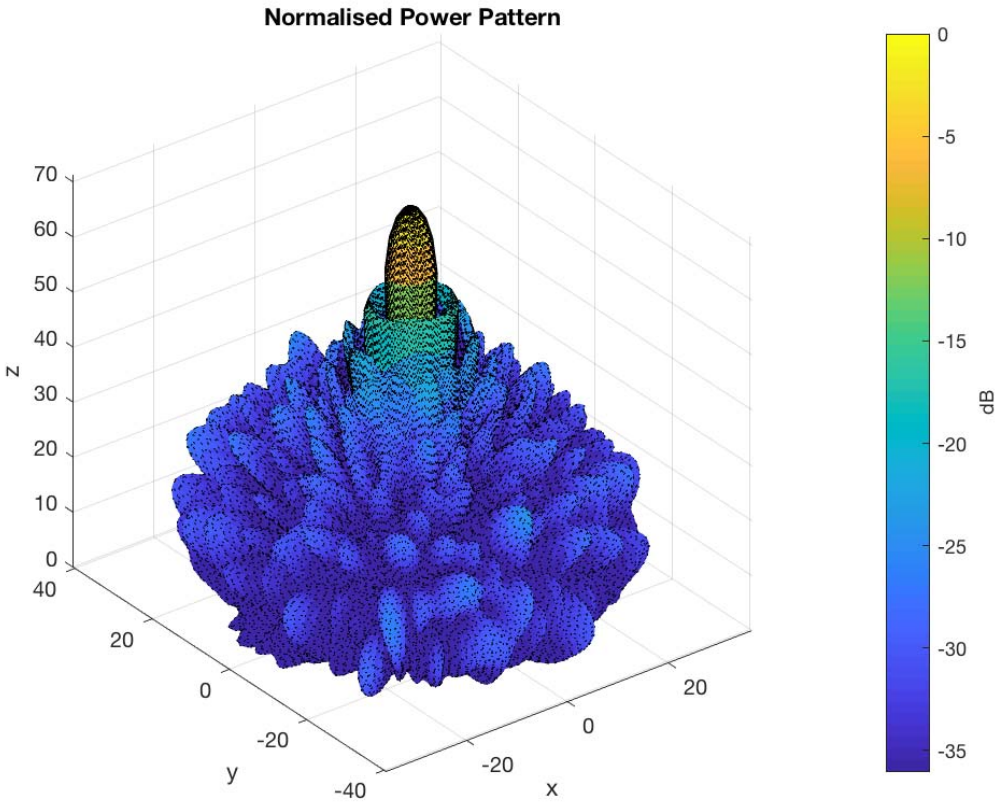

Figure 35: AAVS station pattern, 110 MHz, zenith pointing.

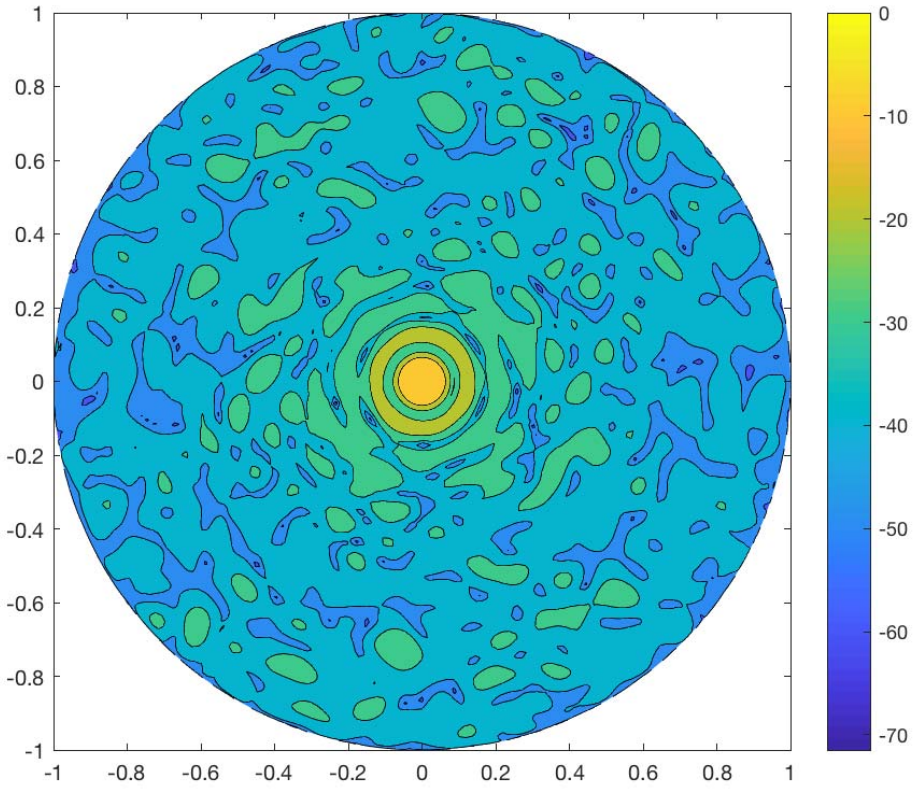

Figure 36: A contour plot of the same beam.

A.8 Phase solution statistics

A preliminary statistical analysis was performed on the gain phase solutions discussed in sections 4.2.1 and 4.2.2. This appendix provides more details of the analysis. In particular, the following calibration coefficients datasets were considered:

Sun-based calibration on 2018-04-05 - Start: 03:21:40 UT (~ 2hrs around Sun transit)
Sky-based calibration on 2018-07-11 (night-time selected subset)
Sun-based calibration on 2018-07-12 – Start: 03:25:26 UT (~ 2hrs around Sun transit)

The night-time subset for the 2018-07-11observation was selected in the time interval: 17:02:06 UT – 20:50:35 UT, in which the Sun does not need to be included in the model and the Galactic plane was rising, hence there is good signal to calibrate on.

The phase solutions in each dataset were divided into 10 minute intervals, in which flagged antennas, reference antenna (antenna 2) and incomplete bins (e.g. intervals in which one or more time samples were missing) were excluded from the statistical calculation.

The variations of the phase gain solution relative to the beginning of each interval were calculated for every antenna at a given time.

Figure 37 shows the phase solution differences for the 2018-04-05 solar observation for the X polarization. In that case, the solutions were given every about 5 minutes.

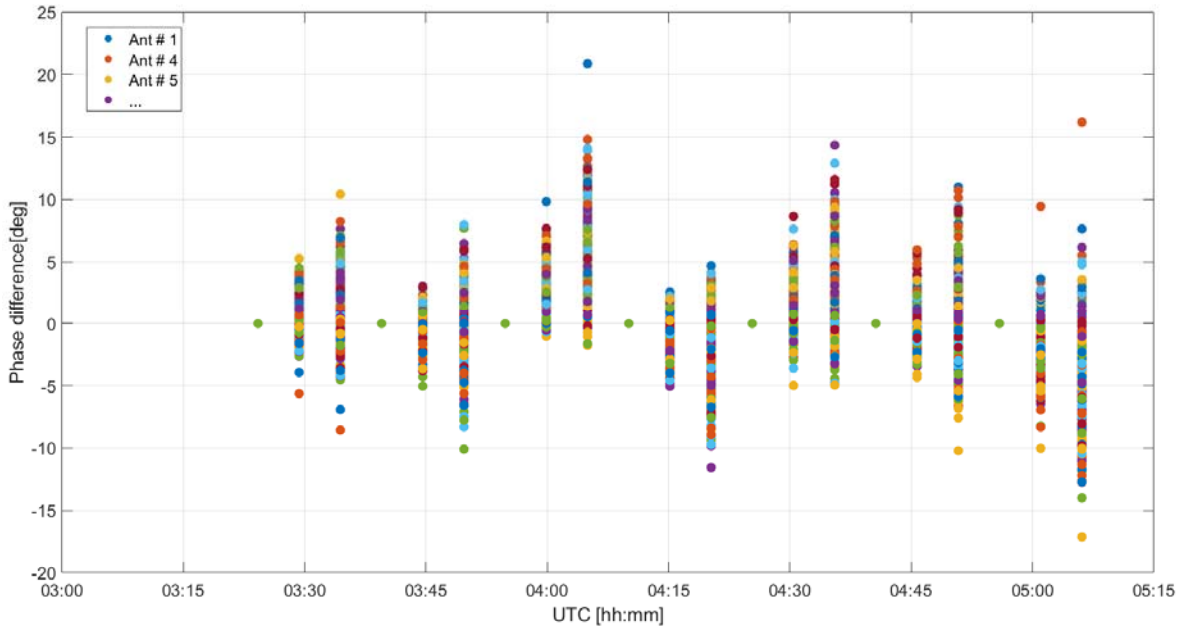

Figure 37: Antenna solution phase drift for the 2018-04-05 sun-based calibration for the X polarization.

The phase difference for the same dataset calculated for the Y polarization is plotted in Figure 38.

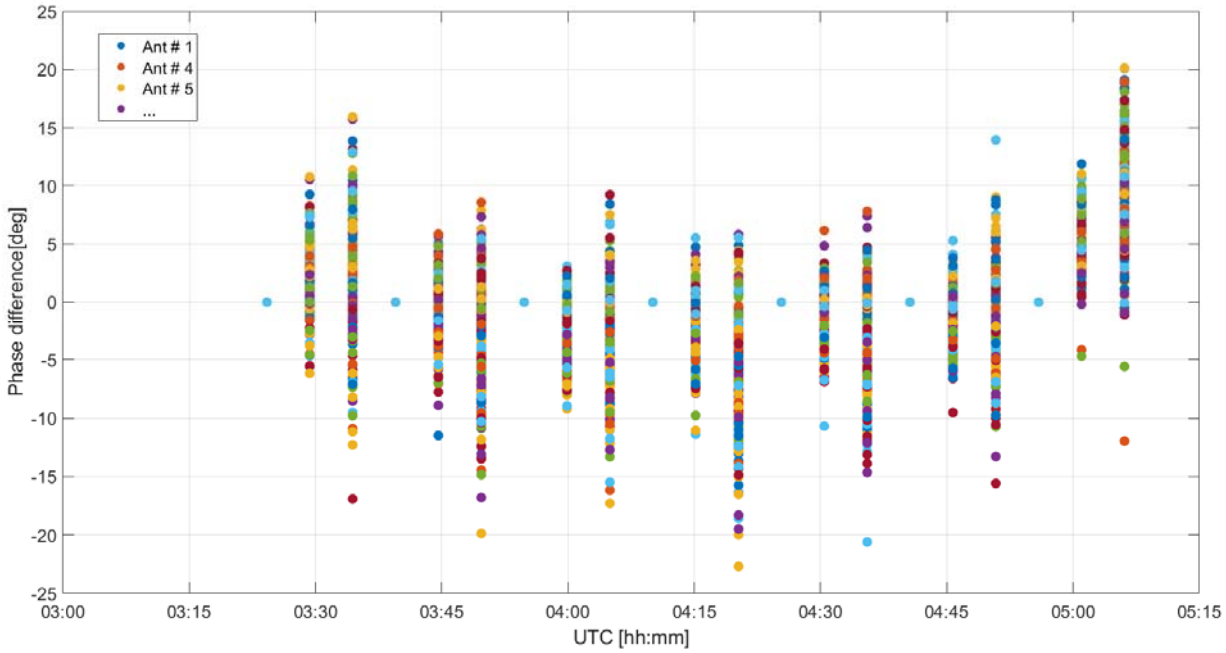

Figure 38: Antenna solution phase drift for the 2018-07-11 sky-based calibration for the Y polarization.

The phase solution variation in the selected data subset for the 2018-07-11 sky-based calibration is shown in Figure 39 for the X polarization. Respect to the solar calibration datasets here the gain solutions were calculated more frequently (approximately every 1 minute).

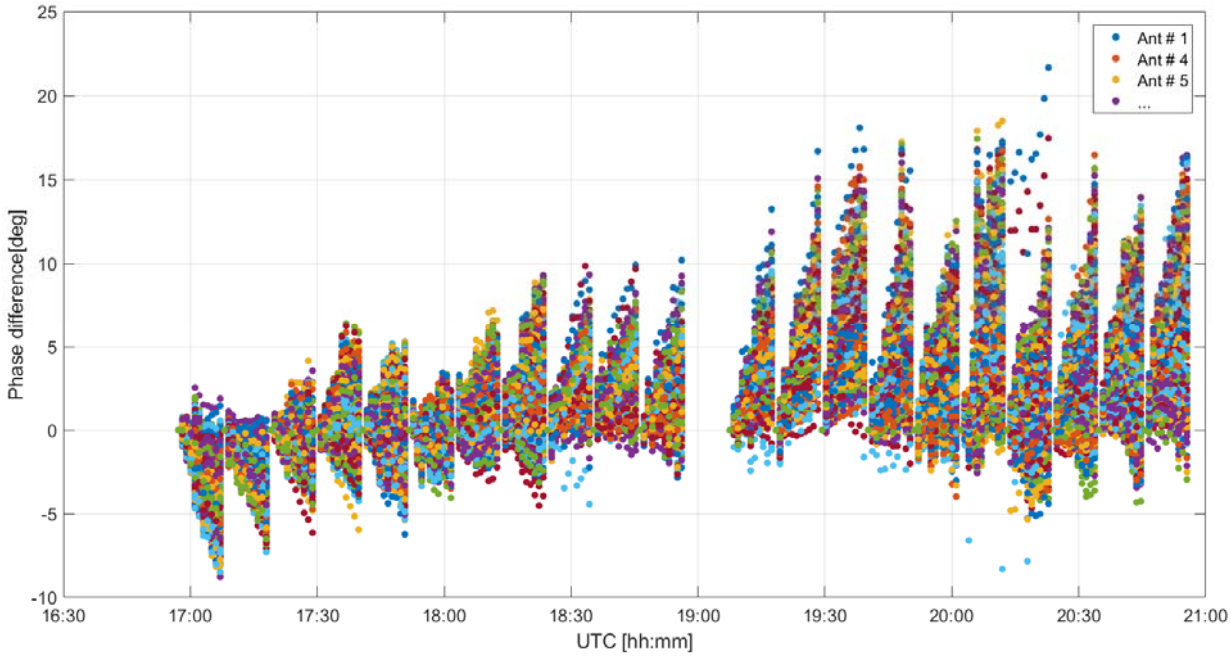

Figure 39: Antenna solution phase drift for the 2018-07-11 sky-based calibration for the X polarization.

In order to evaluate the phase solution stability/variability, the following statistical quantities were derived from the relative phase variation:

Standard deviation of solution variations in each window [Stats_#1]
Maximum standard deviation of the solution differences in every time sample within each window [Stats_#2]
Maximum RMS of the solution differences in every time sample within the each window respect to their mean values in that window [Stats_#3]
Maximum RMS of the solution differences in every time sample within each window respect to their initial values (zero) in the window [Stats_#4]

Figure 40 and Figure 41 show the statistics of the phase solution variations for all antennas, calculated in 10 minute calibration intervals, for the 2018/04/05 solar observation in X-Pol and Y-Pol, respectively.

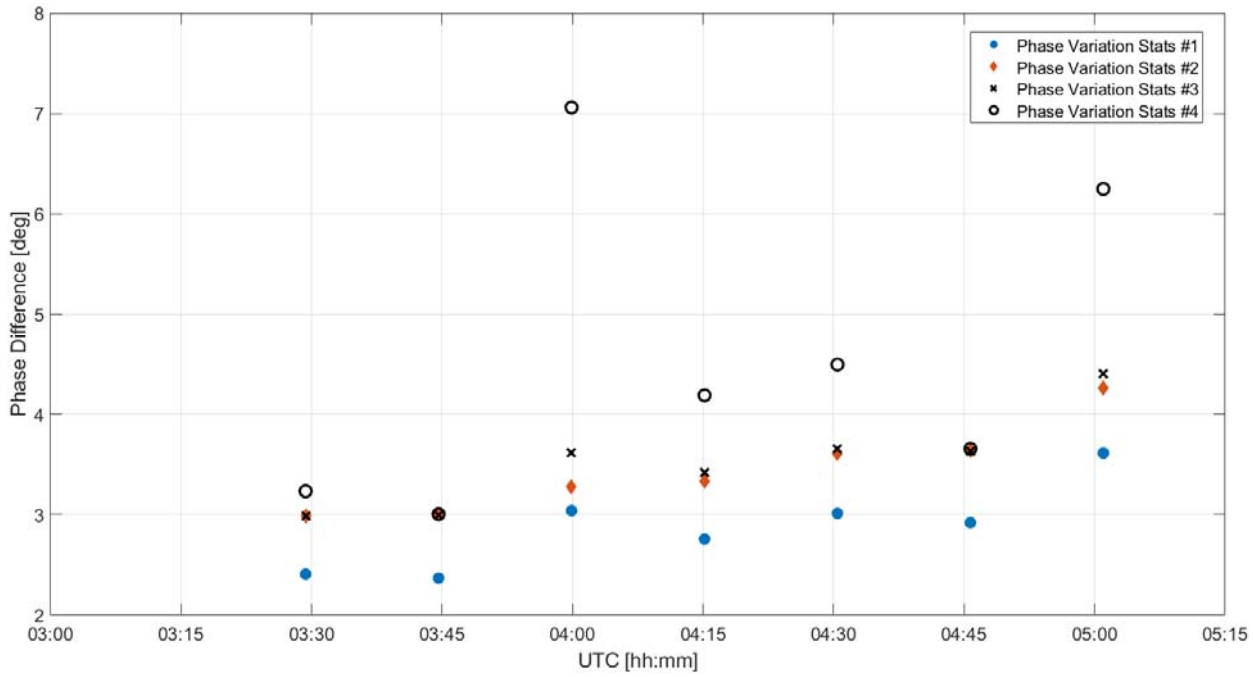

Figure 40: Phase difference statistics of the gain phase calibration for all antennas in X polarization for the 2018-04-05 solar observation.

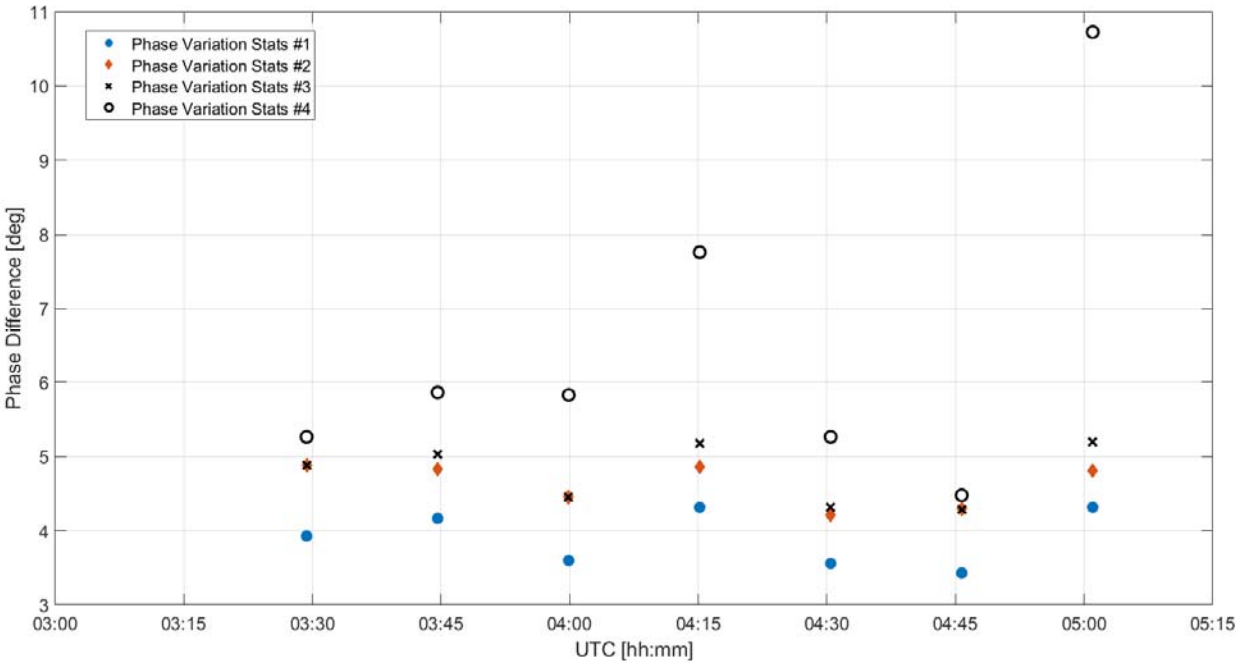

Figure 41: Statistics of the gain phase difference for all antennas in Y polarization for the 2018-04-05 solar observation.

The statistics of the phase solution variations on 10 minute window for the night-time subset on 2018/07/11 sky-based calibration calculated in X-Pol and Y-Pol are shown in Figure 42 and Figure 43, respectively.

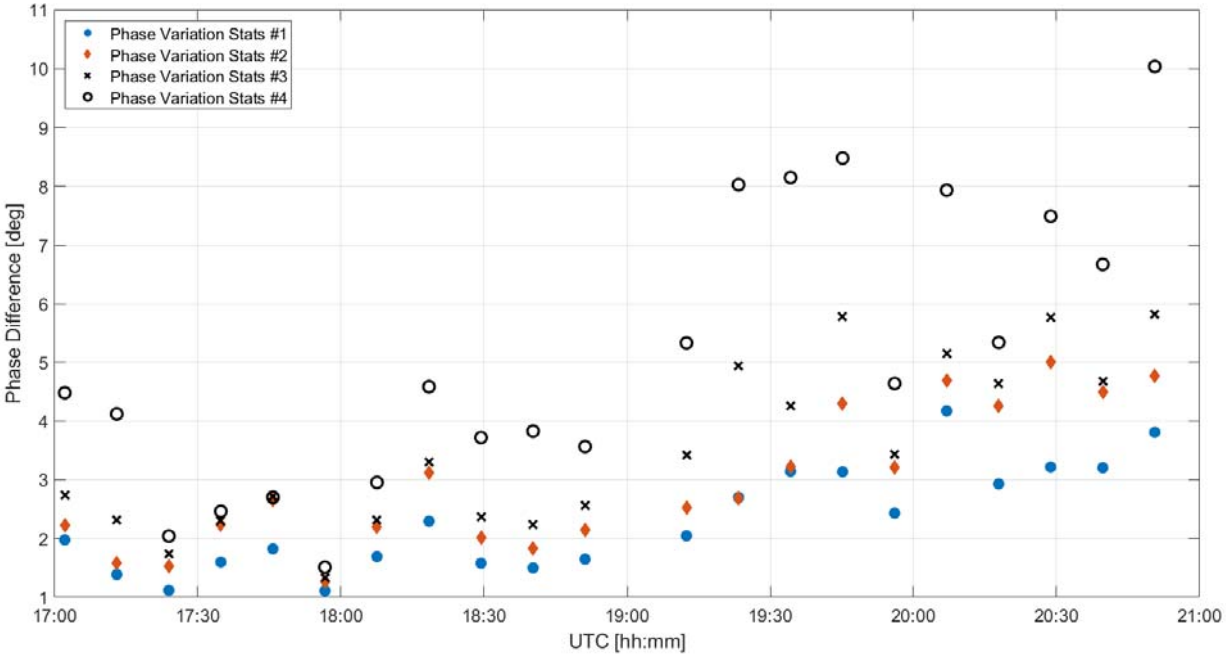

Figure 42: Statistics of the gain phase difference for all antennas in X polarization for the selected 2018-07-11 night-time window.

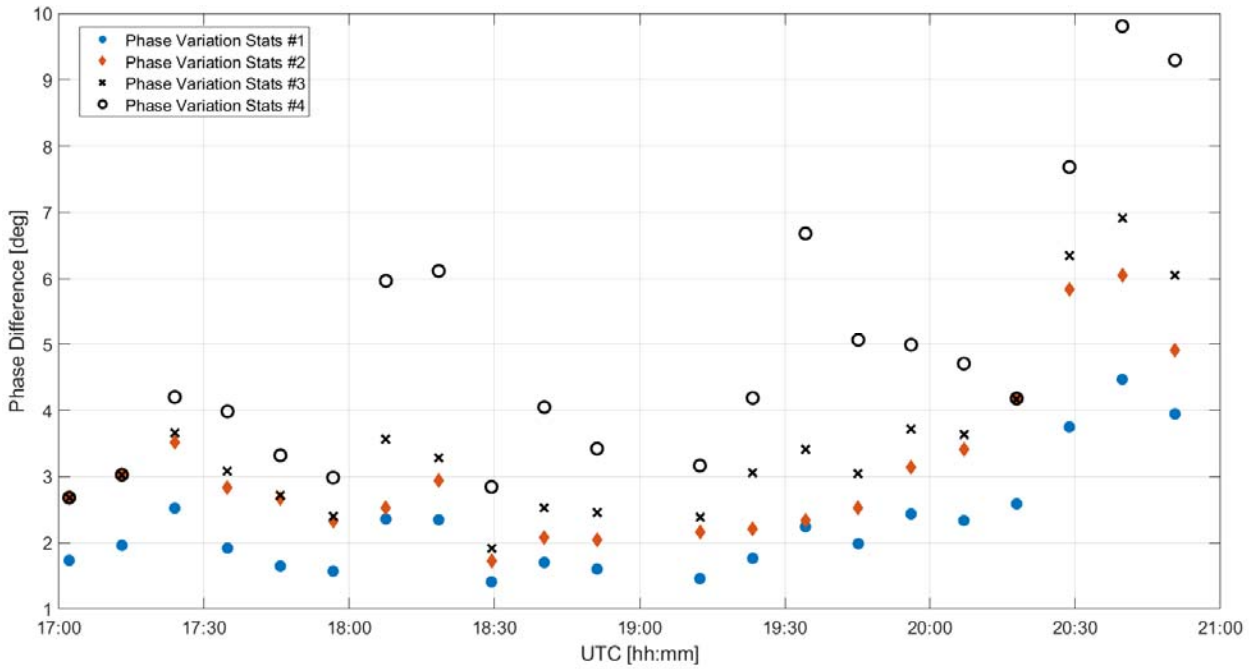

Figure 43: Statistics of the gain phase difference for all antennas in Y polarization for the selected 2018-07-11 night-time window.

Gain solutions were calculated also on 2018-07-12 from about 03:25:26 UT (~2 hrs around using the sun transit) using the Sun as calibration source. The statistical analysis was performed on that phase solution dataset in X-pol (Figure 44) and in Y-Pol (Figure 45).

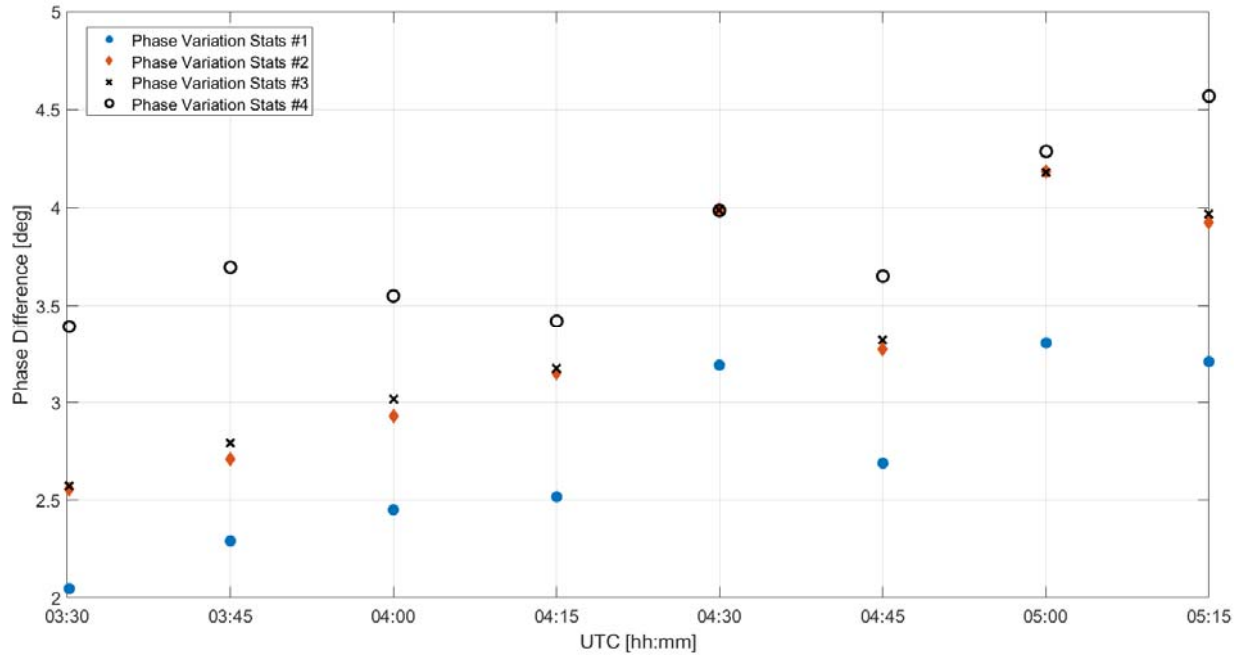

Figure 44: Phase difference statistics of the gain phase calibration for all antennas in X polarization for the 2018-07-12 solar observation.

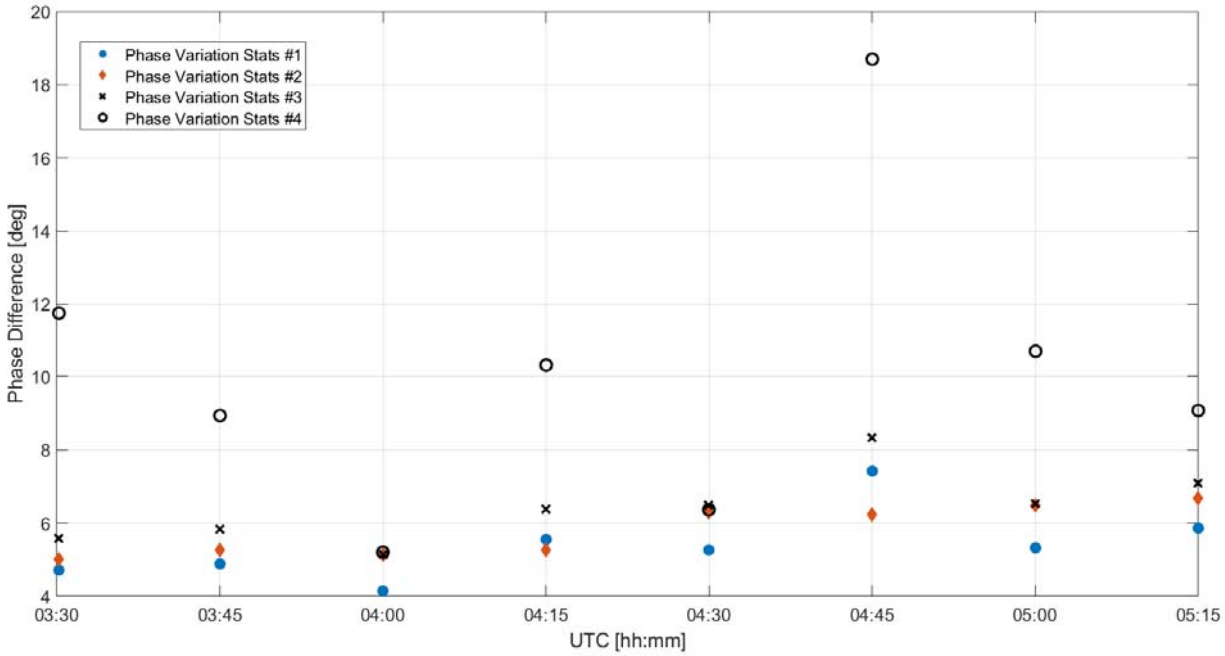

Figure 45: Phase difference statistics of the gain phase calibration for all antennas in Y polarization for the 2018-07-12 solar observation.

Some general considerations can be derived from this preliminary analysis:

The drift of the phase solutions generally increases in time within each 10 minute interval
In general, the phase variation statistical quantities #1,#2,#3 have similar behaviours in X Pol and in Y Pol
Large values of the stats #4 respect to the other stats reflect, in some cases, a significative drift of the phase difference mean value within the calibration window
There is no great difference in the phase drift in the different days, or in day-time or nigh-time for the stats #1,#2 and #3

However, these preliminary results cannot be used to verify if the LFAA stability requirements are met or not. In fact, it is not clear if these variations are due to the incomplete sky model or to the approximation of the telescope model used in the calibration (in which the averaged element pattern approximation was considered) or to an inherent system instability.